New Measurement Techniques for the Assessment of Velopharyngeal Function in Cleft Palate Patients

by

Malcolm John Birch

A thesis submitted for the

Degree of Doctor of Philosophy

at The University of Kent at Canterbury

1995

Abstract

The present day treatment of the cleft palate is very much a multi-disciplinary team approach calling upon the skills of plastic surgeon, orthodontist, maxillo-facial surgeon and speech therapist. The aesthetic result of modern plastic surgery on the lip and face is unquestionably successful; however the improvement to speech due to changes in velopharyngeal function as a result of surgery is not so readily agreed upon. It is generally acknowledged that cleft repair should be carried out as early as possible after birth followed by several years of developmental monitoring; however considerable debate relating to the surgical technique employed and the long term effect of surgery on speech development still abounds.

This thesis undertakes to make a contribution to the debate of efficacy of cleft repair in relation to speech function in the following manner. Firstly a new instrument called a Nasal Resonometer has been specifically designed for use by speech therapists for the pre and post operative assessment of hyper- and hypo-nasal speech. Secondly a new measurement technique involving the computer assisted analysis of x-ray videofluoroscopy images of clinically significant aspects of velar function has been introduced.

Several studies of patients attending the cleft repair clinics over a three year period are presented. The correlations between objective Resonometer measurement, subjective speech therapist analysis, velopharyngeal function and surgical technique are examined.

The extensive clinical use of the Nasal Resonometer and image analysis technique have proven to be a successful addition to routine cleft palate measurements. Further the application of these measurements in specific studies has led to a clearer understanding of the effect of cleft palate surgery and has highlighted future areas of research.

Acknowledgment

The initial impetus for the Nasal Resonometer came from my good friend and colleague Katherine Humphries, Director of Speech Therapy at The London Hospital. Thereafter throughout the entire project she has been a continual source of excellent ideas and has also provided invaluable help in gathering the test data.

I am very grateful for the support of Dr Stanley Klevenhagen who was Director of the Medical Physics Department at The London Hospital during the development phase of this work. More recently I have been extremely fortunate to have the been granted study leave for a critical period in the writing process by Dr David White, Director of Clinical Physics at The Royal Hospitals.

I would like to extend my thanks to Mr Brian Sommerlad, Consultant Plastic Surgeon at St Andrew's Hospital, Billericay. The opportunity to be a part of his Cleft Palate team has been a most rewarding experience. The many discussions of ideas that we have shared have contributed enormously to the video fluoroscopic analysis section of this work.

My Ph.D. tutor, Dr Steve Kelly, has been a source of unstinting support and has provided very practical advise during the writing phase. I shall always be grateful for his thorough proof reading and helpful suggestions.

Lastly and most importantly I would like to thank my wife Portia. Somehow in the midst of carrying her husband through his numerous Ph.D. crises she has brought into this world our beautiful son, Rhoan.

I dedicate this work to you both.

Table of Contents

Abstract

Acknowledgement

Chapter 1 Page 1

Introduction

1.1 Velopharyngeal function. 1

1.2 Hypernasality, hyponasality and nasal emission. 9

1.3 Measurement techniques overview. 11

1.3.1 Pressure/flow measurements. 12

1.3.2 Acoustic measurements 12

1.3.3 Velopharyngeal movement measurements. 15

1.4 Thesis overview. 16

Chapter 2 Page 18

Nasal Resonometer. Theory, Initial Study and Instrument Specification.

2.1 Acoustic theory of the vocal tract. 18

2.2 Initial study. 30

2.2.1 Microphone response. 30

2.2.2 Oral and nasal sound separation device. 33

2.2.3 Clinical study. 37

2.3 Initial instrument specification. 40

Chapter 3 Page 41

Nasal Resonometer. Design, Testing and Results.

3.1 Instrument design. 41

3.1.1 Sound separator design. Page 41

3.1.2 Signal conditioning and hardware implementation. 42

3.1.2.1 Phase lock loop design. 47

3.1.2.2 PLL input filter design. 53

3.1.2.3 Microphone signal amplification and low pass filter. 54

3.1.2.4 Tracking bandpass filters, RMS and A/D conversion. 57

3.1.3 Microprocessor , instrument bus and periphery hardware. 62

3.1.4 Instrument software. 69

3.1.5 Instrument fabrication. 76

3.2 Instrument testing. 78

3.2.1 Low pass, tracking filter and RMS-DC converter tests. 78

3.2.2 Phase lock loop tests. 82

3.2.3 System and microphone tests. 88

3.2.4 Instrument specification. 99

Chapter 4 Page 100

Nasal Resonometer. Clinical Evaluation, Measurement Protocol and Clinical Studies.

4.1 Clinical Evaluation. 100

4.1.1 System response. 100

4.1.2 Evaluation protocol and measurements. 104

4.1.3 Conclusions and measurement protocol. 127

4.2 Clinical Studies. 131

4.2.1 Orthodontic study. 131

4.2.2 Cleft palate and velopharyngeal insufficiency studies. 137

Chapter 5 Page 145

Velopharyngeal movement measurements.

5.1 Current measurement techniques. 145

5.2 Measurement protocol and system specification. 147

5.3 Velopharyngeal measurement system. 150

5.3.1 Hardware and software design. 151

5.3.2 System testing. 157

5.3.2 Clinical evaluation. 158

Chapter 6 Page 160

Velopharyngeal measurement system. Clinical applications.

6.1 Normative data, general clinical results, specific case study. 160

6.1.1 Normative and patient data, typical examples. 160

6.1.2 General clinical results. 162

6.1.3 A specific case study of a pre and post-operative cleft palate re-repair. 165

6.2 Assessment of palate re-repair. 170

6.3 Comparison between velopharyngeal and acoustic measurements. 177

Chapter 7 Page 181

Conclusions and further work.

7.1 Nasal Resonometer. 181

7.2 Velopharyngeal measurements. 183

References Page 186

Appendices Page 197

Chapter 1

Introduction.

1.1 Velopharyngeal Function

The velopharyngeal port is a very complex structure that has been shown (1,2) to employ different closure mechanisms depending on the current activity. The activities of speech, blowing and whistling result in measurably different (3) soft palate and pharyngeal wall movements to those observed during the swallowing process. The essential function of the velopharyngeal port is sphincteric during swallowing (4) and valvular during speech. These actions involve the closure of the pharyngeal port and the physical separation of the oral and nasal cavities. The diagrammatic representation of a typical velar closure cycle during speech is shown in Fig 1a-c.

Further functions of the soft palate (4) and associated musculature are the closure of the nasopharyngeal aperture to facilitate movement of the food bolus from the oral cavity to the pharynx, thereafter preventing passage into the nasal cavity. The tensor and levator muscles enable the pressure equalisation of the middle ear and oral cavity by opening of the eustachian tube.

Fig 1a: Velopharyngeal Schematic

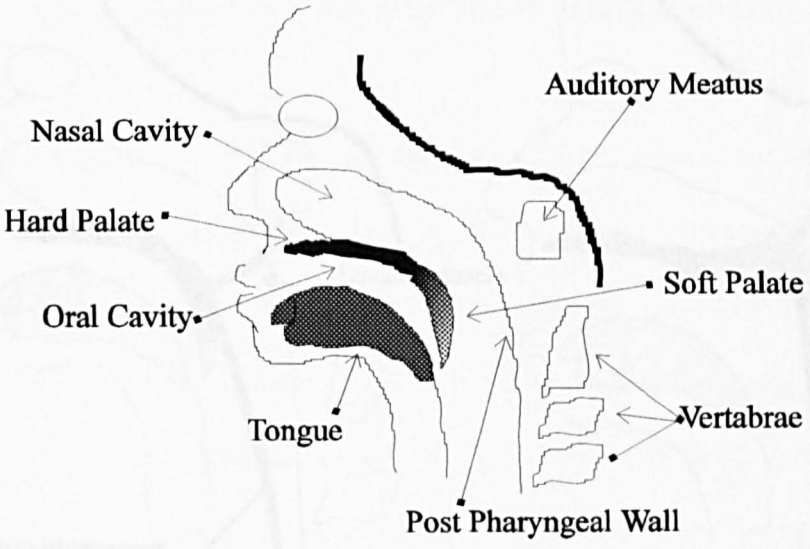

Fig 1b: Nasal Breathing Position

Fig 1c: Velar Closure

Fig 2: Soft Palate Musculature Schematic

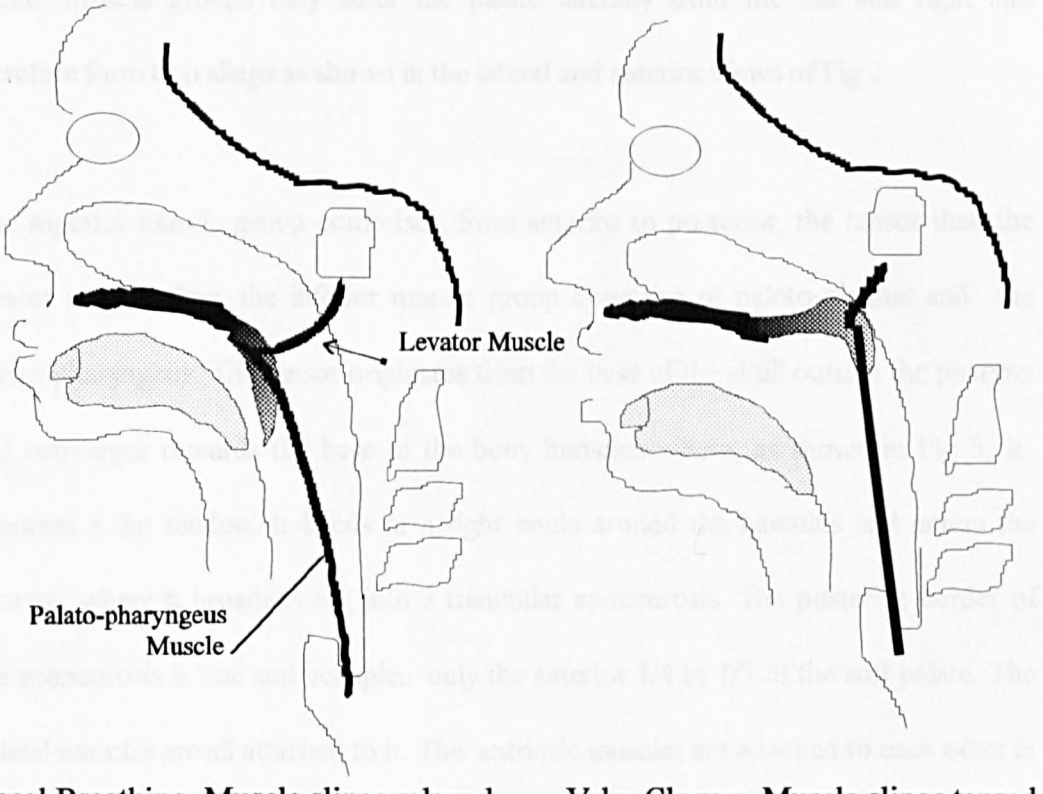

Nasal Breathing, Muscle slings relaxed

Velar Closure, Muscle slings tensed

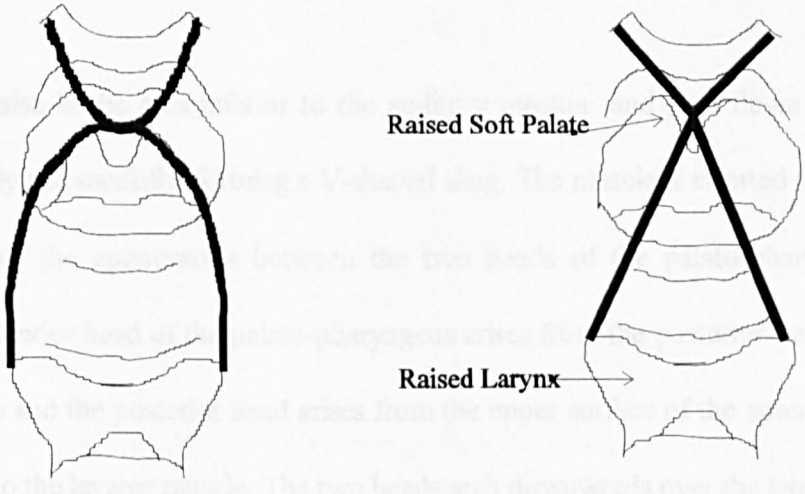

The soft palate is a muscular plate that is attached to the posterior edge of the hard palate. Muscle groups only enter the palate laterally from the left and right and therefore form two slings as shown in the lateral and anterior views of Fig 2.

The superior muscle group comprises, from anterior to posterior, the tensor then the levator muscle sling, the inferior muscle group comprise of paloto-glossus and the palato-pharyngeus. The tensor originates from the base of the skull outside the pharynx and converges towards the base of the bony hamulus where, as shown in Fig 3, it becomes a flat tendon. It bends at a right angle around the hamulus and enters the pharynx where it broadens out into a triangular aponeurosis. The posterior border of the aponeurosis is free and occupies only the anterior 1/4 to 1/3 of the soft palate. The palatal muscles are all attached to it. The extrinsic muscles are attached to each other in the posterior 2/3 of the soft palate forming the slings shown in Figure 2.

The levators arise in the area inferior to the auditory meatus and pass down to the palate anteriorly and medially forming a V-shaped sling. The muscle is inserted into the nasal surface of the aponeurosis between the two heads of the palato-pharyngeus muscle. The anterior head of the palato-pharyngeus arises from the posterior border of the hard palate and the posterior head arises from the upper surface of the aponeurosis just posterior to the levator muscle. The two heads arch downwards over the lateral

Fig 3: Palatal Elevation Musculature
Posterior View

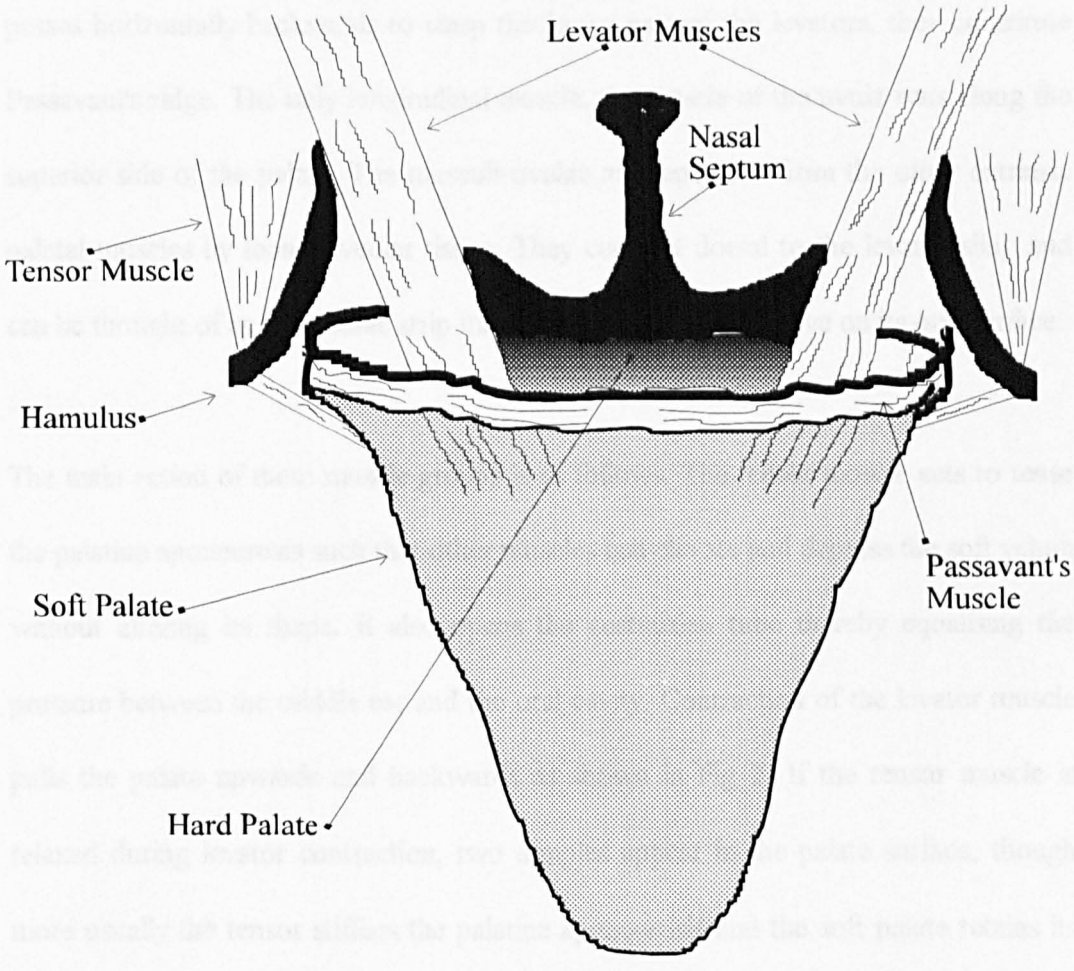

edge of the palate, join, and form a muscle that passes downwards beneath the mucous membrane of the lateral wall of the pharynx as shown in Fig 2.

Some fibres of the palato-pharyngeus, arising at the level of the hard palate, encircle the pharynx inside the fibres of the superior constrictor and form a U-shaped sling that passes horizontally backwards to clasp the lower part of the levators, they constitute Passavant's ridge. The only longitudinal muscle, the muscle of the uvula runs along the superior side of the palate. The musculi uvulae are seperated from the other extrinsic palatal muscles by loose alveolar tissue. They contract dorsal to the levator sling and can be thought of as a bimetalic strip making the palate less concave on its oral surface.

The main action of these muscle groups is as follows. The tensor muscle acts to tense the palatine aponeurosis such that other muscles can elevate and depress the soft velum without altering its shape. It also opens the eustachian tube thereby equalising the pressure between the middle ear and the oral cavity. Contraction of the levator muscle pulls the palate upwards and backwards as shown in Fig 2. If the tensor muscle is relaxed during levator contraction, two dimples appear in the palate surface, though more usually the tensor stiffens the palatine aponeurosis and the soft palate retains its shape.

The lower part of the vertical V-shaped sling of the levator pass through the horizontal U-shaped sling of the Passavant's muscle which as it contracts forms a hard ridge, Passavant's ridge, against which the soft palate is elevated by the levator. The contraction of the upper sling shortens the levator muscles and raises the soft palate, shutting off the nasal cavity from the oro-pharynx. The descending fibres of the sling

reach down to the thyroid cartilage and act as a levator depressor. The anterior head of the palato-pharyngeus muscle is attached to the hard palate and this part acts as a levator of the larynx and pharynx.

It also arches the relaxed palate making it more concave on it's oral surface. The posterior head depresses the whole tensed palate.

The main functions of the soft palate (4) are as follows. The flap-valve action of the soft palate shuts off the oro-pharynx from the oral cavity during chewing so that nasal breathing is unimpeded and closes the naso-pharynx from the nasal cavity during swallowing to prevent food from entering the nasal cavity.

Fig 4: Schematic of Muscle Forces

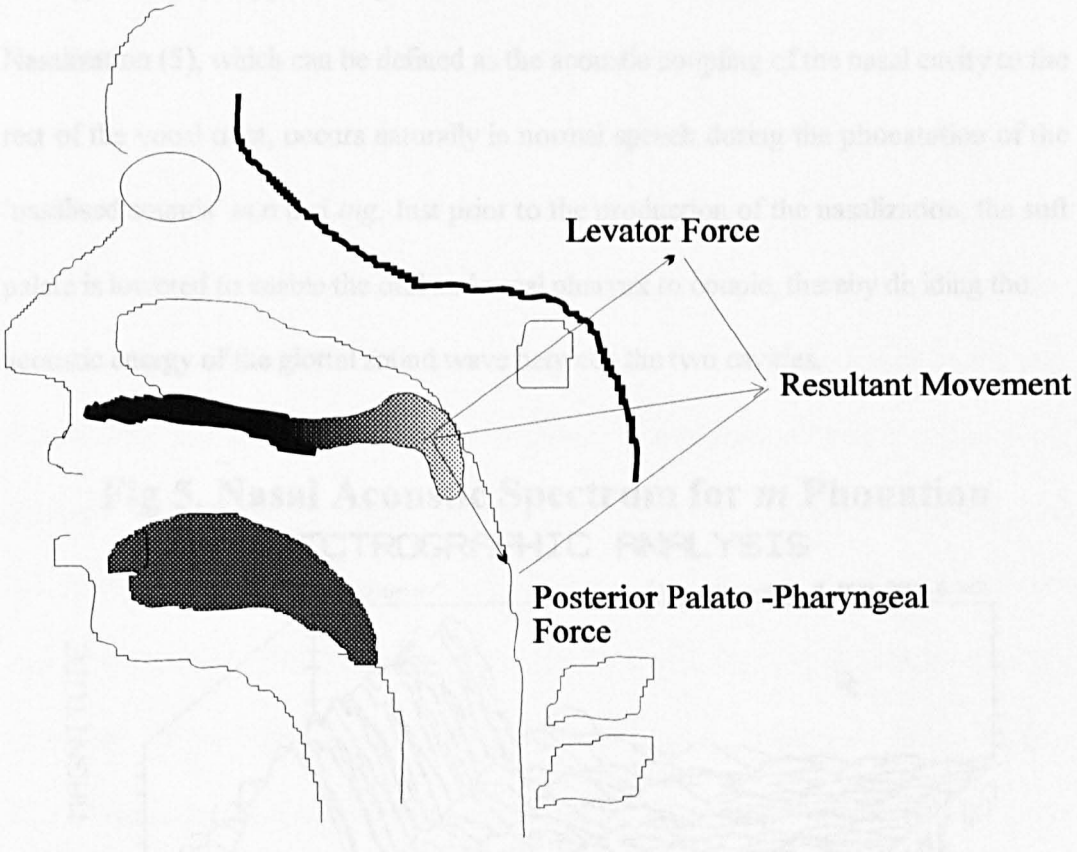

During speech the interim positions that the soft palate reaches are determined by the opposing pulls of the levator and the posterior head of the palato-pharyngeus as shown schematically in Fig 4; thus by the variable positioning of the soft palate within the velopharyngeal port can the acoustic relationship between the resonating chambers of the oral and nasal cavities be altered.

1.2 Hypernasality, Hyponasality and Nasal Emmision

Nasalization (5), which can be defined as the acoustic coupling of the nasal cavity to the rest of the vocal tract, occurs naturally in normal speech during the phonatation of the 'nasalised sounds' *m,n* and *ing*. Just prior to the production of the nasalization, the soft palate is lowered to enable the oral and nasal pharynx to couple, thereby dividing the acoustic energy of the glottal sound wave between the two cavities.

Fig 5. Nasal Acoustic Spectrum for *m* Phonation

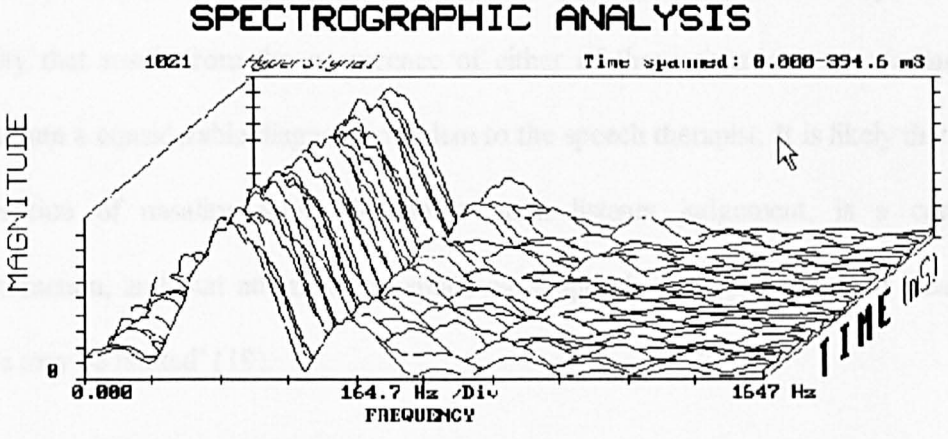

The largely fixed dimensions of the nasal cavity have a highly selective band-pass filtering effect resulting in a typical acoustic output from the nares as shown in Fig 5, consisting of a narrow band fundamental peak with several harmonics.

Hypernasality as the name implies, occurs due to the inadvertent diversion of acoustic energy into the nasal cavity during non-nasalised speech where the degree of coupling

between the cavities can be inappropriate in either degree or timing. The coupling of the nasal resonance system to the vocal tract results in a voice quality that is *perceived* by the listener (6) to have a distinct and undesirable nasal content. Conversely, the condition of hyponasality is due to the lack of acoustic energy present in the nasal cavity as a result of velopharyngeal dysfunction during the production of nasalised sounds or the reduction in nasal output from the nares due to a physical blockage such as a deviated septum. Hyponasality is commoner than hypernasality as it occurs in the commen cold and with enlarged adenoids. Perceptually, the attributes of poor voice quality that result from the occurrence of either of these situations are similar and constitute a considerable diagnosis problem to the speech therapist. It is likely that 'the perception of nasality, while dependant upon listener judgement, is a complex phenomenon, and that attempts to explain nasal speech through perceptual measures alone may be limited' (19).

In normal speakers the division of acoustic energy between the two cavities is not binary (5) in nature and a degree of nasalization is always present. This will depend on a number of factors the most important of which is velopharyngeal opening; with the high vowels *i,u,ae* the tongue is placed high in the oral cavity and facilitates velopharyngeal closure while with the low vowels *a,>*, the tongue position reduces closure effectiveness.

Nasal emission refers to the uncontrolled release of air from the nares via a "shunt" between the oral and nasal cavities, this may be due to a cleft of the hard palate or velopharyngeal inadequacy. The reduction in oral air pressure may cause distortion of sibilant and plosive sounds that rely on pressure building up behind a restricting articulator. The resultant turbulent air flow from the nares or within the nasal cavity may itself generate an acoustic signal that masks phonation and can be mistaken for hypernasality. However the presence of nasal emission is often coincident with hypernasal speech and may represent two facets of the same problem. Subjectively the two effects are difficult to isolate and therefore various instruments have been designed to attempt to measure nasal emission and hypernasality.

1.3 Measurement Techniques Overview

An ideal technique (7) for the assessment of the physical correlates of nasality or nasal emission would meet the following criteria:

- Non-invasive, physically or psychologically.
- Accurate assessment of velopharyngeal function during speech,
- Non-disruptive of articulatory, phonatory, auditory or ventilatory processes.
- Excellent correlation with perceived nasality or highly accurate measurement of nasal airflow.
- Portable, low cost, ease of operation and interpretation.

No instrument has fulfilled all these requirements and in the case of the Nasal Resonometer the prioritising of these criteria at the design stage resulted in an acceptable degree of compromise from the ideal.

1.3.1 Pressure/Flow Measurements.

Nasal airflow has been measured with a pneumotachograph (8,9,10,11) and with a warm wire anemometer (12,13,14) fitted into a nasal mask. In order to relate flow measurements to velopharyngeal function researchers have extended the testing of nasal airflow to include measurements of oral pressure (15), velopharyngeal port area (16,17) and ratiometric oral:nasal airflow (18). Nasal emission is a fairly straightforward concept not subject to much debate; however the associated instrumentation and underlying theories are of considerable interest and while they are outside the realm of this thesis they are included for reference.

1.3.2 Acoustic Measurements

Considerable effort has been expended in the search for a definitive acoustic measurement of velopharyngeal function, the principal advantage being, the non-invasive nature of the instrumentation.

Vocal tract damping, the measure of the elapsed time between an imposed blockage of the supraglottal airway and the cessation of vocal fold vibration (20), has been investigated as an indicator of the efficacy of velopharyngeal port closure. Though the initial variability in results (21) showed that the instrument was not ready for clinical use the sound theoretical basis of the measurement may encourage further research.

Spectral features would appear to provide a useful measure of nasalization as it seems intuitively correct that the perceived presence of a nasal tone must be associated with some quantifiable attribute of the speech spectrum; however the wide ranging search (22,23,24,25) for an *invariant* spectral feature has proven fruitless. Theoretical modelling (5,26,28) of the vocal tract has revealed that the lack of an invariant feature is in fact to be expected (29) although certain spectral characteristics, summarised in Table 1, are generally agreed to be associated with nasalization.

Table 1: Spectral Features of Nasalization	
Feature	Reference
Increased formant bandwidth	23, 24, 28
Formant frequency shift	23, 24, 25, 28, 30, 33
Extra resonances	22, 23, 24, 28, 30
Diminished resonances	22, 23, 24, 28
Noise between formants	22, 23
Decreased overall intensity	24, 28, 31

Oral and nasal sound pressure have been used as an indirect measurement of velopharyngeal opening. The lowering of the velum increases the acoustic coupling to the nasal cavity and the resultant increase in sound pressure has been measured with a nasal microphone (27,34). Although simple, this technique has limited use diagnostically due to the error induced in the measurement by firstly, air turbulence in the nasal cavity being mistakenly measured by the microphone as an acoustic signal from the glottal wave and secondly, the intensity of the nasal acoustic output increasing due to additional phonatory effort. The second measurement uncertainty can be reduced by simultaneously measuring the oral and nasal sound pressures and, presuming that increased vocal intensity effects both to the same degree, then the ratio (35, 36) of nasal to oral pressure will maintain a constant relationship.

The use of an accelerometer in place of the nasal microphone (37) has been found to alleviate the measurement error due to air turbulence and the ratio of nasal

accelerometer to oral microphone signals have been shown to have a significant correlation with perceived nasality (38, 39).

1.3.3 Velopharyngeal Movement Measurements.

The principal methods used to visualise velopharyngeal movements are, optical endoscopy and x-ray fluoroscopy. A typical endoscopic instrument has been the so called 'hard' endoscope (42, 77) which is inserted into either the oral or nasal cavity for direct viewing and audio-visual recording (44) of velopharyngeal movement. The disadvantages of this instrument are, gagging due to the device touching sensitive tissue and the restriction of articulatory function due to the instrument's bulk within the oral cavity. Thin fibre flexible endoscopes (76) entered via the nares (40) have allowed the unhindered articulators to be viewed from above however, the procedure is uncomfortably invasive and only tolerated by the more co-operative patients. The use of endoscopy to ascertain accurate measurements of soft palate movement is severely limited by the distortion of the image dimensions due to optical non-linearity and variation in image magnification with movement. X-Ray fluoroscopy has been extensively (1,2,3,41) applied to the imaging of velopharyngeal movement and the comparison of the reliability of clinical information obtained from fluoroscopic and endoscopic examination (45) clearly points to the use of x-ray. Apart from imaging articulatory movements in several planes simultaneously (3), the physical dimensions of

the velopharyngeal cavity, characteristics of the velar closure cycle and the timing of articulatory movement during speech have been investigated (46,47,48) using x-ray data. The use of image processing (49,50) of fluorographic images has been shown to improve image quality with a commensurate increase in measurement accuracy and a further reduction in the absorbed radiation dose than that achieved (51) using conventional radiographic techniques.

The importance of standardisation of reporting of nasopharyngoscopy and multiview videofluoroscopy has been summarised by an international working group (52) and has been incorporated into the measurement technique proposed in this thesis.

1.4. Thesis Overview

The thesis describes the design and introduction of two measurement techniques into the clinical evaluation of velopharyngeal function. The first is an instrument called the Nasal Resonometer that is intended for use by speech therapists as an aid to assessing hypo- and hypernasal speech, the second is an image analysis measurement system intended for use by plastic surgeons in the pre- and post operative assessment of velopharyngeal movement and closure. Both techniques have found application in the management of patients undergoing the repair of a cleft palate and have also been applied more widely to patients with various velopharyngeal dysfunctions who have attended the Palatal Investigation Unit at St Andrew's Hospital, Billericay.

Chapter one introduces the basics of, velopharyngeal physiology, nasality, emission and gives an overview of the various measurement techniques currently in use. Chapter two describes in detail the theoretical model of the vocal tract, an initial study of hypernasality assessment and a specification for the Nasal Resonometer. Chapter three describes the instrument design, fabrication and laboratory testing. Chapter four reports the clinical evaluation of the instrument, the design of a clinical measurement protocol and results from extensive clinical studies.

Chapter five describes the current velopharyngeal movement measurement techniques, a specification for the image analysis system and the subsequent design and clinical testing . Chapter six describes the application of the system to a specific study of palate repairs, routine clinical use over two years and finally correlates results with other acoustic measurements. Chapter seven draws conclusions on the use of the Nasal Resonometer and the image analysis system. Further proposed extensions to the work are described.

Chapter 2

Nasal Resonometer. Theory, Initial Study and Instrument Specification

2.1 Acoustic Theory of the Vocal Tract.

The simplest theoretical model of the vocal tract consists of a source of sound, a transfer function and a radiated sound wave, stated symbolically as:

$$P(f) = S(f).T(f) \qquad (2.1)$$

and shown schematically in Fig 6.

Fig 6: Filtering Effects of the Vocal Tract

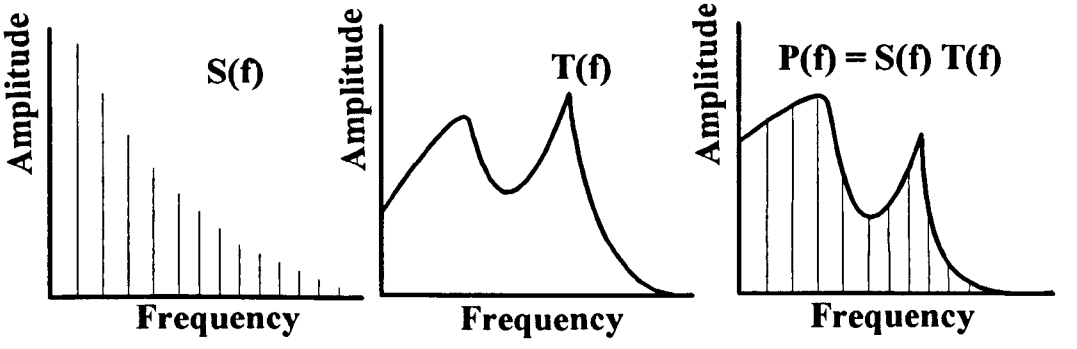

Reproduced from Fant(5).

P(f) represents the output sound pressure frequency spectra radiating from the vocal tract, S(f) represents the input sound spectra to the vocal tract and T(f) represents the filter transfer function that modifies the input sound spectrum to the output radiated sound wave.

Physically, the glottis provides the source of sound S(f) , the vocal tract consisting of the cavities of the larynx, oral pharynx and oral cavity modifies T(f) the glottal sound spectra, and the output sound P(f) radiates from the labia, nares or both. In some instances the nasal

pharynx and nasal cavity also couple to the vocal tract via a lowering of the soft palate to form an adjunct to the oral pathway.

The source of sound in speech can originate from both the glottis and from higher in the vocal tract, consecutively these are appropriately described by speech therapists as voiced and unvoiced sounds.

Voiced sounds are produced by the vibration of the glottis which is produced in the following manner. Exhalation from the thoracic cavity is initially obstructed by the closure of the vocal folds resulting in a sub-glottal pressure rise. This pressure increases to the point when the folds are forced apart which enables the rapid increase of airflow across the glottis, the resultant local pressure drop due to the Bernoulli effect in conjunction with the natural fold elasticity causes the glottis to close again and the cycle is repeated. The vibrating glottal mass results in compression and rarefaction of the air in contact with the surfaces of the vocal folds which in turn transmits acoustic energy, by transfer of momentum between adjacent gas molecules, along the column of air within the vocal tract . Some examples of voiced sounds are the vowels, *a* sound as in 'car' and *e* sound as in 'feet'.

Unvoiced sounds are produced by articulators, for example the tongue or labia, partially or completely blocking the air flow from the thoracic cavity. The resultant turbulent air flow through a restricted orifice provides the source of sound, some examples of unvoiced sounds are the fricatives *s* sound as in 'see' and *f* sound as in 'fee'.

The acoustic properties of the vocal tract modify the spectral characteristics of both voiced and unvoiced sounds by the processes of damping and filtration. In this manner certain frequencies are selectively transmitted and others attenuated, the spectral peaks that occur in the output P(f) as a result of this process are known as *formants* , Fig 6 shows the spectrum for a two formant voiced sound. The peaks in the transmission through the vocal tract due to the filter function T(f), occur at specific frequencies known as *resonant frequencies*; they are independent of the sound source S(f) and highly dependant on the physical dimensions of the various cavities. Fig 6 shows that the formant and resonant frequency are synonymous and in the case of voiced sounds, the formant frequency is a property of the vocal tract filter function

(5). Harmonics occurring in the sound source will only inadvertently coincide with the peaks in the filter function. Hence the formant frequency is independent of the sound source and depends upon the positions of the various articulators modifying the dimensions and hence resonant properties of the vocal tract cavities.

The simplest physical model of the sound system that has been utilised (53) is the Helmholtz resonator which consists of a single cavity, closed at one end to represent the glottis and open at the other to atmosphere via the oral cavity and interlabial orifice as shown in Fig 7, the nasal cavity is not added.

Fig 7: Single Helmholtz Resonator Model

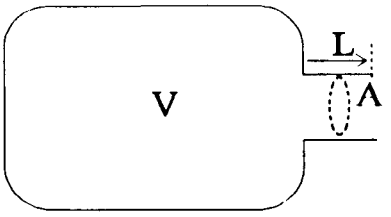

A Single Helmholtz Resonator

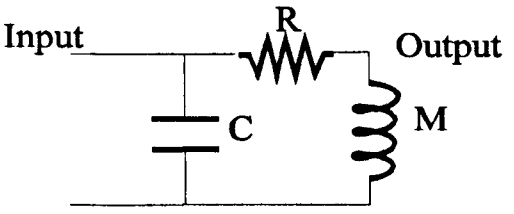

The Equivalent Circuit

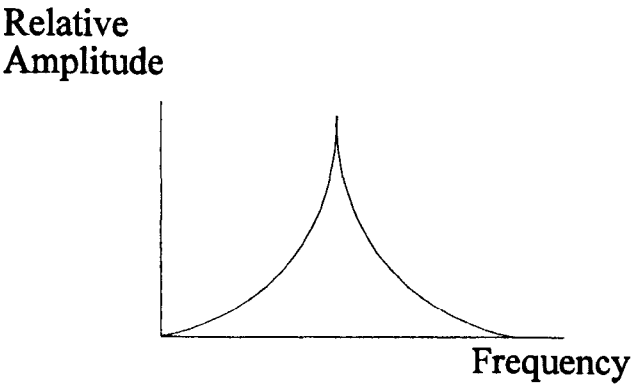

The Resonant Response Curve

The total volume of the vocal tract is represented by the volume V, the length of the interlabial channel by the length L and the area of the lip opening by the area A. The acoustic properties of the resonator depend upon the chamber volume and shape of the channel but not on the exact shape of the chamber. The electrical analog of this simple model is given by the equivalent circuit in Fig 7 where the capacitor C equates to the chamber volume V, inductance M to the interlabial channel defined by L and A, the damping property of the resonator due to energy dissipation is represented by the electrical energy lost in R . Using the actual vocal tract dimensions, the values of C, M and R can be calculated such that the frequency response of the equivalent circuit driven from a constant amplitude input corresponds to the acoustic resonant frequency curve for the particular vocal tract configuration as shown in Fig 7.

Adjusting the resonator dimensions and therefore the electrical analogue values causes the resonant peak to shift along the frequency axis and also alters the filter bandwidth, that is the frequency range between the -3dB or half-power points. The resonant frequency f_r is inversely proportional to C and/or M as follows.

$$f_r \propto 1/\sqrt{(C.M)} \qquad (2.2)$$

Acoustically the resonant frequency is lowered by increasing the resonant chamber volume (V), increasing the interlabial channel length (L) or decreasing the area (A) of the lip opening. The tuning property of the resonator or bandwidth of the resonant curve is a function of the length (L) and area (A) of the output channel, the longer the length and smaller the neck area the sharper will be the resonant peak. The dissipation of acoustic energy due to resistive losses will cause a detuning of the system and a consequential widening of the resonant bandwidth.

This very simple model of a single resonant chamber to represent the vocal tract is unfortunately inadequate. In the case of most oral vowel and consonant sounds the coupling of the oral and pharyngeal cavities is restricted to varying degrees by the position of the tongue. A more representative model of this situation is a double chamber Helmholtz resonator as shown in Fig 8.

Fig 8: Double Helmholtz Resonator Model

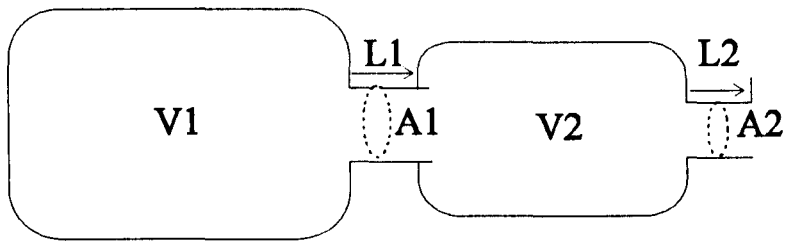

A Double Helmholtz Resonator

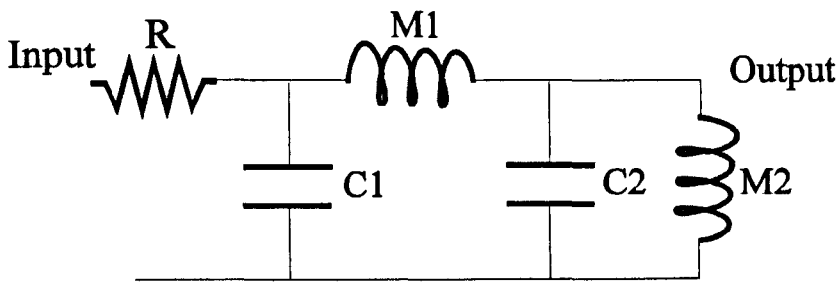

The Equivalent Circuit

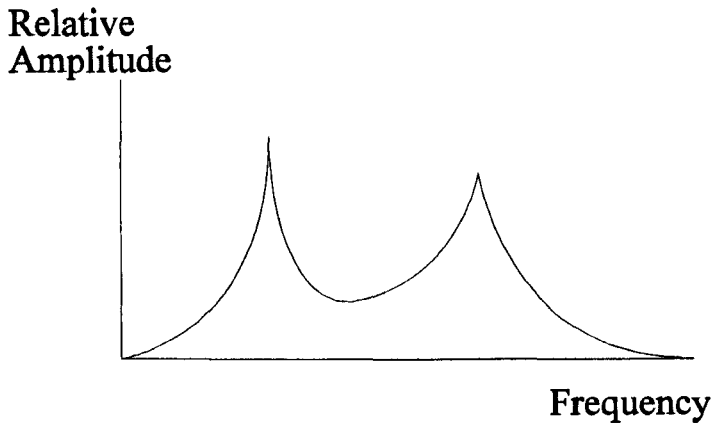

The Resonant Response Curve

In the double Helmholtz resonator the acoustic tract is modelled as the velopharyngeal cavity volume (V1), the length (L1) and area (A1) of the constriction between the tongue and palate, the oral cavity volume (V2), the length of the interlabial channel (L2) and the area of the lip opening (A2). The electrical analog, as in the case of the single resonator, models these 'lumped constant' acoustic parameters of cavity volume and channel conductivity as respectively capacitance (C1,C2) and inductance (M1,M2). The resultant double peaked resonant curve in Fig 8 depends on the presence of both cavities although each peak may be

more closely associated with one cavity. As the amount of coupling increases so the association decreases and it is not valid to consider a particular resonant frequency to be an invariant feature of a particular cavity (5,26,28). This is an important consideration as there is considerable coupling between the oral and pharyngeal cavities in vowel sounds due to the low proximity of the tongue and the palate. The limitation of the double Helmholtz resonator model is due mainly to the restricted frequency range in the output that will occur for a particular set of dimensions. Calculations for this model require that the cavity dimensions are small compared to a quarter wavelength and the higher frequencies that occur in speech are therefore not adequately represented.

The limitation imposed by the 'lumped parameters' Helmholtz models was overcome (26) by remodelling the vocal tract as a series of concentric cylinders of varying radius and length placed end to end and driven from a piston delivering a volume velocity i_o as shown in Fig 9.
In this case the vocal tract is considered as a tube closed at the glottal end and open at the labial. The column of air within the tube propagates the compressional sound wave to the open end where a wave of rarefaction is reflected back to the closed glottal end. This process is continued and a series of standing waves is established with a characteristic spacing of nodes and antinodes determining the resonant properties of the column. The first resonant mode corresponds to a node and antinode, that is a quarter wavelength, coinciding with the open and closed ends of the tract, therefore in a typical male tract of length 17cms the lowest resonant frequency would be 500Hz. In a perfectly symmetrical tube, higher modes of vibrations, corresponding with odd multiples of the quarter wavelength, would produce evenly spaced harmonics of the fundamental at 1500Hz, 2500Hz and so on. The vocal tract however consists of constrictions and expansions along its length and coincidence of an antinode with a constriction will lower the resonant frequency (5) whereas constriction at a node will raise the frequency.

Fig 9: Concentric Cylinders Model

Reproduced from Dunn (26)

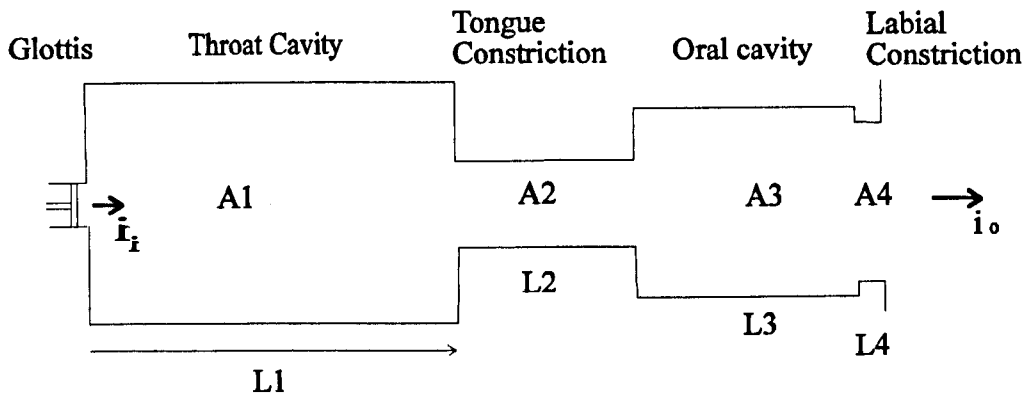

Vocal Tract Model

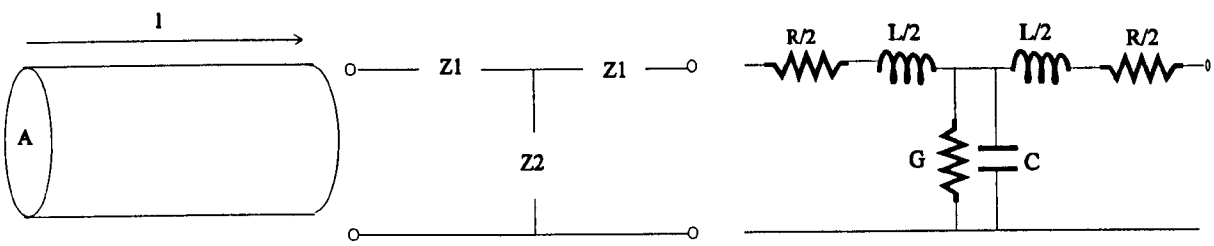

Cylindrical Section represented by T Impedance Network

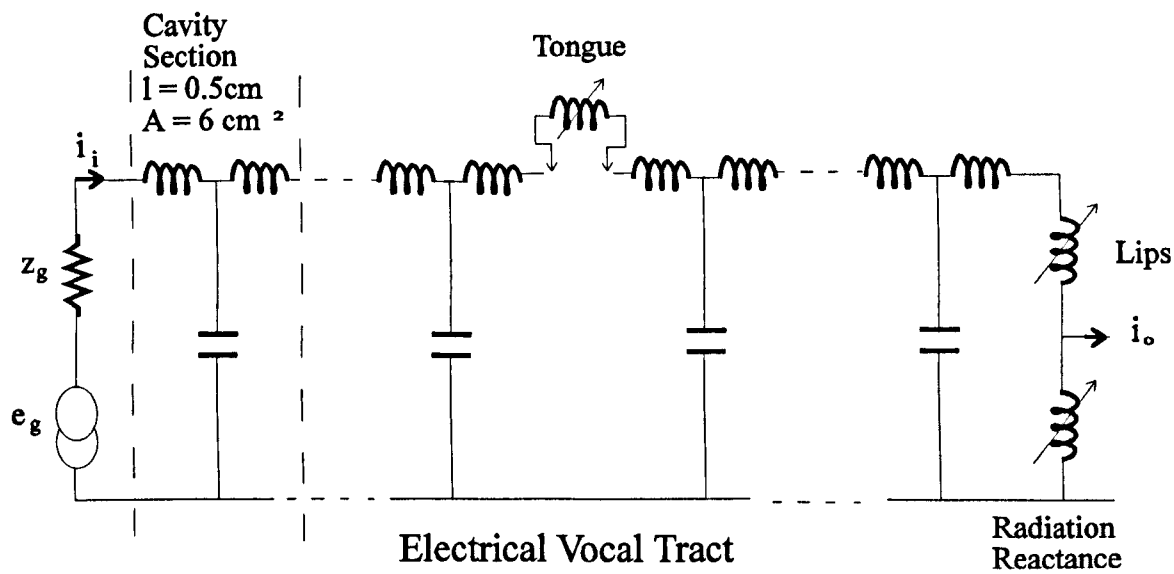

Electrical Vocal Tract

The principal advantage of this cylindrical model is that the acoustical masses and compliancies are uniformly distributed throughout each uniform cylindrical section leading to a more accurate resonant frequency value and the occurrence of additional resonances due to reflections at the points of impedance change in the tract.

Figure 9 shows a single cylinder of length l and uniform area A. When a plane acoustic wave passes through it is analogous to an electrical transmission line (26). The distributed acoustic elements of mass and compliance are analogous to the electrical resistance, inductance and capacitance and can be represented as a T impedance network as shown in Figure 9. The characteristic impedance of the transmission line Z_0 and propagation constant Γ are related to the circuit elements, inductance L, capacitance C, resistance R, admittance G, distributed per unit length, by the following equations (5,26).

$$Z_1 = Z_0 \tanh(\Gamma l/2) \qquad (2.3)$$

$$Z_2 = Z_0 \operatorname{csch} \Gamma l \qquad (2.4)$$

$$Z_0 = \sqrt{\{(R + jwL)/(G + jwC)\}} \qquad (2.5)$$

$$\Gamma = \sqrt{\{(R + jwL)(G + jwC)\}} \qquad (2.6)$$

The inductance L and capacitance C per unit length of the acoustic transmission line are

$$L = \delta/A \qquad (2.7)$$

$$C = A/\delta c^2 \qquad (2.8)$$

where c = sound velocity, δ = density of air, $w = 2\pi f$.

Assuming that the losses due to R and 1/G are small then the resonant frequencies of the system are determined by the L and C elements and the resonant bandwidths by R and G.

The Electrical Vocal Tract, EVT, as shown in Figure 9 has been constructed (5,6,26,28) based upon the transmission line, acoustic cylinder analogy. The EVT component values are calculated by subdividing X-Ray images of the vocal tract during vowel production into cavity sections of 0.5cm length and estimating the cavity area. The glottal sound source is modelled using a current source e_g, with a slope of -12dB/decade driving the transmission line through a

high impedance z_g of approximately 22kΩ . Correlation between subject and EVT values(5) are displayed graphically in Fig 10.

Fig 10: Subject/EVT Vowel Formants

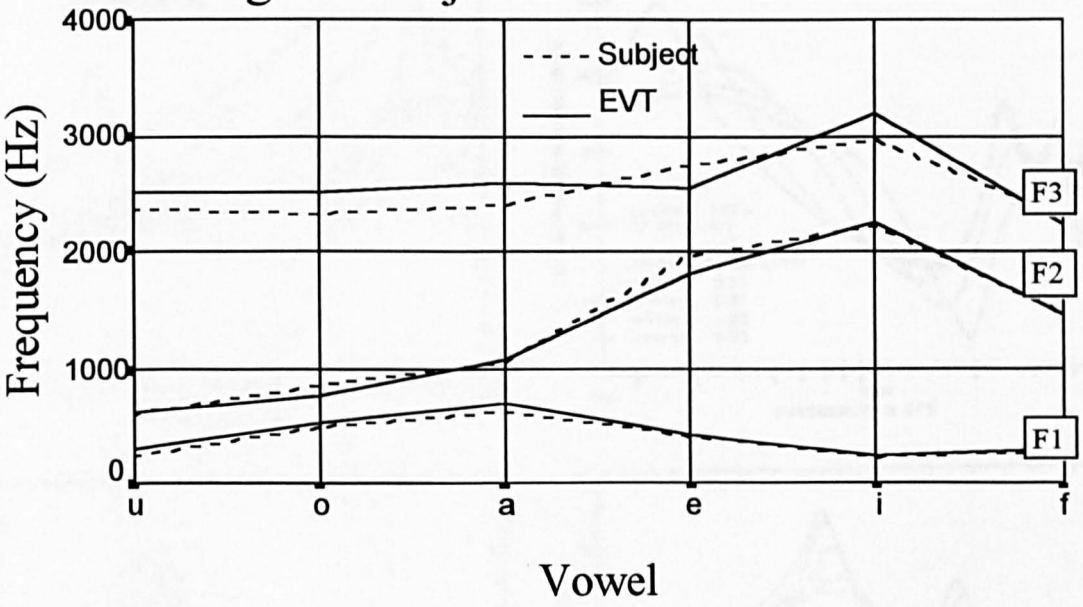

Spearman correlation coefficients at a significance level of 0.05 are, first formant F1 > 0.99, second formant F2 > 0.99 and third formant F3 > 0.84. Application of this model (5, 26) using various vocal tract dimensions have led to the following generalisations.

- The uncoupled resonant frequencies of the oral and pharyngeal cavities lie between F1 and F2, the coupled formant frequencies.
- F1 and F2 never coincide nor do they have an F1-pharyngeal cavity, F2-oral cavity affiliation as the Helmholtz resonator suggests.
- If F1 and F2 are well separated than it is possible to say that F1 is dependent upon one cavity and F2 is dependant upon on another cavity otherwise they are inter dependant to varying degrees.
- F3 usually originates from the longest cavity.

Spectral plots of the frequency amplitude relationship using the EVT(28) are shown in Fig 11.

Fig 11: Relative Acoustic Output Amplitude/Frequency Spectrum of the EVT for Several Vowels with Varying Degrees of Nasal Coupling

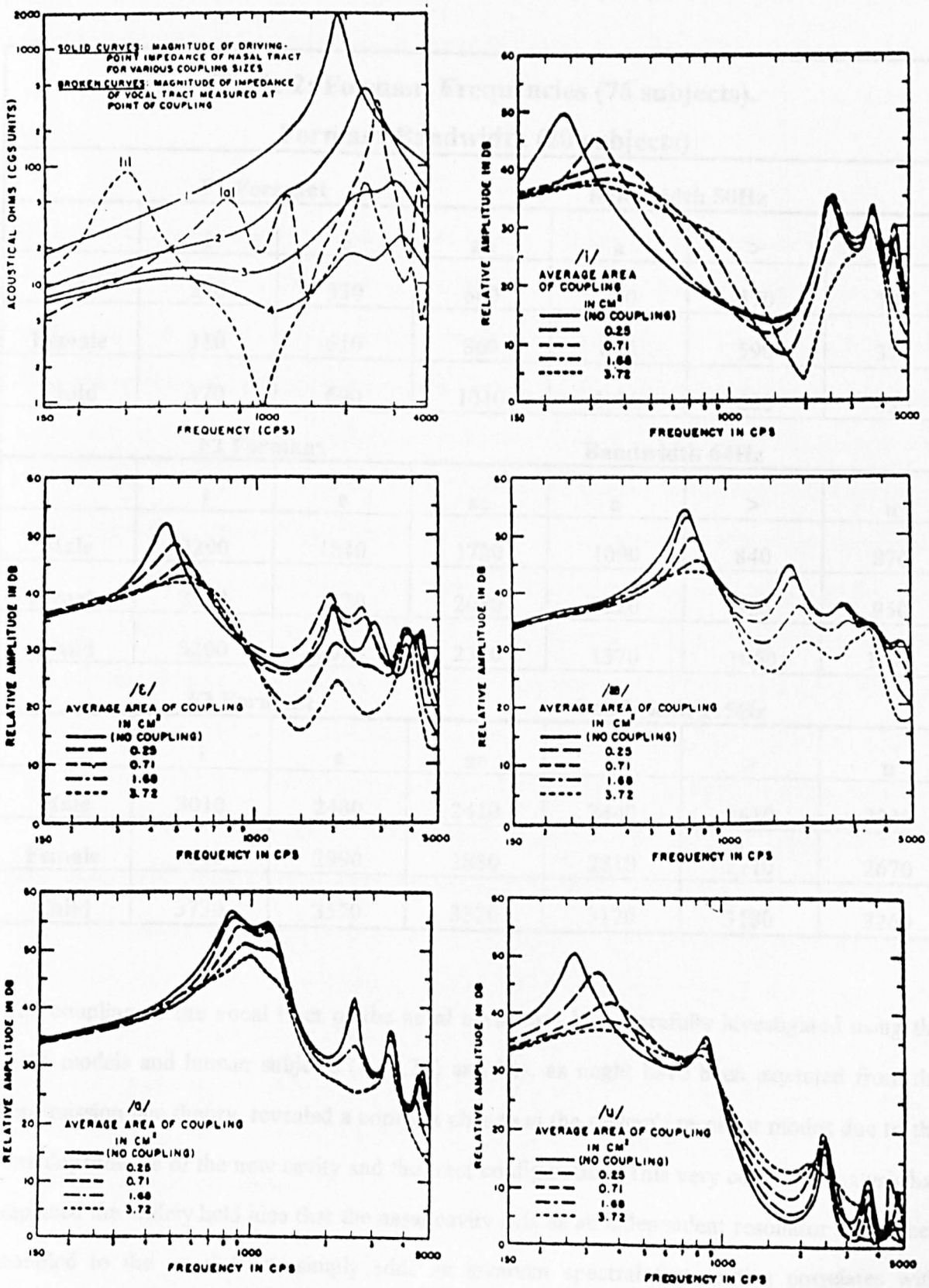

Formant frequencies measured from 76 subjects(43) and formant bandwidths measured from 20 subjects(54) are given in Table 2.

Table 2: Formant Frequencies (76 subjects).
Formant Bandwidth (20 subjects)

F1 Formant				**Bandwidth 50Hz**		
	i	**e**	**ae**	**a**	**>**	**u**
Male	270	530	660	730	570	300
Female	310	610	860	850	590	370
Child	370	690	1010	1030	680	430
F2 Formant				**Bandwidth 64Hz**		
	i	**e**	**ae**	**a**	**>**	**u**
Male	2290	1840	1720	1090	840	870
Female	2790	2330	2050	1220	920	950
Child	3200	2610	2320	1370	1060	1170
F3 Formant				**Bandwidth 115Hz**		
	i	**e**	**ae**	**a**	**>**	**u**
Male	3010	2480	2410	2440	2410	2240
Female	3310	2990	2850	2810	2710	2670
Child	3730	3570	3320	3170	3180	3260

The coupling to the vocal tract of the nasal cavity has been carefully investigated using the EVT models and human subjects (5,22,28) and has, as might have been expected from the transmission line theory, revealed a complex change in the system's resonant modes due to the interdependence of the new cavity and the tract configuration. This very complete analysis has replaced the widely held idea that the nasal cavity acts as an independent resonator that, when coupled to the vocal tract, simply adds an invariant spectral feature that correlates with perceived nasalisation. The distribution of acoustic energy between the nasal and oral cavities

is a function of the impedance of the pharyngeal oral cavity configuration and the degree of coupling to the nasal cavity. The former is highly dependant on the position of the articulators. Therefore the effect of the *same* degree of nasal coupling on a high vowel such as *i* where the tongue takes up a superior posture compared to a low vowel such as *a* will be markedly different.

Figure 11 shows the relative acoustic output amplitude frequency spectrum for several vowels with varying degrees of nasal coupling. All the vowels show a shift upwards in frequency of the first formant, reduction in formant amplitudes and a widening of formant bandwidth with increased coupling. The damping properties of the nasal tract which are due to its convoluted shape forming a large surface area accounts for the common features of amplitude reduction and widening bandwidth. The upward shift of formant frequency with degree of coupling can be accounted for by the relative difference in the acoustical impedance at the input to the nasal cavity as seen from the vocal tract. As the relative magnitude of the nasal tract load decreases with respect to the vocal tract source impedance so the nasal cavity starts to look more like a short circuit and has a more marked effect on the output compared to the case when the nasal impedance is relatively higher. The graphs of acoustic impedance against frequency with the EVT configured as the vowels *i* and *a* compared with 4 degrees of nasal coupling show that, in the region of the first formant, the difference between the EVT and nasal impedance for the high vowel is considerably greater than for the low vowel.

As a result, the first formant frequency shift due to nasal coupling in the case of the high vowel is markedly greater than the low vowel. The effect of differential acoustic impedance is also demonstrated by comparison of the amplitude frequency graphs for the high vowels *i,u* to, the low tongue position and therefore lower impedance vowels *ae,a* and also the mid tongue position forming the inbetween impedance of the vowel. Appendix 1 gives a list of vowel symbols and associated sounds.

2.2 Initial Study

In order that the principals on which an instrument designed to measure hyper- and hypo-nasality might be based could be tested an initial study (55) was instigated. It was proposed that the study have the following aims.

- To test the principal, that a simple index of hyper-nasality based on a ratiometric measurement of radiated sound pressure from the nasal cavity with respect to the oral cavity correlates with perceived hyper-nasality.
- To measure the index of nasality for a normal group and hyper-nasal group.
- To establish the acoustic frequency bandwidth of the measurement that produced any significant results.
- To test the reliability of the rating of perceived hyper-nasality amongst a group of trained observers.
- To test the effective acoustic isolation of the device used to separate and isolate the oral and nasal radiated pressures.
- To test the response of the microphones in free field conditions over the measurement bandwidth.

The test equipment used in the initial study comprised of a Spectral Dynamics SD345 Spectrascope III, two Sennheiser high quality omnidirectional microphones type MKE 2R, a Bruel and Kjaer sound level meter Type 2230, a KEF high fidelity loudspeaker Type 101, a Khron-Hite signal generator Type 2400 and a Toshiba audio stereo cassette deck Type D10. Specifications for these test instruments are given in Appendix 2.

2.2.1 Microphone response

The initial test arrangement for the measurement of the two Sennheiser microphones is shown in Figure 12. The Khron-Hite signal generator output or the analog tape recorder are impedance matched with the KEF loudspeaker using the driver circuit shown which also

incorporates a threshold level detector to trigger the spectrum analyzer to begin measurements. The sound pressure at the inputs to the microphones were monitored with the sound level meter and set initially to 70dB(A) at 1KHz.

Fig 12: Microphones Response Test

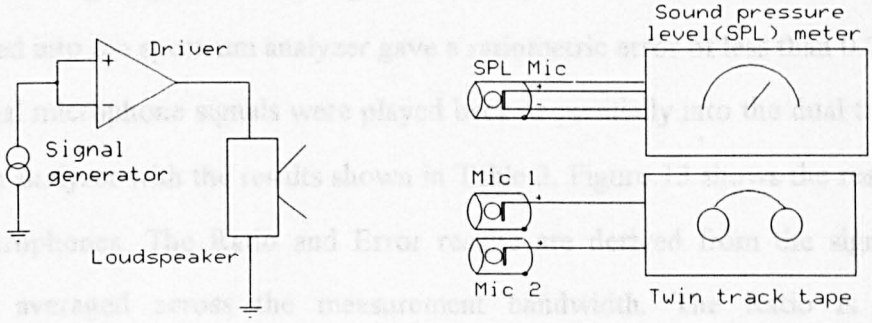

Microphones signal recording

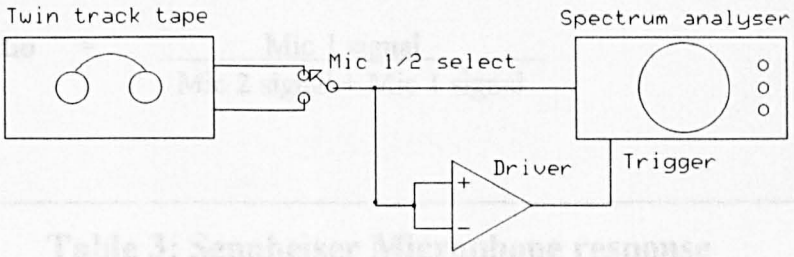

Microphone signal playback

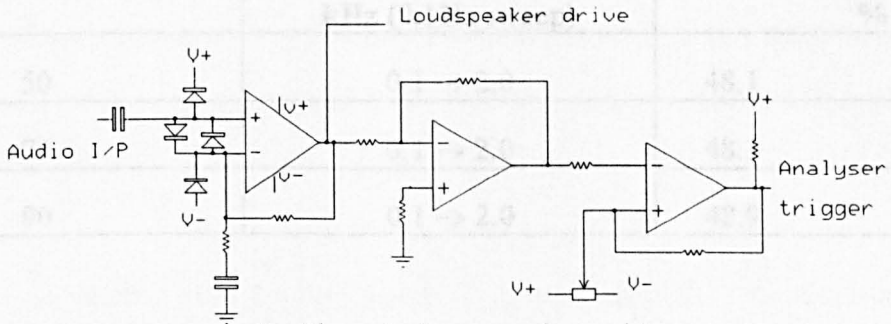

Audio driver circuit

The ratiometric measurement technique envisaged for the clinical instrument precluded the need for absolute measurements of sound pressure; however, the expression of the microphones' response as a ratio of one with respect to the other, required that the testing be

done simultaneously. Therefore, the microphones and sound level meter were mounted in a custom designed jig to ensure that the plane of each device was orthogonal to and equidistant from the loudspeaker and, shaped so as to minimise acoustic reflection. The outputs from the Sennheiser microphones were recorded on twin channel analogue tape; the channel gains of the recorder had been set by the introduction of an identical swept frequency tone into each channel from the signal generator. The gains were adjusted such that the resultant test signals when replayed into the spectrum analyzer gave a ratiometric error of less than 0.25%.

The individual microphone signals were played back sequentially into the dual trace facility of the spectrum analyzer with the results shown in Table 3. Figure 13 shows the results from two pairs of microphones. The Ratio and Error results are derived from the signal from each microphone averaged across the measurement bandwidth. The Ratio is the ratio of microphone signals as shown.

$$\text{Ratio} = \frac{\text{Mic 1 signal}}{\text{Mic 2 signal} + \text{Mic 1 signal}}$$

Table 3: Sennheiser Microphone response

Nominal pressure dB(A)	Measurement Band kHz (0.1Hz sweep)	Ratio %	Error
50	0.1 → 2.0	48.1	1.9
70	0.1 → 2.0	48.3	1.7
90	0.1 → 2.0	48.9	1.1

A more detailed study of the microphones response to frequency modulation, amplitude modulation and angular dependency is shown in Chapter 3.

Fig 13: Signal Ratio vs Frequency

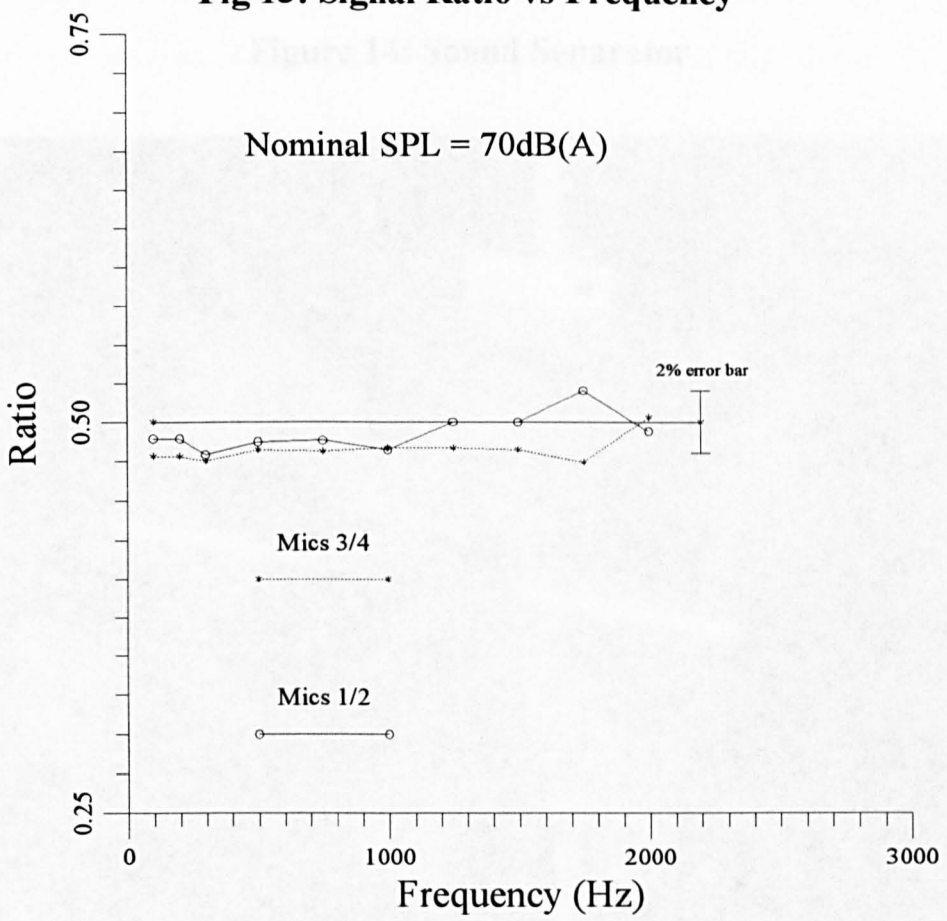

2.2.2 Oral and nasal sound separation device.

The measurement of the ratio of oral to nasal radiated sound pressure relies on the effective separation and isolation of the two radiated sound waves from the nares and oral cavity. Therefore a device known as a 'sound separator' was designed and tested according to the following principals.

- Acoustic outputs from the oral and nasal cavity should have an effective isolation of the order of 20dB to minimise errors due to cross coupling of the signals to approximately 0.2%.
- The geometry of the device should enable repeatable patient alignment and the effect of movement should be assessed.
- The device should not interfere with articulation.

Figure 14: Sound Separator

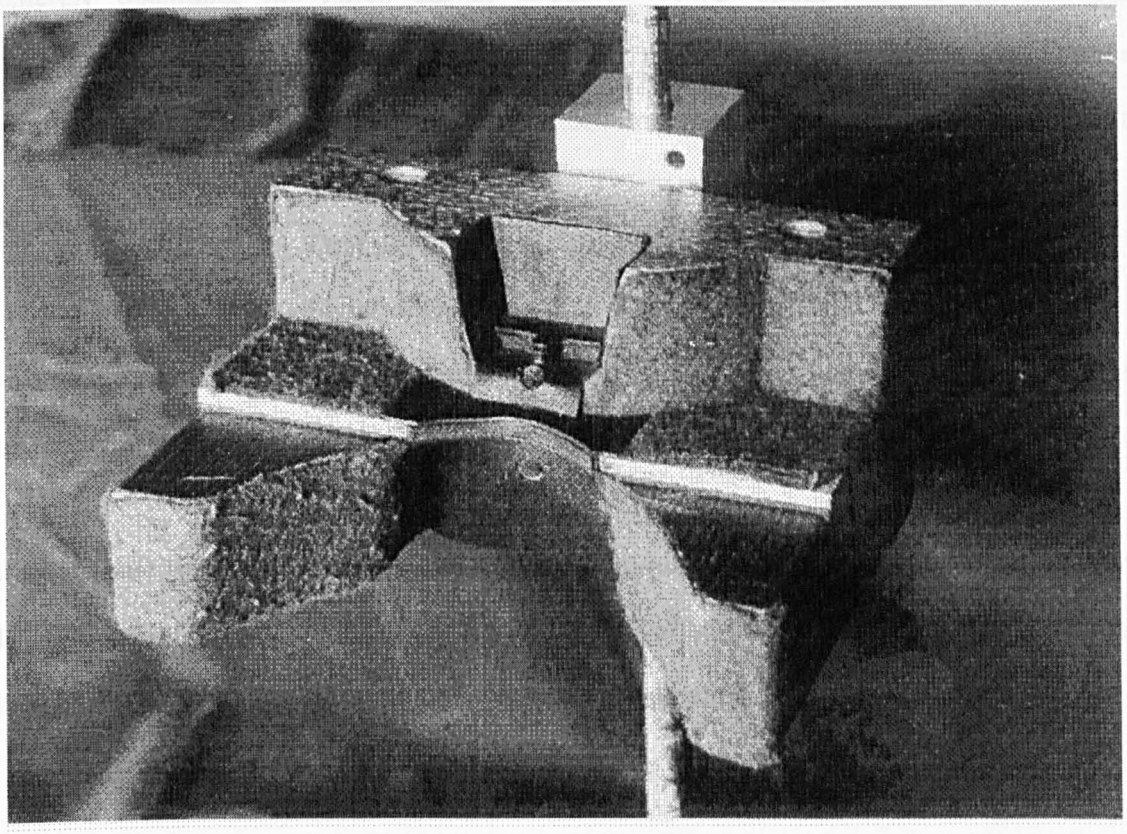

The sound separator shown in Figure 14 was fabricated in wood covered in felt and rubber.

The geometrical design was such that, with the patient aligned by placing the upper lip against the 'lip ledge' and the inferior surface of the nasal septum resting on the 'nose ledge', then the microphones were equidistant from the nares and lips. The contour of the 'lip ledge' was estimated from measurements of the upper lip margin of several children in the age range 8 to 15 years. The nasal and oral sections were specifically shaped for maximum sound dispersion and covered in thin rubber sheet to enable hygienic swabbing. The sound separator was attached to a bench stand via easily adjustable clamps so that height and angle of the device could be tailored to each patient.

Isolation between the microphones was assessed by using a human subject as a source of sound. The oral acoustic signal cross coupling into the nasal microphone was tested by completely occluding the nares during sustained vowel phonations of normal speech intensities. Similarly the nasal acoustic signal cross coupling into the oral microphone was tested during sustained phonation of the nasal consonant *m*, where the lip opening is firmly shut. Results were as follows.

Oral to Nasal isolation: Typically 16dB.

Nasal to Oral isolation: Typically 15dB.

This 'leakage error' introduced to microphone signals of equal intensity produces a ratiometric error of 0.6%.

The errors due to misalignment of the patient or movement during the measurement period were assessed by introducing head movement in the vertical and horizontal plane as shown in Figure 15 during sustained phonation of the nasal consonant *n* .

Figure 15: Patient Misalignment

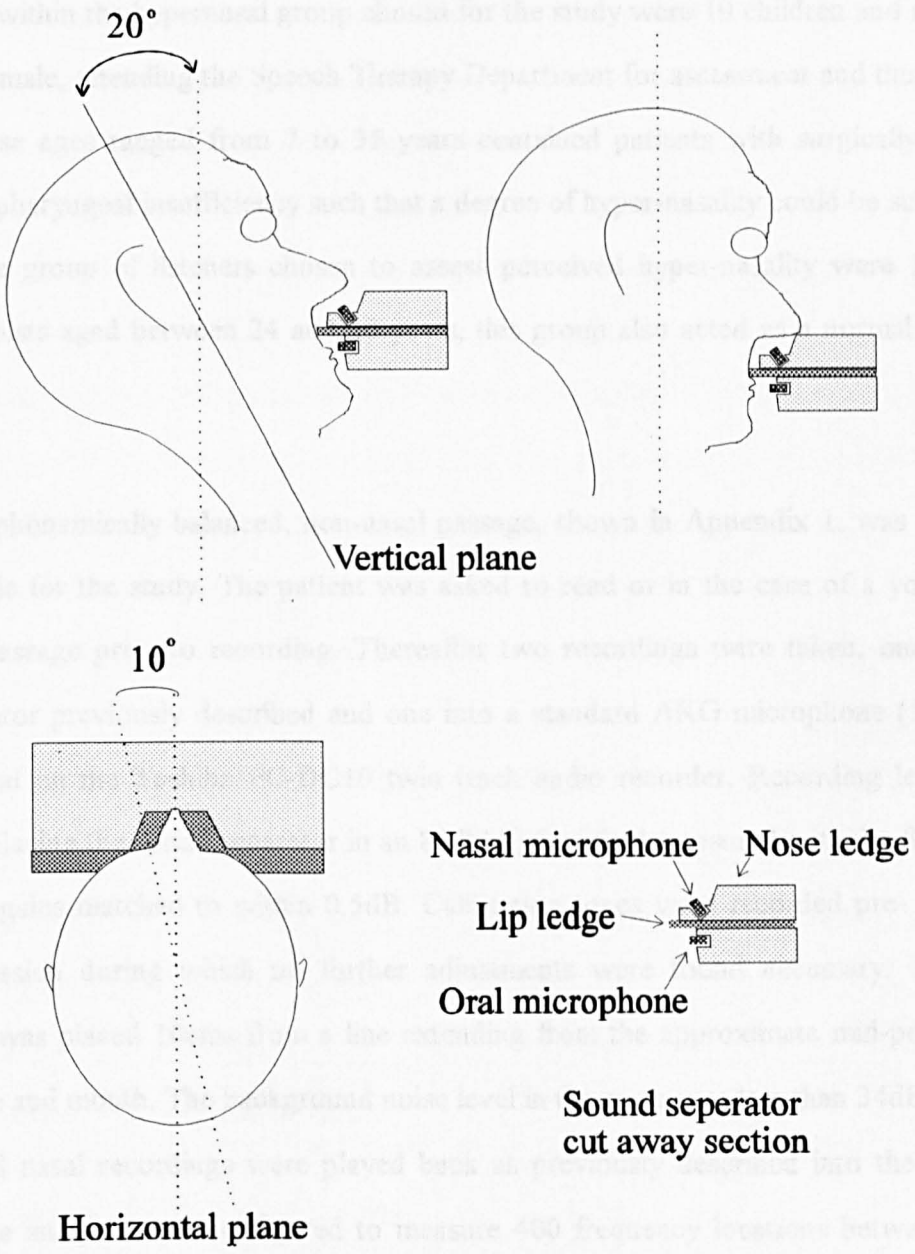

The recorded oral and nasal signals were averaged by the spectrum analyzer over the measurement periods and the oral:nasal ratio compared. Results were as follows.

Maximum ratiometric signal change: 20° Vertical displacement: 15%

10° Horizontal movement: 5%

A further study of the clinical version of the sound separator is given in Chapter 3.

2.2.3 Clinical study.

The subjects within the hypernasal group chosen for the study were 19 children and adults, 10 male and 9 female, attending the Speech Therapy Department for assessment and therapy. The subjects whose ages ranged from 7 to 35 years contained patients with surgically repaired clefts or velopharyngeal insufficiency such that a degree of hyper-nasality could be subjectively detected. The group of listeners chosen to assess perceived hyper-nasality were 10 female speech therapists aged between 24 and 40 years, this group also acted as a normal group of speakers.

A 70 word, phonemically balanced, non-nasal passage, shown in Appendix 1, was used as a speech sample for the study. The patient was asked to read or in the case of a young child repeat this passage prior to recording. Thereafter two recordings were taken, one into the sound separator previously described and one into a standard AKG microphone (56) , both were recorded on the Toshiba PC-DC10 twin track audio recorder. Recording levels were adjusted by placing the sound separator in an 80db(A) free field measured with the SPL Meter and channel gains matched to within 0.5dB. Calibration tones were recorded pre- and post-recording session during which no further adjustments were found necessary. The AKG microphone was placed 10cms from a line extending from the approximate mid-point of the subjects nose and mouth. The background noise level in the room was less than 34dB(A).

The oral and nasal recordings were played back as previously described into the spectrum analyzer. The analyzer was configured to measure 400 frequency locations between 200Hz and 1200Hz, each set of measurements were summed to give an RMS value of the intensity level and 128 sets were averaged to give a final figure. The average value for each signal was expressed as a ratio, normalised (100%) to the highest ratio as follows.

$$\text{Ratio (\%)} = \frac{\text{nasal signal}}{\text{nasal signal} + \text{oral signal}} \qquad (2.9)$$

The standard microphone recordings were replayed as a set of 25 subjects, 6 of which were retests with at least 10 samples between test and retest. The first set of subjects were not scored by the 10 listeners. The listeners were then instructed to score the degree of hyper-nasality present on a scale of 0 to 100% where 0% denoted no detectable hyper-nasality. The worst hyper-nasal case, as judged by an experienced speech therapist, was then played to the listeners and assigned 100% followed immediately by the complete set of recordings.

Pearson(absolute scores) and Spearman(rank order) correlation coefficients were used as a test of bivariate correlation between, oral:nasal ratio (measured using the sound separator) and the hyper-nasality scores (assigned by the speech therapists), and also the speech therapists test/retest scores. Results are shown in Table 4 and in Figure 16. A two tailed test of significance(p) was applied to test the null hypothesis which in all cases was rejected.

Table 4: Correlation Coefficients of Oral:Nasal signal ratio with Speech Therapists Assessment

Speech Therapist	Signal ratio	Correlation Coeff'	Significance (p)
Mean of scores	Measured ratio	0.78	<0.001
Rank of means	Rank of ratios	0.76	<0.001
Mean of ranks	Rank of ratios	0.67	<0.001
Sp Th test mean	Sp Th retest mean	0.90	<0.001

The mean of the scores from all therapists for all subjects was 48.5 with a standard deviation of 10.5. The correlation between speech therapists assessment of hyper-nasality and the oral:nasal ratio is consistently high which implies that this measurement method has potential as an index of hyper-nasality. The test-retest correlation tends to suggest that therapists are quite consistent in their judgement of this speech impairment. However it must be acknowledged that the statistical analysis shows a high *correlation* between assessment

methods which only implies that the trend or ranking of the scores is in agreement. Comparison of the absolute scoring between therapists and oral:nasal ratio shows good correlation but has a wide *variation* as can be seen in Figure 16 and the large standard deviation.

Fig 16: Correlation of Oral:Nasal Signal Ratio with Perceived Nasality

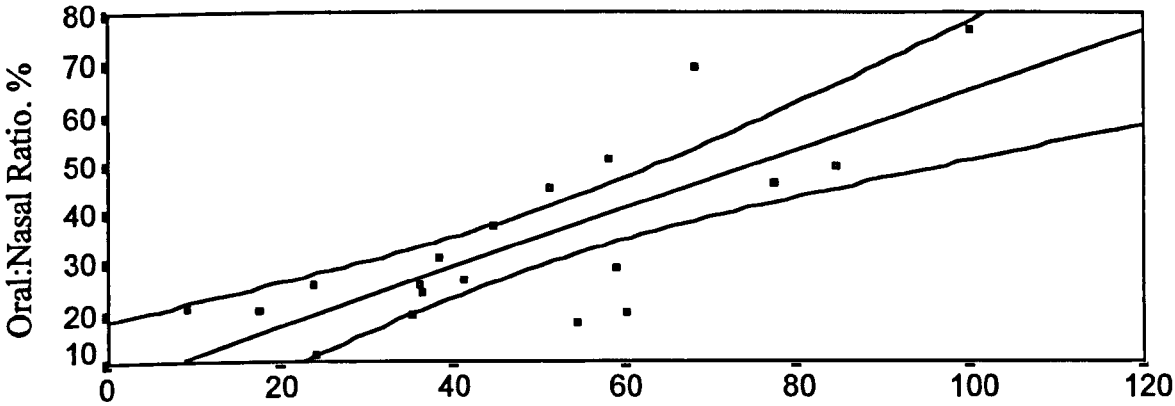

Linear regession shown with 95% confidence levels.

The conclusion of the initial study is therefore that the oral:nasal ratio as given in equation 2.9 may form a useful relative index of hyper-nasality but was unlikely to give an absolute measurement. Based upon this initial study and further data given in this chapter a specification for a clinical instrument called a Nasal Resonometer was written.

2.3 Initial Instrument Specification

- The instrument must separate the oral and nasal sounds emerging from their respective cavities during normal speech without impeding phonation. The effective isolation between the sounds must be greater than 15dB.
- The instrument must continuously measure the sound wave radiating from the nares and oral cavity and display in real time a graphical representation of the oral:nasal ratio.
- Overall measurement bandwidth: 100Hz - 5kHz;

  First formant measurement bandwidth: 100Hz - 1200Hz.
- The instrument must be capable of discriminating hyper- or hypo- nasality in the presence of other normal and abnormal speech sounds.
- The instrument must produce figures for average and peak ratios during the measurement period.
- The instrument must be capable of use in a bio-feedback mode whereby a clinician can on a single measurement, and on a treatment session basis:

  Set and monitor an 'oral:nasal ratio target to be achieved'.

  Monitor the success rate of the patient in achieving the set targets.

  Monitor the trend of the measurement averages.
- The oral and nasal sounds should be available to the clinician to monitor via a switchable volume controlled loudspeaker output.
- The instrument must provide outputs and inputs, of the oral and nasal sounds, to and from any standard stereo audio cassette recorder.
- The instrument must be, compact, portable and easy to use. On-line help and hard copy of results must be available.

Chapter 3

Nasal Resonometer. Design, Testing and Results

3.1 Instrument Design

The principal components of the instrument, designed to meet the requirements of the initial specification described in Chapter 2, are shown in block diagram in Figure 17.

Figure 17: Instrument Block Diagram

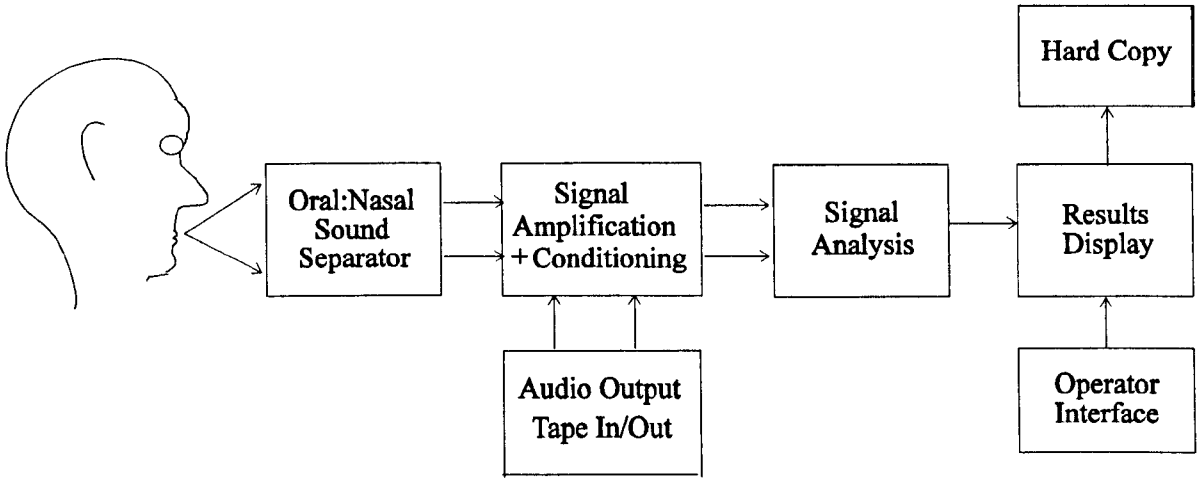

3.1.1 Sound separator design

The principal of the sound separator remained as in the initial study. The nasal and oral sound pressures are continuously monitored by two miniature, omnidirectional, electret transducer microphones mounted within the body of the sound separator. The design of the original device has been considerably simplified by eliminating the bulk of material below the lip shelf in the lower oral section and removing the recess for the nasal microphone. Two side members have been added to the lower section to improve acoustic isolation between the upper and lower sections. In order that the various contours of individual upper lip margins can be accomodated, a slim bag of soft wax material has been added to the lip shelf. The soft

wax moulds itself to the shape of the patient's upper lip area and forms an effective acoustic seal and a comfortable cushion. A photograph of the clinical version of the sound separator is shown in Figure 18.

Figure 18: The Clinical Sound Separator.

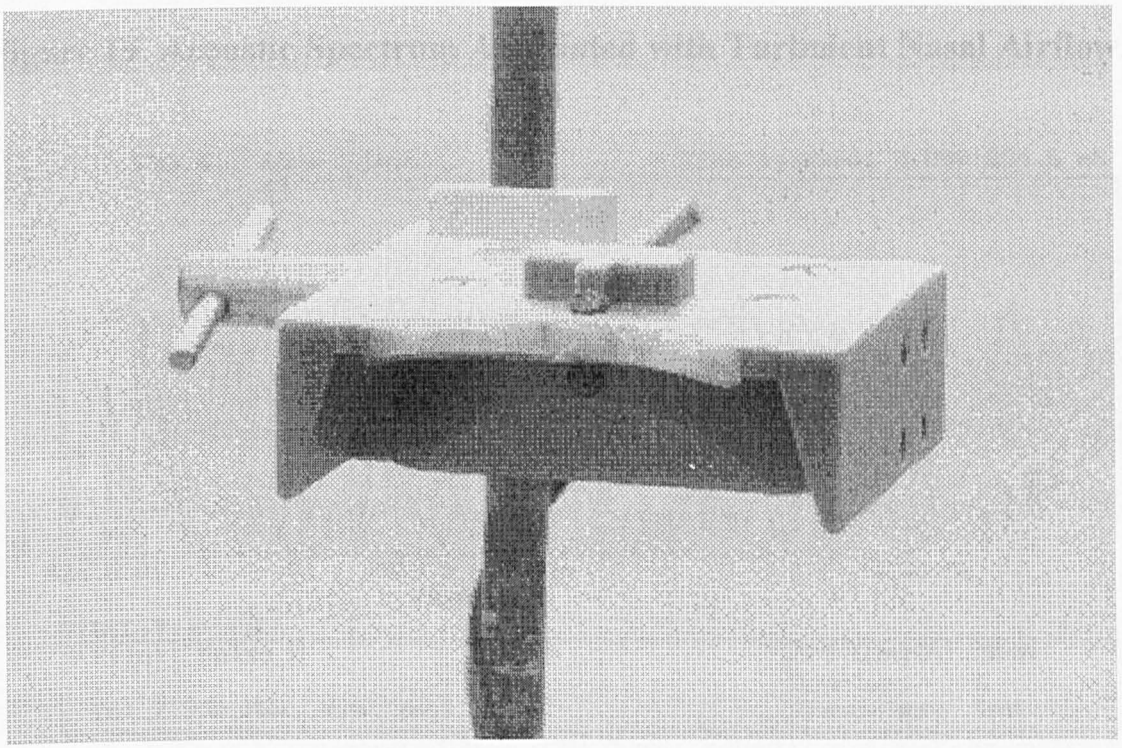

3.1.2 Signal conditioning and hardware implementation.

The measurement index is based upon the ratio of the nasal to oral sound pressures present during the phonation of various vowel or other appropriate test sounds; the clinical phonatory test material will be described in Chapter 4. The results of the initial study, based on the use of a spectrum analyser operating over a relatively broad band, have shown an encouraging correlation with subjective measurements. These results however are inevitably prone to error due to noise in the signal which arises from uncontrolled phonatory effects that occur as a result of the presence of a cleft palate or impaired velar function. As previously described, the uncontrolled presence of nasal air flow due to emmission is principally responsible for the difficulty that both, speech therapists assessing abnormal nasality and, any instrument designed

to detect hyper- or hypo-nasality, has in forming a reliable measurement index. The effect of turbulent air flow on a microphone is to introduce a broadband signal formed of randomly changing spectral peaks that produce an effect that acoustic engineers term 'wind-rush' or 'popping'. Figure 19 shows the acoustic spectrum from the nasal microphone of the sound separator in the presence of turbulent nasal air flow.

Figure 19. Acoustic Spectrum Associated with Turbulent Nasal Airflow.

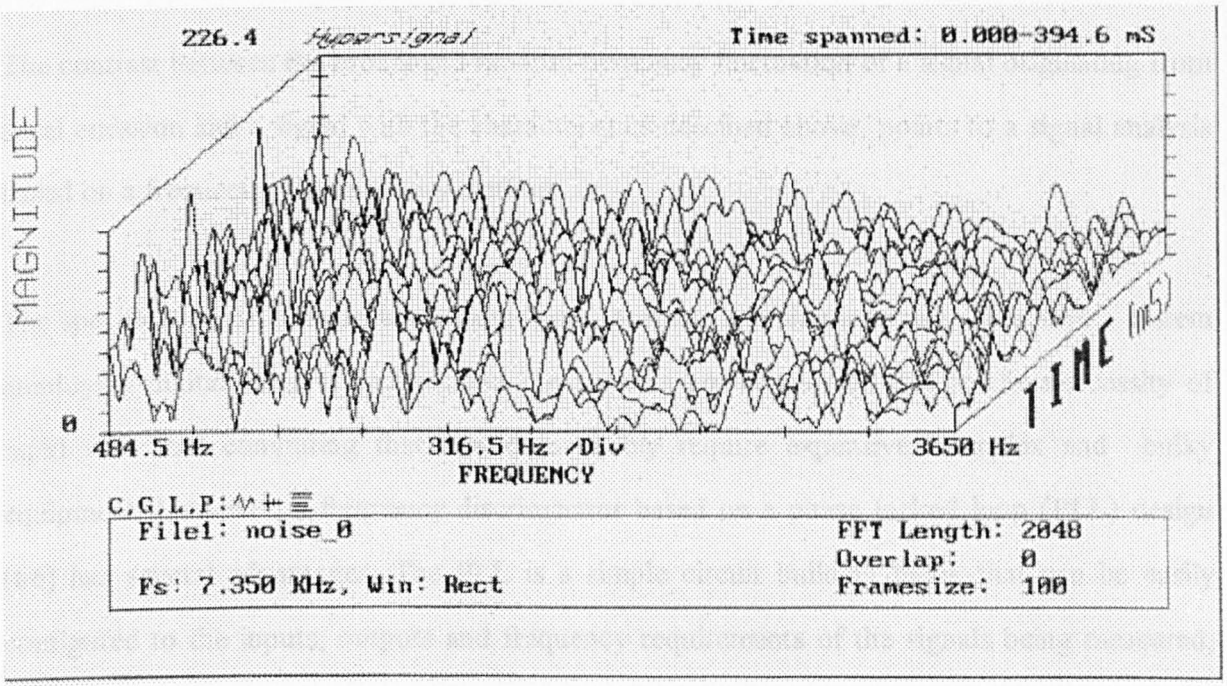

The likely presence of this broadband noise during measurements taken from patients and, the widespread frequency locations of the first formants of the vowel sounds in the audio spectrum requires a signal analyis method that is capable of firstly, rejecting broadband signals as noise and secondly, locking onto and measuring steady or slowly varying narrow band signals. The data from Table 2 and the graphs of Figure 11 can be summarised for the vowel first formants as follows.

First formants occur in the range: 110Hz to 1100Hz

Typical formant bandwidth: 50Hz

Typical formant frequency shift due to varying degrees of nasal coupling: 300Hz

The rate at which the formant frequency shifts, is associated with the rapidity with which the velum position changes, thereby dynamically altering the degree of nasal coupling. X-Ray studies of the movement and timing of the velum (48,60,68) in both normals and patients, which are described extensively in the second half of this thesis, can be summarised as follows.

Normal velar closure/opening time: 100ms to 160ms
Impaired velar closure/opening time: 100ms to 350ms

The contrast between the broadband random frequency fluctuation of a signal originating from nasal emission and a signal with the characteristics descibed above points to a signal analysis based on a frequency disciminatory method.

The specification calls for an instrument that is portable and simple to use. Therefore a system employing digital spectral analysis and display was not considered due to the neccessity of rapid real time computing that would inevitably require expensive, complex and bulky equipment. However, a frequency discriminator based on a phase locked loop (PLL) design (66) has several advantages. The PLL is a simple circuit building block that can be easily configured to the inputs, outputs and frequency requirements of the signals being measured, the components are readily available, cheap and easily incorporated onto standard circuit layouts.

The PLL is composed of three main elements, a phase detector which is essentially a multiplier, a low pass filter and a voltage controlled oscillator, as shown in Figure 20. All three elements are connected together in a closed loop. The phase detector compares the phase of the input signal to that of the voltage controlled oscillator (VCO). The output of the phase detector is therefore proportional to the phase difference of its two inputs. This output is low pass filtered to eliminate high frequency components and the resultant signal is used to control the VCO.

Fig 20: Basic Phase Lock Loop(PLL)

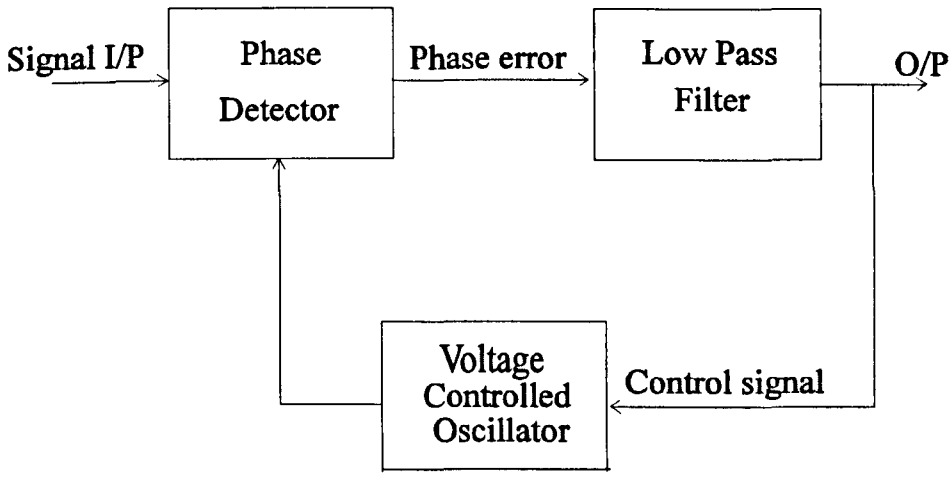

The control voltage applied to the VCO changes the oscillator's frequency in a direction that reduces the phase difference between the signal input to the phase detector and the oscillator. In this way, a signal containing predominately one frequency will be locked on to by the PLL and the control signal will tend towards a DC value. In the case of an audio signal containing randomly fluctuating spectral peaks, the PLL is often out of lock and searching for a frequency on to which it may lock. If the low pass filter has a short time constant, this operation of searching is fast, so that the PLL spends brief periods locked to the various components of the input signal. The control signal can therefore be used in the instrument as an indication of the lock quality.

Good lock quality would tend towards a DC or slowly changing value due to the presence of a predominant first formant frequency. In contrast, poor lock quality, due to the presence of an uncontrolled air flow originating from nasal emmision, would be a rapidly changing value. The discrimination between lock qualities can be made by digitising the control signal and continuously inputting the results into a simple microprocessor. An appropriate algorithm, contained in the microprocessor's software, can therefore decide, based on the absence of emmisive noise and the presence of a signal of known characteristic, when to commence a

real time measurement of the oral:nasal ratio. The schematic of the measurement principal is shown in Figure 21.

Fig 21: Measurement Principal: Schematic

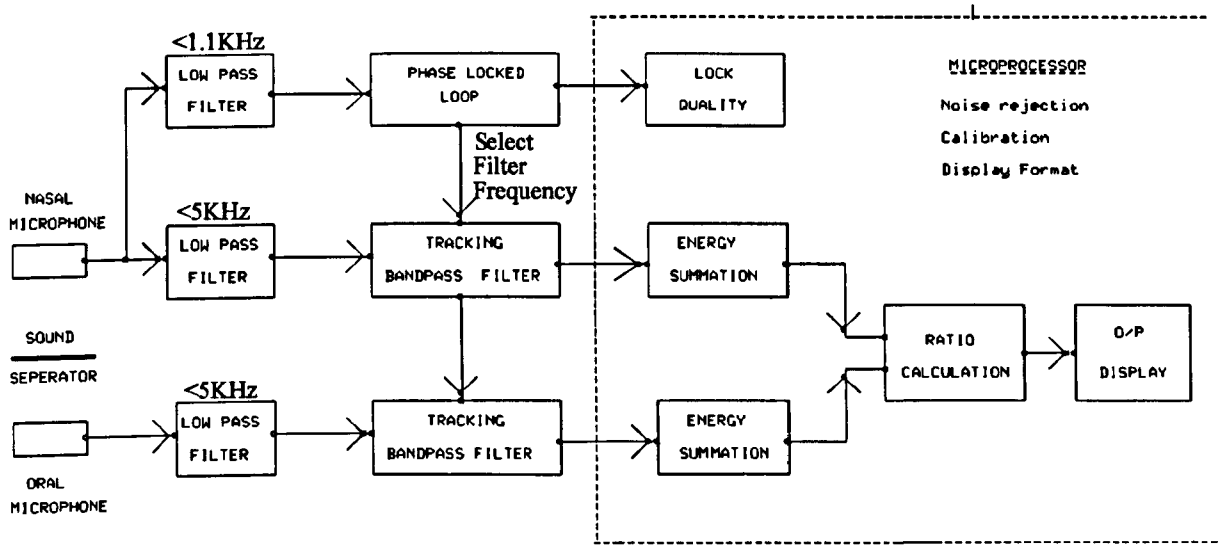

A further refinement to the reduction of noise present in the measurement is to employ a narrow band signal sampling technique. In contrast to measuring broadband, the VCO frequency, suitably divided down, can be used to drive the centre frequency of a tracking narrow bandpass filter to the centre of the measured signal hence narrowing the measurement bandwidth and improving the signal to noise ratio . In this manner, formants with widely differing frequencies originating from various phonations can be selectively detected, locked on to and filtered by the measuring system. In addition, the shift in a formant frequency due to the presence of hyper-nasality will also be tracked by the bandpass filters. In this instance the relatively slow change in frequency is discriminated positively by the algorithm as a noise free signal and the measurement commenced. The s/n ratio that the instrument would encounter during clinical use was estimated to be of the order of 0dB based on the assumption that, perceptually the acoustic signal due to nasal emmission was of a similar magnitude to the speech signal. The process of discrimination is called phase lock detection and the microprocessor is acting as the lock detector (67).

3.1.2.1 Phase Lock Loop design.

The principal of phase locking is simply, to detect a *phase difference* between a signal and oscillator and thereby adjust the oscillator *frequency.* It would appear that this loop could simply be closed, as in the case of operational amplifier feedback, with some gain. However, in a PLL there is an integration that occurs within the loop: *phase* is detected and *frequency* is adjusted. This introduces a 90^0 phase shift into the loop and therefore any further shift, resulting in a 180^0 phase difference at unity gain, will result in loop oscillations. To avoid this instability a second order loop design was chosen, using passive low-pass filtering within the feed-back loop and a type II phase detector. This type of loop also produces a `flywheel effect' due to the type II phase detector producing no output (actually very high impedance) at phase lock and therefore the voltage held on the filter capacitor will continue to instruct the VCO to maintain the same output frequency. The type II phase detector is an edge sensitive device, producing positive or negative pulses of varying width depending on the phase relationship of the signal and oscillator; this detection method is therefore not dependant on the signal duty cycle. In addition, this type of detector instructs the VCO to produce minimum frequency during loss of lock which can be unambiguously discriminated by the lock detector.

Another important consideration when choosing to use a second order loop design was the opportunity to tailor the response time and the stability (damping) time of the loop. In this application, the ability of the instrument to delineate noise from signal is based upon the lock detector discriminating between the loop's characteristic response to the occurrence of these different situations. Figure 22 shows the PLL in more detail and the Bode plots of the PLL, VCO and low pass filter. The stability of the loop requires that a good phase margin is maintained between 180° and the phase shift around the loop, at unity gain. The addition of R8 in series with C9 in the low pass filter adds a second zero to the PLL Bode plot at f1,

thereafter the loop gain rolls off at 6dB/octave in the region of unity gain and the loop is stable.

Fig 22: PLL Design

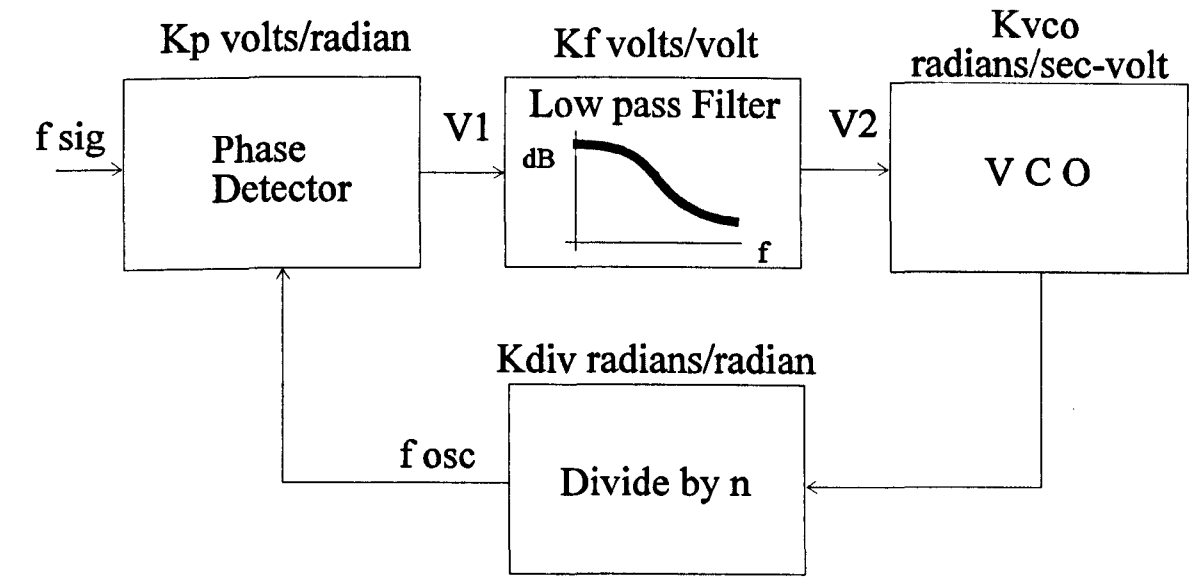

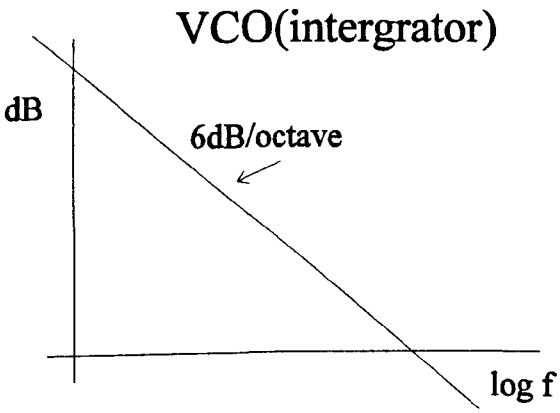

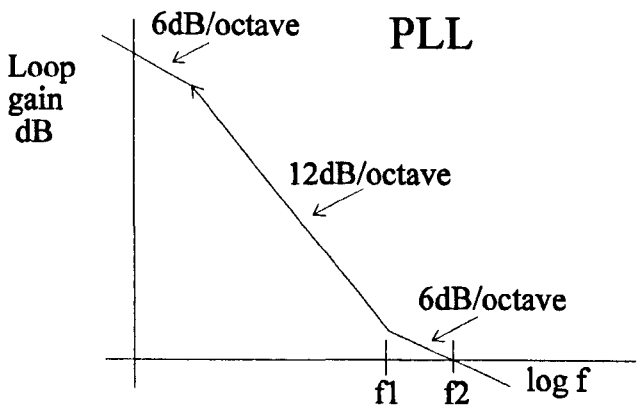

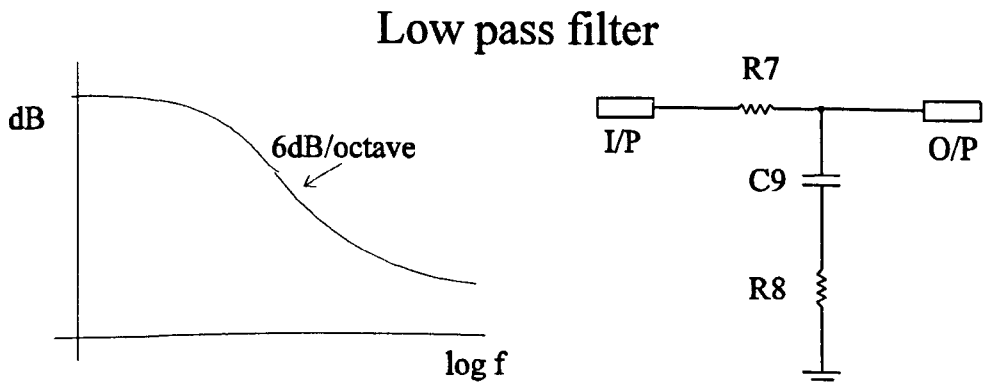

The properties of this `lead-lag' filter are derived from, the desired loop response to enable the delineation of signal from noise and, with reference to Figure 22, the loop equations shown below.

Device	**Function**	**Gain**	**Calculation**
Phase detector	$V1 = Kp.\ \Delta\phi$	Kp	$\Delta\phi$ = phase difference, f sig $\rightarrow$ f osc $Kp = 12\ V/2\pi = 1.91V/radian$
Low pass filter	$V2 = Kf.V1$	Kf	$Kf = \frac{1 + jwR8C9}{1+jw(R7C9+ R8C9)}$ volts/volt
VCO	$d\phi_{out}/dt = Kvco.\ V2$	Kvco	VCO range: 78kHz $\rightarrow$ 780kHz V2 range: 0 $\rightarrow$ 12 volts $58.5kHz/V=3.67 \times 10^5$ rds/sec-V
Divide by n	$\phi_{out} = (1/n)\ \phi_{in}$	Kdiv	Kdiv = 1/n = 1/1200 radians/radian

The overall loop gain can be written as,

$$\text{Loop gain} = Kp.Kf.(Kvco/jw).Kdiv \qquad (3.1)$$

The PLL chosen for the instrument was the Motorola 14046B. This CMOS device incorporates both the type II phase detector and VCO, the choice of the VCO maximum and minimum frequencies are set by the external components R3, R4 and C14 as shown in Figure 23. The type II phase detector has the disadvantage of being relatively noise prone compared to a type I, therefore in order that the input frequency range be limited to the signal range of interest and cut off thereafter sharply , a low pass filter based on the 4 pole Chebyshev design precedes the phase detector, as shown in Figure 24. The design figures were originally based on an input frequency range to the PLL of 65Hz to 650Hz and the instrument was tested accordingly. Subsequently, the range was expanded to incorporate the higher first formant frequencies present with young children and altered to an upper limit of 1100Hz.

The divide by n gain factor, Kdiv, was calculated by consideration of the desired input frequency range to the PLL, in conjunction with the requirement that the tracking bandpass filters would be driven from a signal derived from the PLL oscillator. The tracking bandpass filter, described later, was configured using switched capacitor filters that required a clocking frequency to signal frequency ratio of 100. A further refinement to the signal analysis was incorporated in the design of the tracking filters which enabled the microprocessor to switch their centre frequencies to 2x, 3x and 4x that of the first formant frequency to detect and measure the presence of harmonics. These considerations indicated a factor of 1/1200 for Kdiv.

The value of Kdiv and the PLL input frequency range therefore fix the VCO frequency range. The VCO gain factor, Kvco, is derived from the maximum VCO frequency range divided by the maximum control voltage V2 and was calculated as 3.67×10^5 radians/volt.

The phase detector gain factor, Kp, is derived by the maximum phase difference that the detector will encounter divided into the maximum output V1 and was calculated as 1.91 volts/radian.

The low pass filter gain factor, Kf, was calculated by consideration of the desired loop response. As shown previously, varying degrees of nasal coupling result in a typical formant frequency shift of 300Hz The most rapid movement of the velum measured in normal subjects is 100ms and therefore a rate of frequency shift of 5Hz was used as a criterion below which the signal would be considered noise free and measurements commenced. An arbitrary figure of 250Hz (f2 in Figure 22) was chosen as the frequency at which the loop reaches unity gain, a rate of frequency shift at this value seemed unlikely ever to occur. For an adequate phase margin, the low pass filter breakpoint (f1 in Figure 22) was therefore set at 50Hz thereby determining the low pass filter values of R7,R8,C9 in Figure 23 as,

$$R8C9 = 1/2\pi f1 \qquad (3.2)$$

The value of R7 in the low pass filter was therefore calculated using a loop gain of unity at a frequency of 250Hz.

The design of the PLL was completed as follows, referring to Figure 23.

The inputs to the phase detector Motorola 14046B, $IC13_{pins\ 14,3}$ result in a phase difference signal at pin 13, PC2 Out. This signal is low pass filtered by the lead lag arrangement of R7,R8,C9, buffered by $IC2_{pins\ 12,13,14}$ the output of which acts as the VCO control voltage input to $IC13_{pin\ 9}$. This control voltage, after attenuation by R5,R6 and buffering by $IC2_{pins\ 8,9,10,}$, provides the lock quality indication to the microprocessor.

Fig 23: Phase Lock Loop PCB

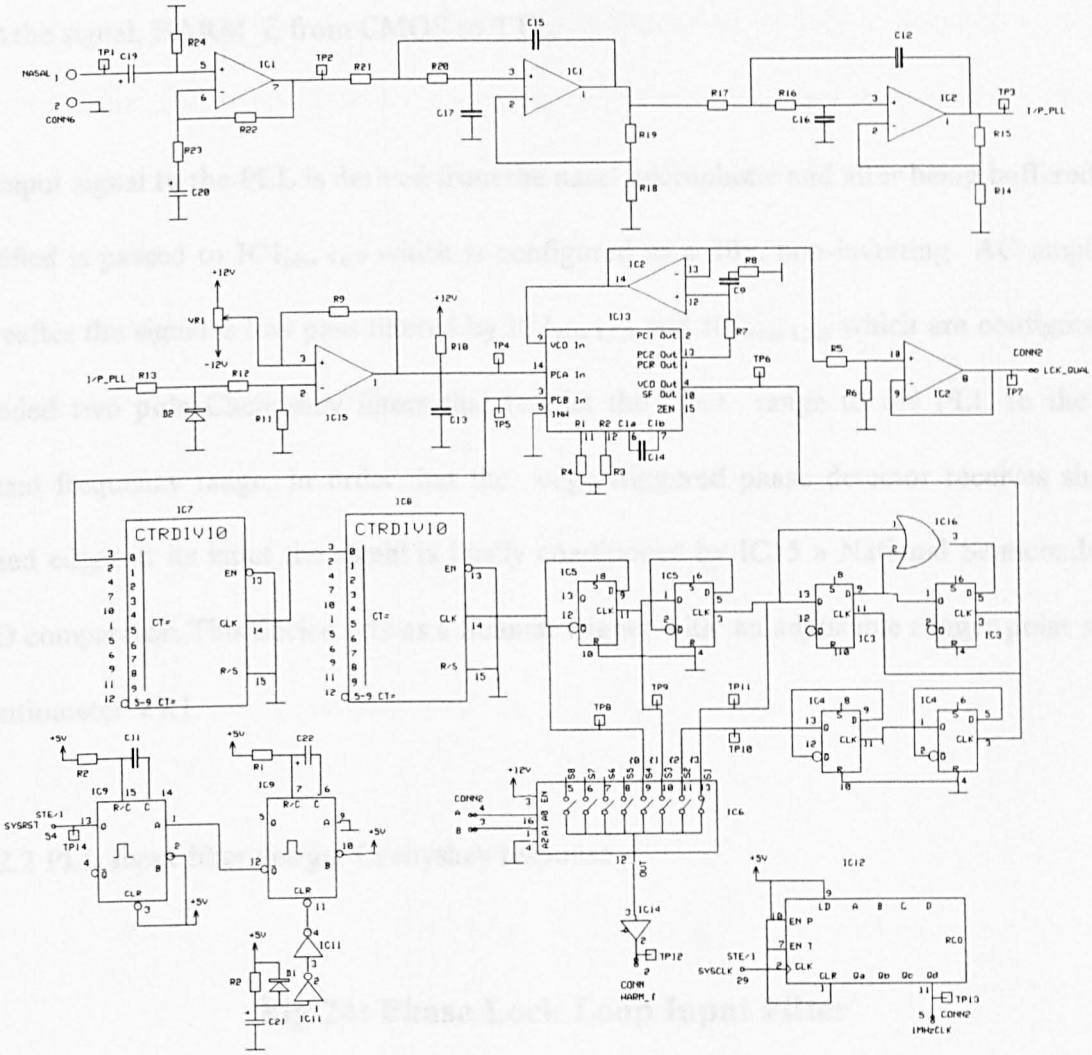

The VCO output from IC13$_{pin\ 4}$ is fed back to the phase detector input via the divide by n circuit comprising of ICs 3,4,5,7,8. The configuration of the D type latches IC3 and nor gate IC16 divide the VCO frequency by 3; thereafter IC5 divides this signal by 4 followed by ICs 7,8 which are cascaded decade counters giving a division of 100. The overall division factor is therefore 1200. IC4 additionally divides the VCO frequency by 4. The inputs to IC6, taken from these various frequency divisions make up 4 signals, phase locked to the measurement signal, at 100x, 200x, 300x and 400x the fundamental frequency. IC6 is an analogue

multiplexer Analog Devices 7501 that switches the appropriate clock frequency to the bandpass filters under the control of the microprocessor. IC14 is a Motorola 4504 that level shifts the signal, HARM_f, from CMOS to TTL.

The input signal to the PLL is derived from the nasal microphone and after being buffered and amplified is passed to $IC1_{pins\ 5,6,7}$ which is configured as a 10x, non-inverting AC amplifier. Thereafter the signal is low pass filtered by $IC1_{pins\ 1,2,3}$ and $IC2_{pins\ 1,2,3}$ which are configured as cascaded two pole Chebyshev filters that restrict the input range to the PLL to the first formant frequency range. In order that the edge triggered phase detector receives sharply defined edges at its input the signal is finally conditioned by IC15 a National Semiconductor 393D comparator. This device acts as a Schmitt trigger with an adjustable trigger point set by potentiometer VR1.

3.1.2.2 PLL Input filter design, Chebyshev response

Fig 24: Phase Lock Loop Input Filter

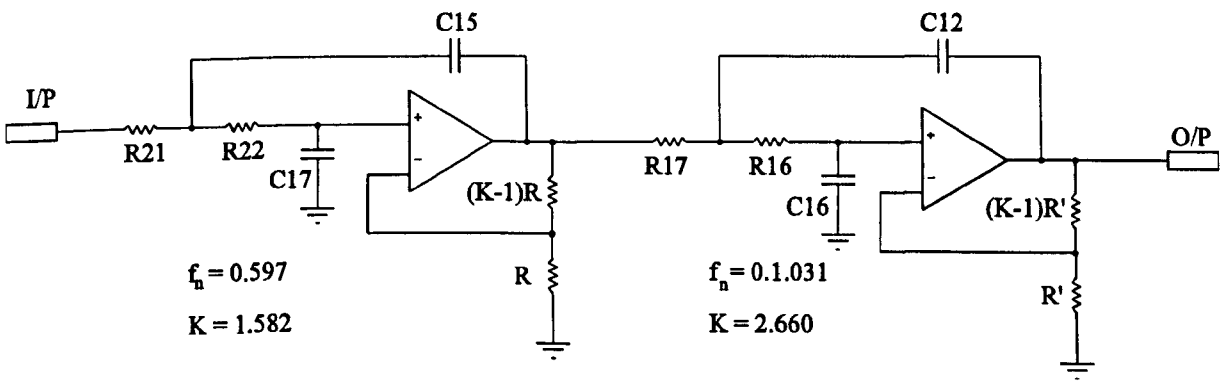

In order that the input frequency range to the PLL was sharply defined by an input filter with a steep roll off, a 4-pole Chebyshev active filter was chosen. The bandpass ripple was

designed to be no more than 0.5dB and the centre frequency initially set to 650Hz. The 24dB/octave roll off ensured a clearly delineated measurement bandwidth from extraneous signals and provided an effective anti-aliasing filter. The relatively large phase shift associated with this filter design was not considered to be problematic due to the lock detector effectively only sampling signals with slow frequency changes and the averaging of several measurements by software during the sampling period. Passive component values where chosen according to the following equation and Figure 24, IC1 and IC2 are Texas Instruments 074 quad operational amplifiers.

$$RC = 1/2\pi f_c f_n \qquad (3.3)$$

where f_c = passband end frequency

f_n = normalising factor

3.1.2.3 Microphone signal amplification and low pass filter.

Fig 25: Microphone Matching Circuit

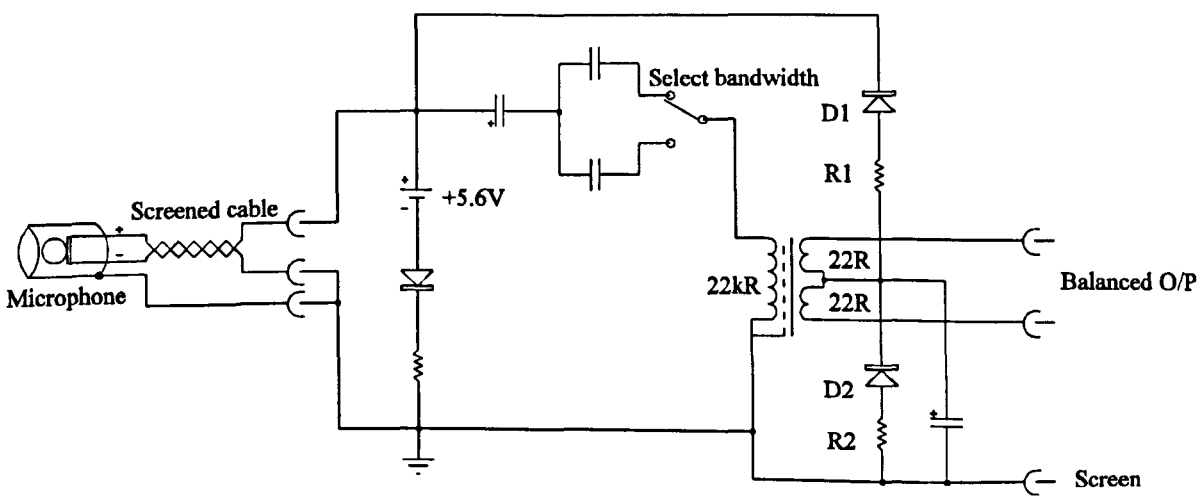

The microphone chosen for the clinical instrument was the Sennheiser 2-3 omnidirectional electret type. The output from the microphone is connected to the matching and power supply module shown in Figure 25 by screened twisted pair cable. The microphone output is AC coupled to the balanced driver transformer via the bandwidth selector switch and selected capacitor. The electret capsule within the microphone, powered by the 5.6Volt battery, requires a minimum load impedance of 330Ω. A balanced differential output signal transformer with an input impedance of 22kΩ and an output impedance of 22Ω, provides a signal level of 5.1mV/Pa into an open circuit. The resistor, diode chain R1,2 D1,2 biases the balanced secondary output of the transformer to the middle of the battery voltage. The output of the preamplifier module is connected via screened twisted pair cable to the input of the Resonometer Audio/Keyboard PCB shown in Figure 26.

The oral and nasal input signals OR+/- and NAS+/- from the microphone matching circuits are connected to the Audio/Keyboard PCB and amplified by the 10x gain differential amplifiers, IC $2_{pins\ 8,9,10}$ and IC $2_{pins\ 12,13,14}$. The outputs drive the signals OROUT and NASOUT, which are available via front panel connectors, for dual channel recording on audio tape. In a similar manner, previously recorded signals ORIN and NASIN are replayed from tape into the instrument via the front panel. The 1x gain inverting amplifiers, $IC2_{pins\ 1,2,3}$ and $IC2_{pins\ 5,6,7}$ enable either the microphone or the audio tape signal to be monitored. The output of these inverting amplifiers drive $IC3_{pins\ 1,2,3}$ and $IC3_{pins\ 5,6,7}$ which are configured as low pass filters with a Bessel response and a -3dB passband of 5kHz. These anti-aliasing filters limit the input signal frequency range to the measurement band as shown in Figure 21. This response was chosen as the passband of the filter of this type has maximally flat time delay or, in other words, the output phase shift is linear with frequency. Component values where chosen

according to equation 3.3 with f_n = 1.272 and K = 1.268. The output of the nasal channel inverting amplifier also provides the signal PLL which is the input to the PLL filter as described in section 3.1.2.1.

Fig 26: Audio / Keyboard PCB. Audio Section

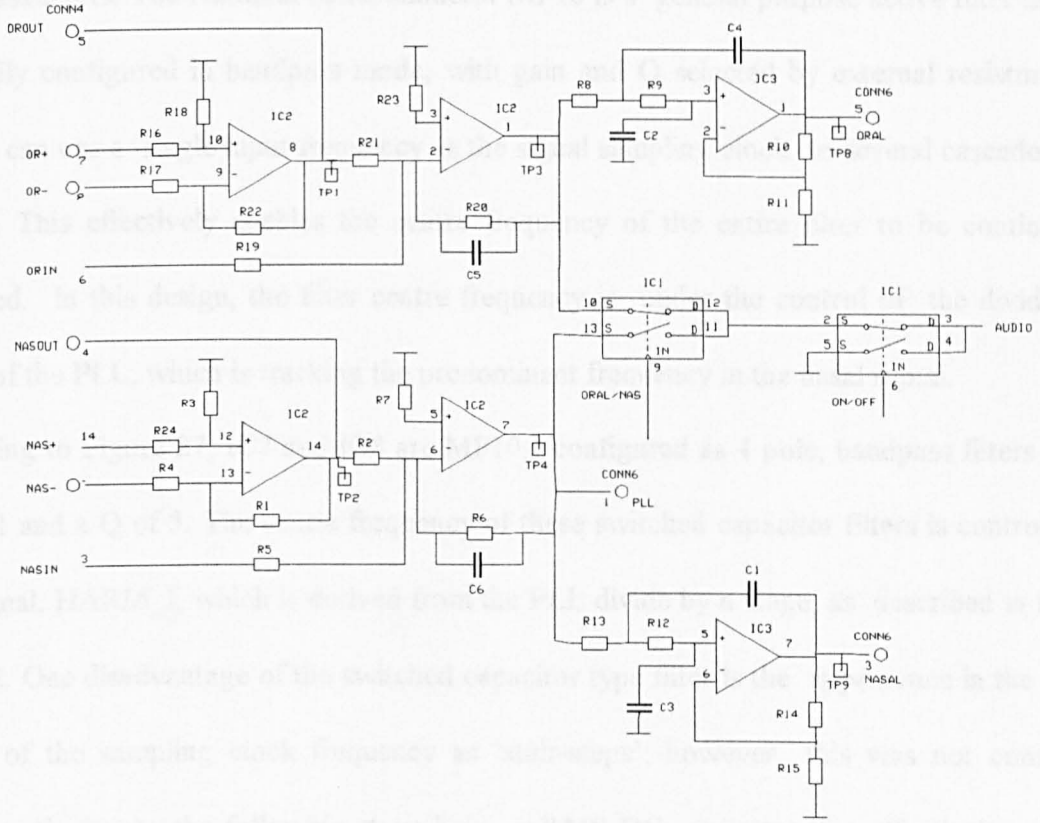

3.1.2.4 Tracking bandpass filters, RMS and A/D conversion.

Following the amplification and low pass filtering of the microphones' output the resultant signals, ORAL and NASAL, are passed to the tracking bandpass filters. Thereafter, the summation of the harmonics of these signals is achieved by the microprocessor switching the centre frequency of the filters, measuring each output in turn and summing the results as shown schematically in Figure 21. Switched capacitor type filters were chosen as the tracking bandpass filters. The National Semiconductor MF10 is a general purpose active filter that can be easily configured in bandpass mode, with gain and Q selected by external resistors. The device can use a single input frequency as the signal sampling clock to several cascaded filter stages. This effectively enables the centre frequency of the entire filter to be continuously adjusted. In this design, the filter centre frequency is under the control of the divide by n stage of the PLL, which is tracking the predominant frequency in the nasal signal.

Referring to Figure 27, IC7 and IC8 are MF10s, configured as 4 pole, bandpass filters with a gain x1 and a Q of 5. The centre frequency of these switched capacitor filters is controlled by the signal, HARM_f, which is derived from the PLL divide by n stage, as described in section 2.1.3.2. One disadvantage of the switched capacitor type filter is the appearance in the output signal of the sampling clock frequency as 'stair-steps'; however this was not considered problematic due to the following stage being a RMS-DC converter that effectively acts as a low pass filter. The power supply requirements of the MF10 are restricted to +/- 7 volts and it was therefore necessary to regulate the instrument's +/- 12 volt supplies using regulators REG 1/2. A further x3 gain stage was added using the inverting amplifiers $IC9_{pins1,2,3}$ and $IC9_{pins\ 5,6,7}$ in order to maximise the dynamic range.

Fig 27: Data Acquisition PCB. Dynamic Filtering / RMS:DC Conversion

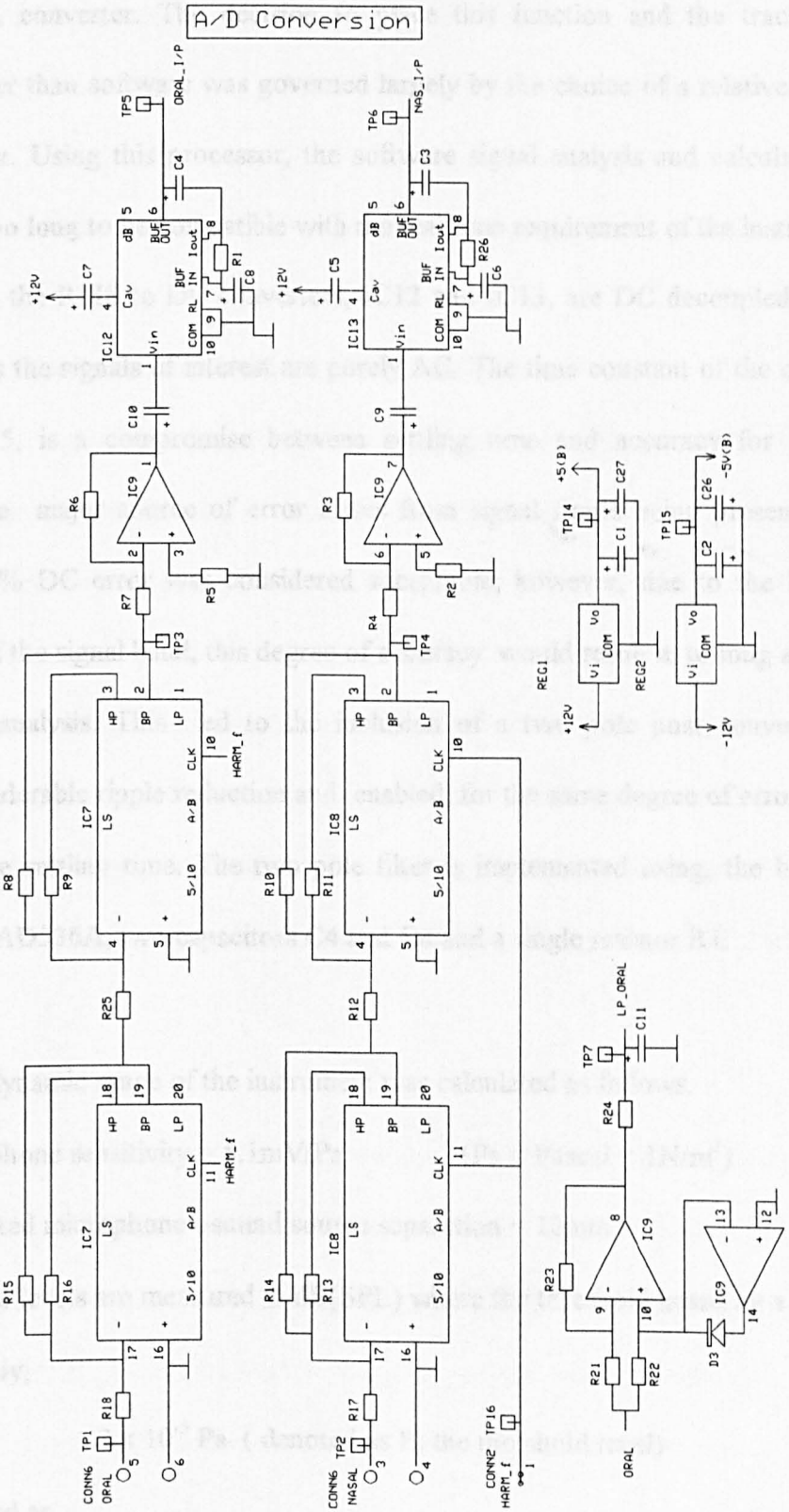

The RMS to DC conversion of the signals was implemented in hardware using the Analogue Devices 536A converter. The decision to place this function and the tracking filters in hardware rather than software was governed largely by the choice of a relatively simple 8 bit microprocessor. Using this processor, the software signal analysis and calculation time was shown to be too long to be compatible with the real time requirement of the instrument.

The inputs to the RMS to DC converters, IC12 and IC13, are DC decoupled by capacitors C9 and C10 as the signals of interest are purely AC. The time constant of the conversion, set by C7 and C5, is a compromise between settling time and accuracy for a given input frequency. The major source of error arises from signal ripple being present in the RMS output. A 0.1% DC error was considered acceptable; however, due to the low frequency components of the signal band, this degree of accuracy would result in to long a time constant for real time analysis. This led to the inclusion of a two pole post converter filter that provided considerable ripple reduction and enabled, for the same degree of error, a substantial decrease in the settling time. The two pole filter is implemented using, the buffer amplifier present in the AD536A, two capacitors C4 and C8 and a single resistor R1.

The required dynamic range of the instrument was calculated as follows.

Microphone sensitivity = 5.1mV/Pa (Pa = Pascal = $1N/m^2$)

Estimated microphone→sound source separation = 10mm

Sound pressure levels are measured in dB(SPL) where the threshold heard by a normal person is approximately,

2×10^{-5} Pa (denoted as P_o the threshold level)

which is defined as,

0dB(SPL) where $dB = 20 \log_{10}(P/P_o)$

Conversational speech at 1metre produces approximately 65dB(SPL)

At 1 metre, pressure range. $0 \rightarrow 65$ dB(SPL)

At 10mm, pressure range. $80 \rightarrow 145$ dB(SPL) (adjusting for inverse square law)

Therefore, the amplifier gains through the instrument were calculated as follows.

At the input to the A/D converter.

Microphone sensitivity = 100mV/Pa

Choosing an 8 bit conversion for a 5 volt input range gives a resolution of 19mV/bit

giving, measurement resolution = 0.2 Pa (approximately)

and therefore maximum range (8bits) = 51.2 Pa.

or a measurement range of, $80 \rightarrow 128$ dB(SPL)

The theoretical pressure range that the microphones were likely to be subjected to is subject to the error associated with the estimate of typical microphone to sound source distance, that is the distance to the nares or labia. However, using the figures shown above it was decided that the instrument design would be based on an overall signal gain of 28dB and an 8bit resolution.

The design of the A/D conversion and interface to the microprocessor was accomplished using the Analogue Devices 0808 as shown in Figure 28. This device incorporates an 8 channel input multiplexer, a successive approximation 8 bit A/D conversion, microprocessor compatible control logic and tri-state bus digital outputs. The multichannel facility of this device enabled the microprocessor to easily read the digital values of the signal conditioned

microphone outputs and the condition of the lock quality signal, LCK_QUAL from the PLL. A further signal, LP_ORAL, derived from the signal ORAL using a modulo x1 amplifier $IC9_{pin\ 8,9,10}$, is required by the software as a measurement trigger.

Fig 28: Data Acquisition PCB. A/D and STE Bus Interface Section

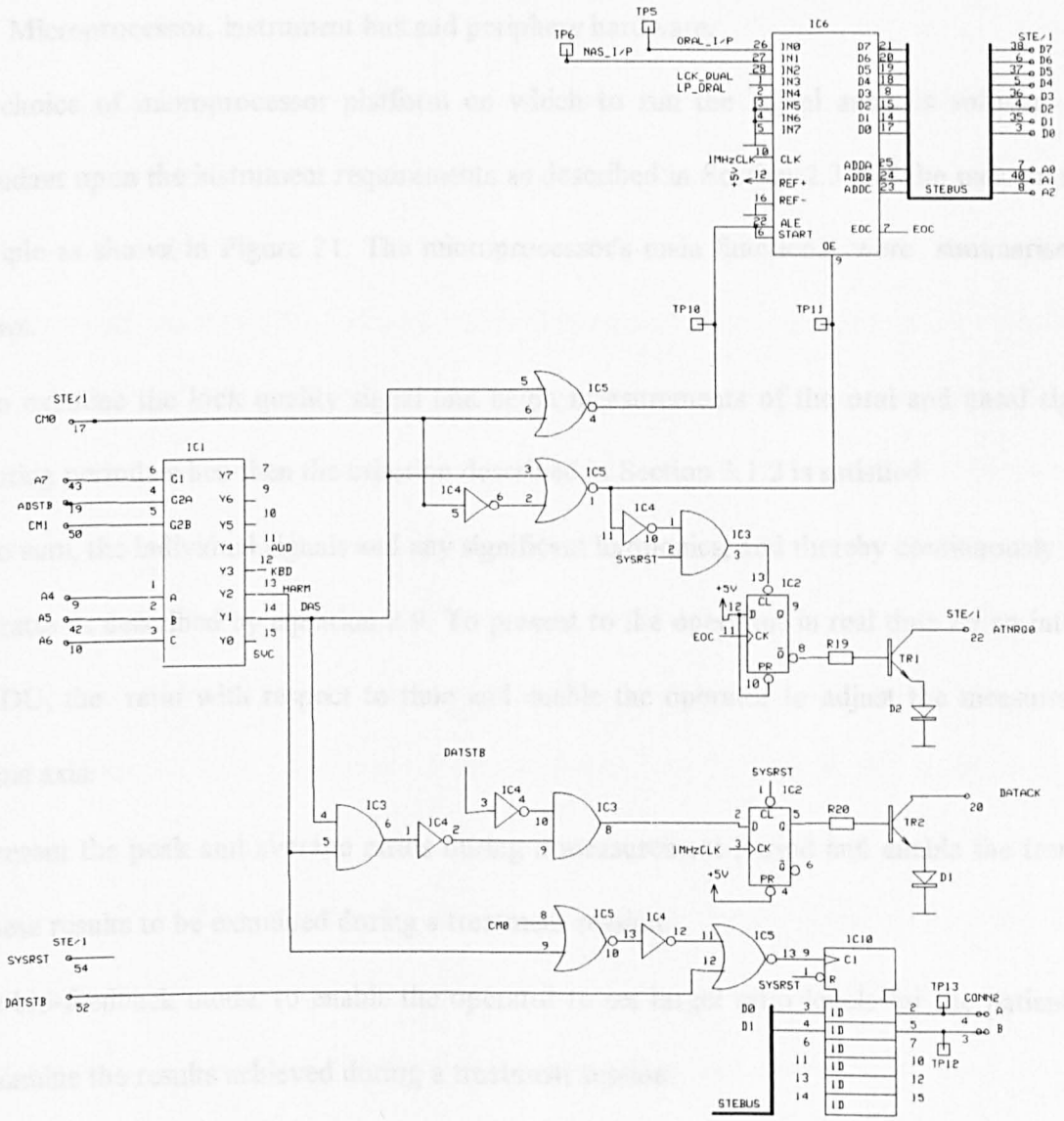

The successive approximation conversion technique, although relatively slow at a 100μsec per 8 bit conversion compared to other A/D techniques, was chosen due to the inclusion of a 256 resistor network that guarantees the monotonicity of the output.

The method of delineating signal from noise is dependant upon the detection of a slow shift in frequency and therefore does not require a particularly high signal sampling rate.

3.1.3 Microprocessor, instrument bus and periphery hardware.

The choice of microprocessor platform on which to run the signal analysis software was dependant upon the instrument requirements as described in Section 2.3 and the measurement principle as shown in Figure 21. The microprocessor's main functions were summarised as follows.

- To examine the lock quality signal and begin measurements of the oral and nasal signals during periods when then the criterion described in Section 3.1.2 is satisfied.
- To sum, the individual signals and any significant harmonics, and thereby continuously form a ratio as described by equation 2.9. To present to the operator, in real time on an integral VDU, the ratio with respect to time and enable the operator to adjust the measurement time axis.
- Present the peak and average ratios during a measurement period and enable the trend of these results to be examined during a treatment session.
- In bio-feedback mode, to enable the operator to set target ratio levels for the patient and examine the results achieved during a treatment session.
- To enable the operator to enter patient details and provide a hardcopy record of all the above results.
- To enable the operator to select a variable amplitude audio output of either channel.

- To enable factory calibration of the instrument such that the frequency gain response of each channel could be matched.

The 8 bit Zilog Z80 microprocessor was chosen for this design. The calculation of dynamic range for the instrument in Section 3.1.2.4 shows that an 8 bit data depth satisfies the resolution and range required of the instrument and this industry standard processor, running at 4MHz, was considered to be fast enough to meet the real time requirement.

To allow the microprocessor access to the various signals from the signal conditioning circuits as described in Section 3.1.2 , the operator keyboard, VDU, hardcopy printer and control of the audio output, the instrument design was based upon the STE1000 microprocessor bus (69). This industry standard system of interconnection enables the design to be independent of generic device families and enables a straight forward asynchronous interface to the bus of the various signal conditioning cards and periphery devices. One of the principal advantages of this bus is the large number of commercial cards and modules available which enabled the appropriate microprocessor card and VDU module to be selected.

Figure 29 shows the instrument interconnections. The Z80 PCB is a low cost commercial card, manufactured by Arcom, that includes a 4MHz Z80, 32K ROM, 4K RAM, 4 channel Clock Timer Counter (CTC) and a dual asynchronous receiver-transmitter (DART) serial port. One channel of the CTC is programmed to provide the appropriate baud rate for the DART channel that communicates with the printer. The data sampling system is interrupt driven at the appropriate rate for the oral/nasal channel switching and settling time on the signal conditioning cards. Therefore two CTC channels are cascaded to provide real time interrupts, at programmable equal intervals, to the processor for the purpose of timing the data acquisition. The signal sampling is explained in more detail in Section 3.1.4.

Fig 29: Instrument Interconnections

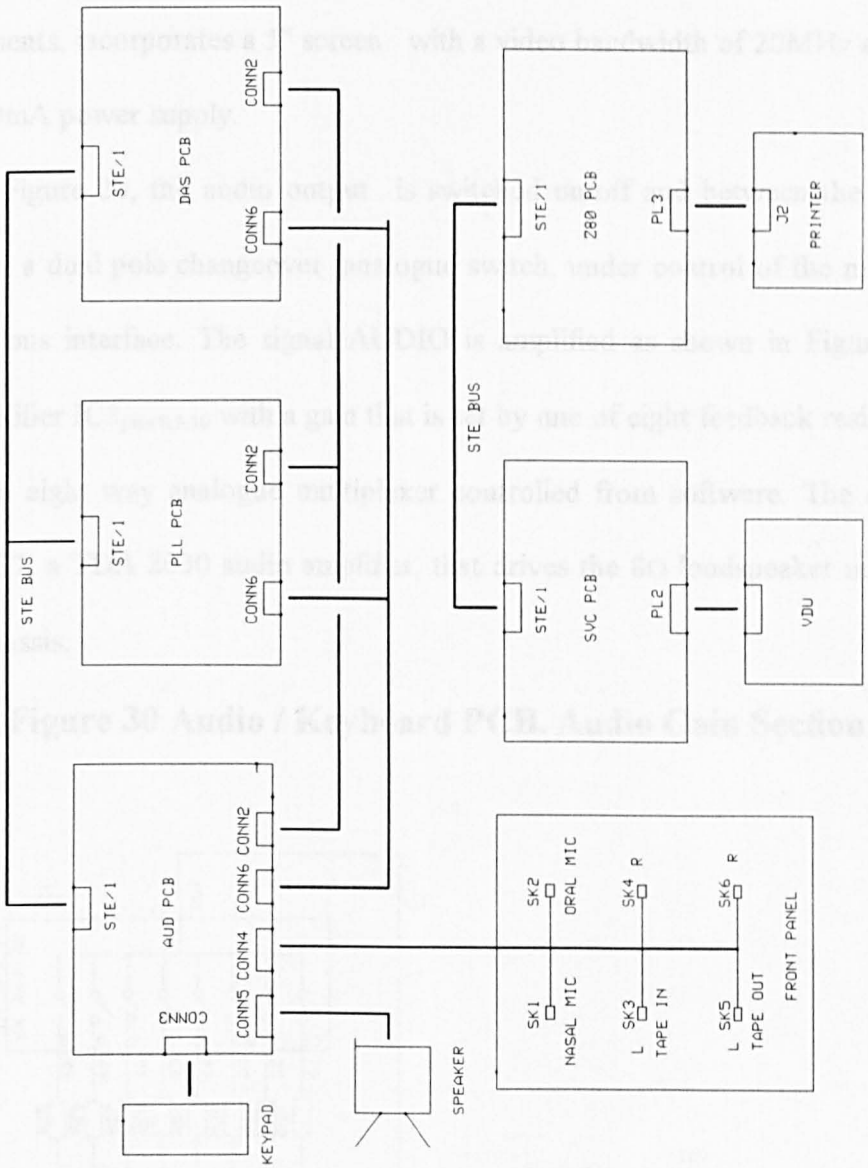

The SVC PCB is manufactured by Arcom and is capable of displaying 80 columns by 25 rows of text on a VDU with a standard video composite mode input. As an STE bus compatible module, the various registers and memory associated with the control and display of the VDU, simply appear in the CPU I/O address field. The SVC has an on-board video controller that

supports hardware scroll, several character attribute modes, graphics and a 9x12 ASCII character set. The VDU, manufactured by Vaco, is open chassis mounted specifically for OEM instruments, incorporates a 5" screen with a video bandwidth of 20MHz and requires a +12 volt, 800mA power supply.

Referring to Figure 26, the audio output is switched on/off and between the oral or nasal signal by IC1, a dual pole changeover analogue switch, under control of the microprocessor via the STE bus interface. The signal AUDIO is amplified as shown in Figure 30, by the inverting amplifier $IC3_{pins\ 8,9,10}$ with a gain that is set by one of eight feedback resistors selected using IC6, an eight way analogue multiplexer controlled from software. The output is AC coupled to IC7, a TDA 2030 audio amplifier, that drives the 8Ω loudspeaker mounted in the instrument chassis.

Figure 30 Audio / Keyboard PCB. Audio Gain Section

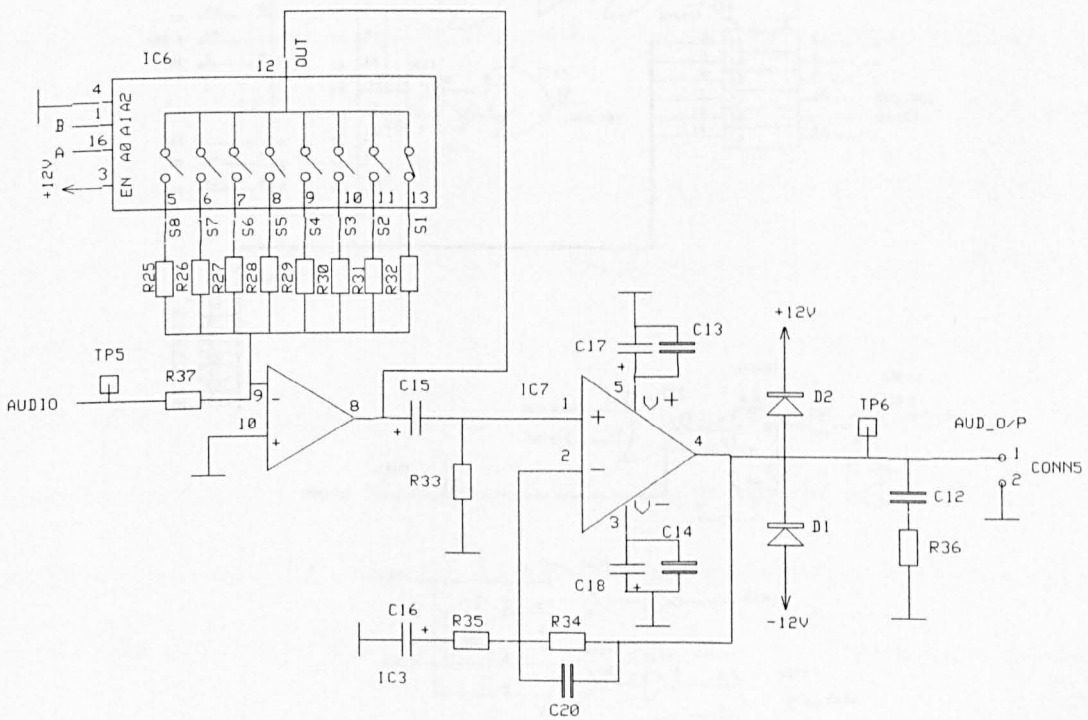

Referring to Figure 31, the operator's keyboard interfaces to the STE bus via IC4 and IC5.

Fig 31: Audio / Keyboard PCB. Keyboard Interface Section.

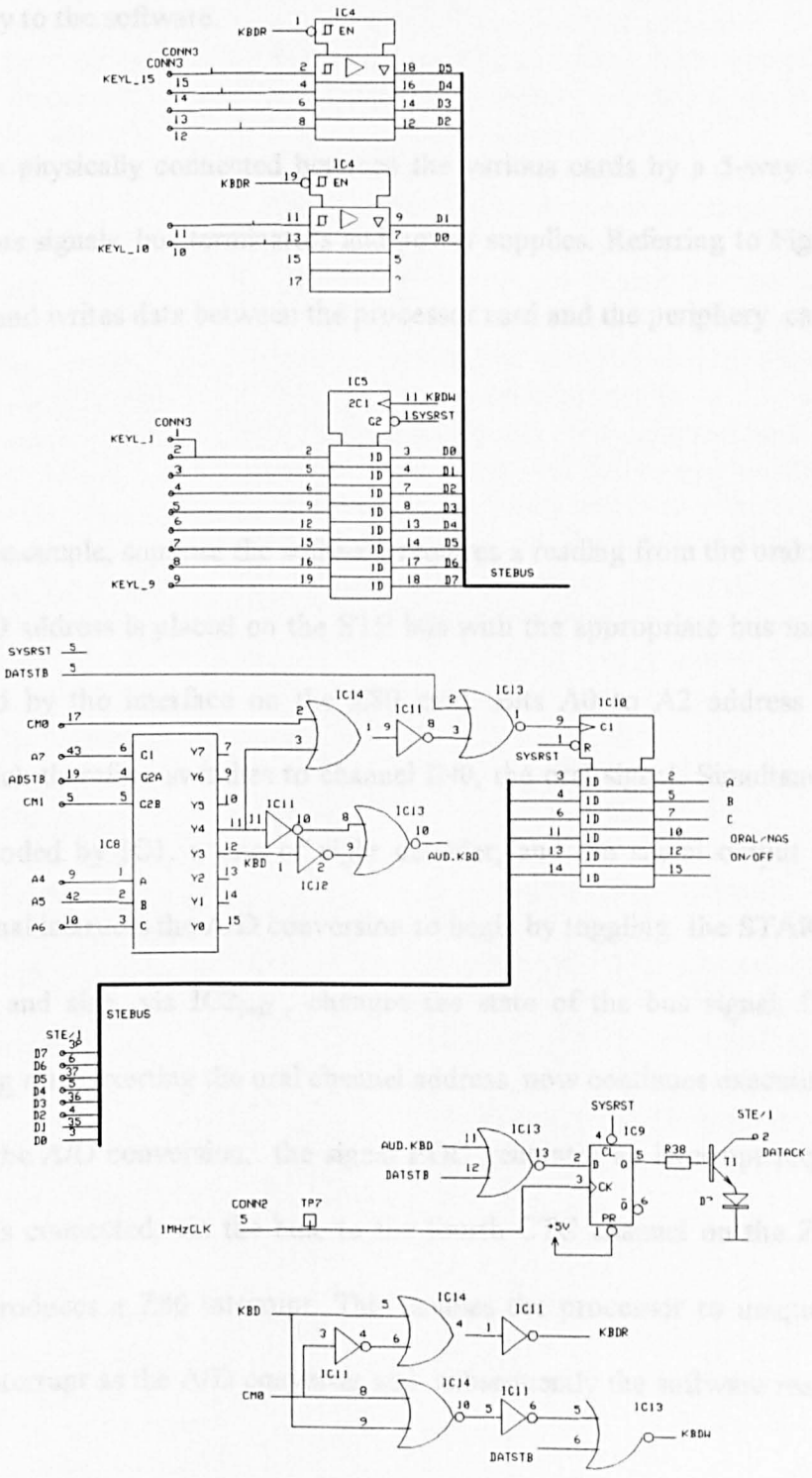

The processor writes a single logic zero to one line of the 8 bit latch IC5, this signal will be switched through the key matrix to IC4 by the action of a single key being depressed by the operator. This signal, read from IC4, in combination with the signal written to IC5, uniquely identifies the key to the software.

The STE bus is physically connected between the various cards by a 5-way backplane that carries all the bus signals, bus terminators and power supplies. Referring to Figure 28 the bus interface reads and writes data between the processor card and the periphery cards as follows.

For the sake of example, suppose the software requires a reading from the oral microphone. A unique 8 bit I/O address is placed on the STE bus with the appropriate bus management and timing provided by the interface on the Z80 card. Bits A0 to A2 address IC6, the A/D multiplexer which therefore switches to channel IN0, the oral signal. Simultaneously, bits A4 to A7, are decoded by IC1, a one of eight decoder, and the signal output DAS becomes active. This signal instructs the A/D conversion to begin by toggling the START input on the A/D converter and also, via $IC2_{pin2}$, changes the state of the bus signal, DATACK. The processor, idling since exerting the oral channel address, now continues executing code. At the completion of the A/D conversion, the signal EOC generates an interrupt request, ATNRQ. This interrupt is connected, via the bus, to the fourth CTC channel on the Z80 card which consequently produces a Z80 interrupt. This enables the processor to uniquely identify the source of the interrupt as the A/D converter and subsequently the software reads the digitised oral signal.

Fig 32: Main Software Modules

Module: Main

Power up
Initialize hardware
Monitor function keys
Call function
Handle errors

Module: Fnc1

Initialize screen
Display hospital details
Display header details
Monitor keys
Decode and display results
Edit screen
Call next function

Module 3: Fnc3

Initialize screen
Draw axis and annotate
Normalize average ratios
Display average ratios/test
Interrupt when screen is full
Monitor keys
Call next function

Module: Fnc4

Initialize screen
Draw axis and annotate
Calculate % success
Display % success
Display cursor setting/test
Wrap screen around when full
Monitor keys
Call next function

Module: Fnc2

Initialize the screen
Draw axis and annotate
Scale the time axis according to the operator request
Output any recent prior data to avoid loss
Monitor the keys
Monitor the oral signal for a threshold
After the threshold is detected continuously assess the lock quality
If phase lock is detected commence measurements
Set up interrupt timing for data acquisition
Sample the oral and nasal signals and their harmonics with appropriate timing
Continuously sum the results and form a ratio
Normalize the results and display graphically in real time
Continuously calculate and display the average ratio
Set the aiming cursor for the success measurement
Continuously monitor the degree of success
Continuously monitor the peak ratio
Call the next function

Module: Help

Provides help screens on the following topics.
The measurement principles
Setting up and care of the instrument
Setting up the patient for a measurement
How to operate the instrument
Results and how to interpret them
The principal and operation of the target cursor
How to record and playback from audio tape

3.1.4 Instrument software

The software was written predominately in the C language with some modules written directly in Z80 machine code. The code was developed using a Microtec high level cross compiler and assembler. When assembled into machine code, the software was loaded and run on the target processor using an ARS Microsystems in circuit emulator.

The software was organised into four main modules, FNC1 to FNC4, that corresponded to the operator's keyboard request for one of the four display screens to be switched to the VDU. The main functions within each module are shown in Figure 32.

3.1.4.1 Screen 1.

The first screen, generated and controlled by software module FNC1, is shown in Figure 33 and enables the operator to enter treatment and patient details.

Figure 33: Nasal Resonometer. Patient Details Screen

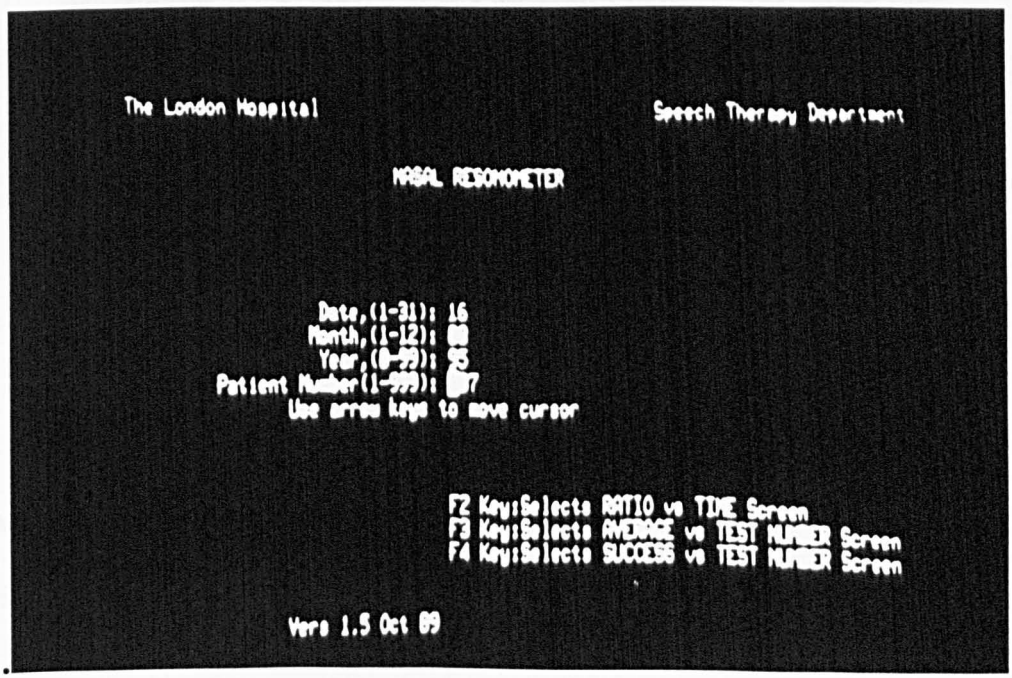

3.1.4.2 Screen 2. Phase lock and data acquisition.

The second screen shown in Figure 34, generated and controlled by software module FNC2, is the main data acquisition and display interface. The operator can select the following.

- The maximum x-axis time scale to suit the phonatory test material.
- The position of the horizontal patient aiming cursor, used in biofeedback mode.
- Recall of the last measurement for comparison purposes.
- The audio output channel and amplitude.
- The help screens.

Figure 34. Nasal Resonometer. Main Clinical Data Screen .

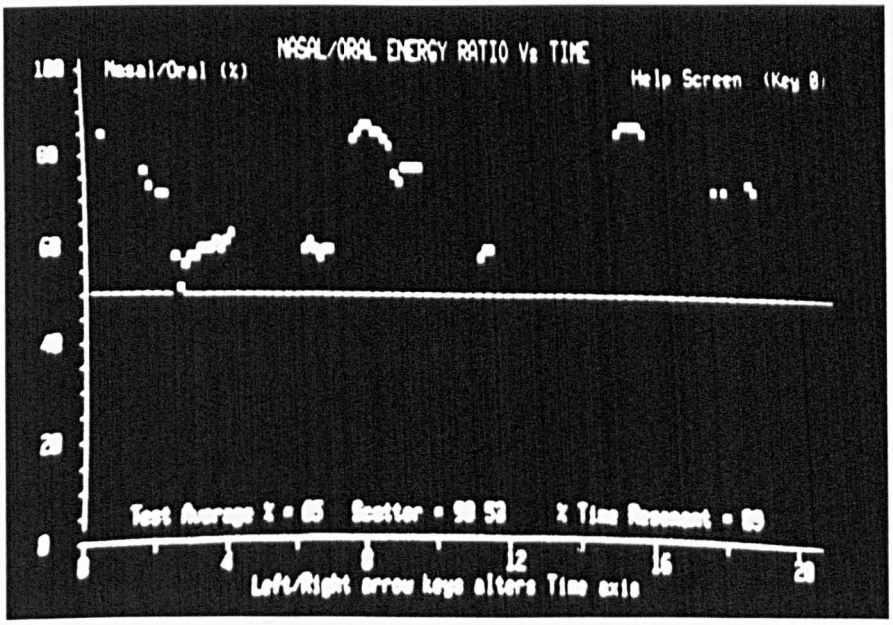

The main data acquisition routines within the FNC2 module are OPSYSCODE and C_INTERRUPT, and are listed in Appendix 3. Referring to this code, the main features of

these modules are as shown in the flow chart shown in Figure 35 and the timing diagrams as shown in Figure 36 and 37.

Fig 35: Software Flow Diagram

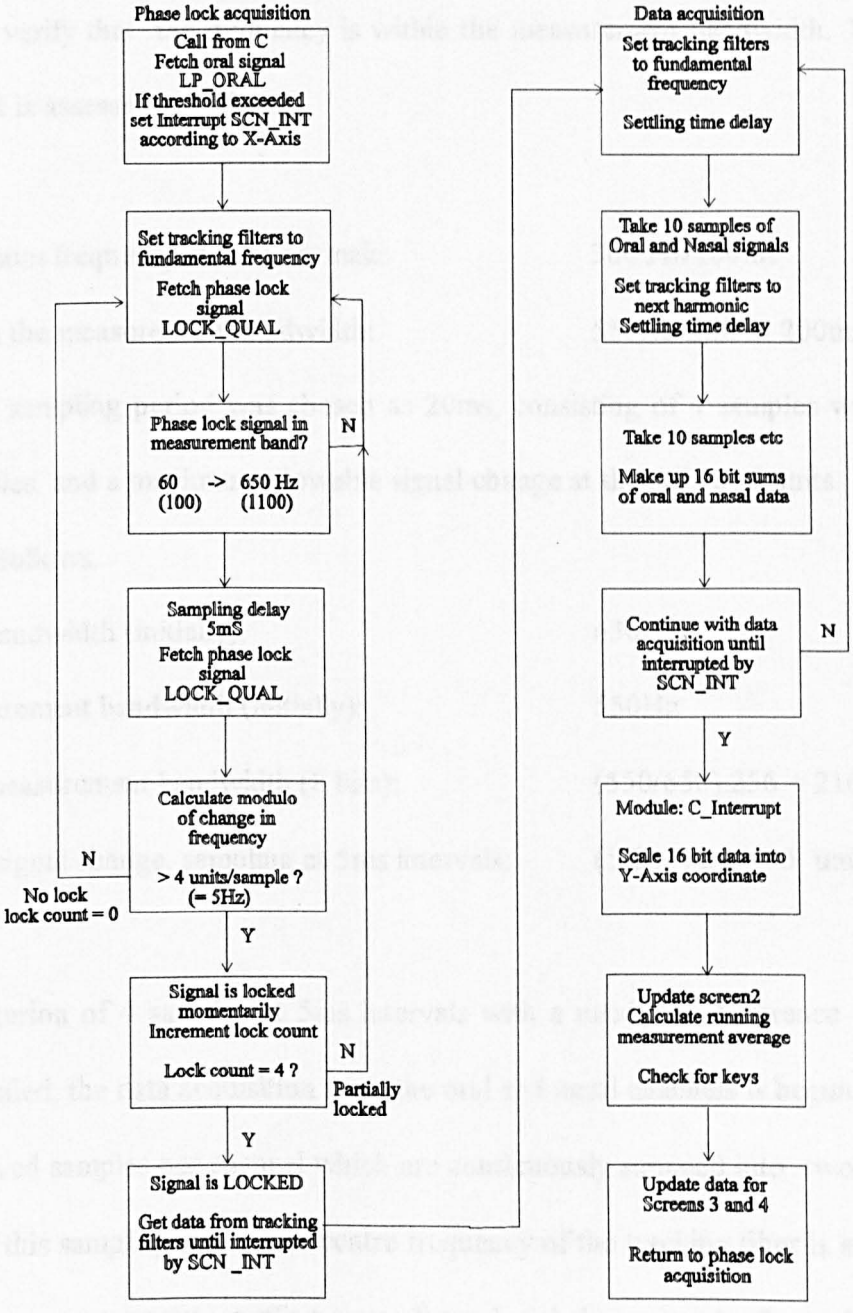

Phase lock acquisition is, as explained in section 3.1.2.1, based upon the detection of a shift in frequency of the nasal signal of less than 5Hz. The machine code software in OPSYSCODE establishes that an oral signal threshold has been exceeded, calculates an interrupt interval for C_ Int according to the operator's requested measurement period and then monitors the phase lock signal to verify that the frequency is within the measurement bandwidth. Thereafter the frequency shift is assessed as follows.

Maximum frequency shift in normals:	300 Hz/100ms
Within the measurement bandwidth:	550Hz shift in 200ms (5Hz)

Therefore the sampling period was chosen as 20ms, consisting of 4 samples with 5ms delay between samples, and a maximum allowable signal change at the A/D of 5 units.
Calculated as follows.

PLL bandwidth (initially):	650Hz
Measurement bandwidth (initially):	550Hz
A/D measurement bandwidth (8 bits):	(550/650).256 = 216 units
Max. signal change, sampling at 5ms intervals:	(5/200).216 = 5 units

When the criterion of 4 samples at 5ms intervals with a maximum difference of 5 units per sample is satisfied, the data acquisition from the oral and nasal channels is begun. This consists of 10 interleaved samples per channel which are continuously summed into two 16 bit words. At the end of this sampling period the centre frequency of the tracking filter is switched to the next harmonic, an appropriate settling time allowed and the next set of samples taken. This process continues until interrupted by C_Int, thereafter the data is passed to the C code C_INTERRUPT module, processed and displayed as a data point on the screen. If the

Figure 36: Phase Lock Acquisition Timing

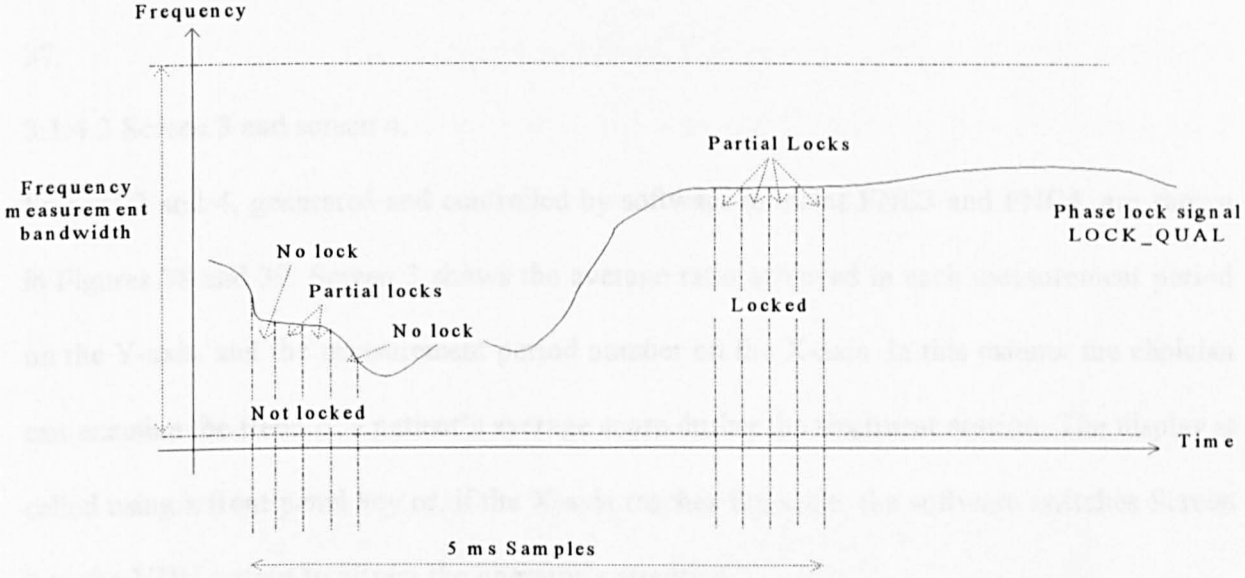

Figure 37: Data Acquisition Timing

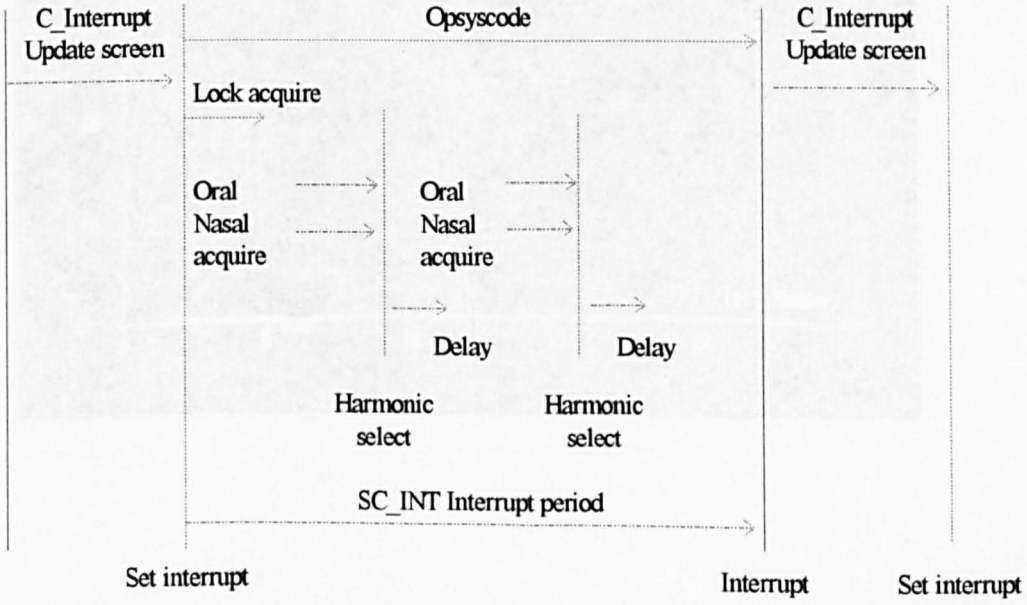

measurement period has not been exceeded the control flows back to OPSYSCODE and the process of lock acquisition is restarted. This process is shown diagrammatically in Fig 36 and 37.

3.1.4.3 Screen 3 and screen 4.

Screens 3 and 4, generated and controlled by software modules FNC3 and FNC4, are shown in Figures 38 and 39. Screen 3 shows the average ratio achieved in each measurement period on the Y-axis, and the measurement period number on the X-axis. In this manner the clinician can examine the trend of a patient's average score during the treatment session. The display is called using a front panel key or, if the X-axis reaches full scale, the software switches Screen 3 to the VDU output to attract the operator's attention.

Figure 38: Screen 3. Average Ratio Scored in Consecutive Tests

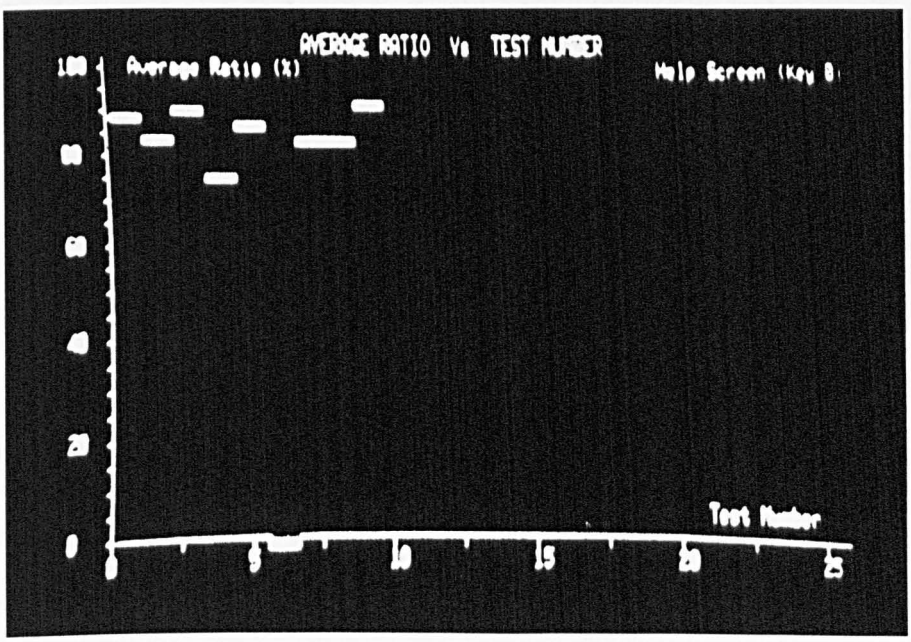

Figure 39 shows Screen 4 which displays the success rate of the patient in achieving the oral:nasal ratio target, set using the aiming cursor on Screen 2, by the clinician. The success rate is shown on the Y-axis and is calculated from the percentage of time during the measurement period when the patient achieved a nasal:oral ratio less than the aiming level. Also shown, as a dotted line, is the aiming level that was set for each measurement period. The X-axis shows the measurement period number.

Figure 39: Screen 4. Success Achieved in Consecutive Tests

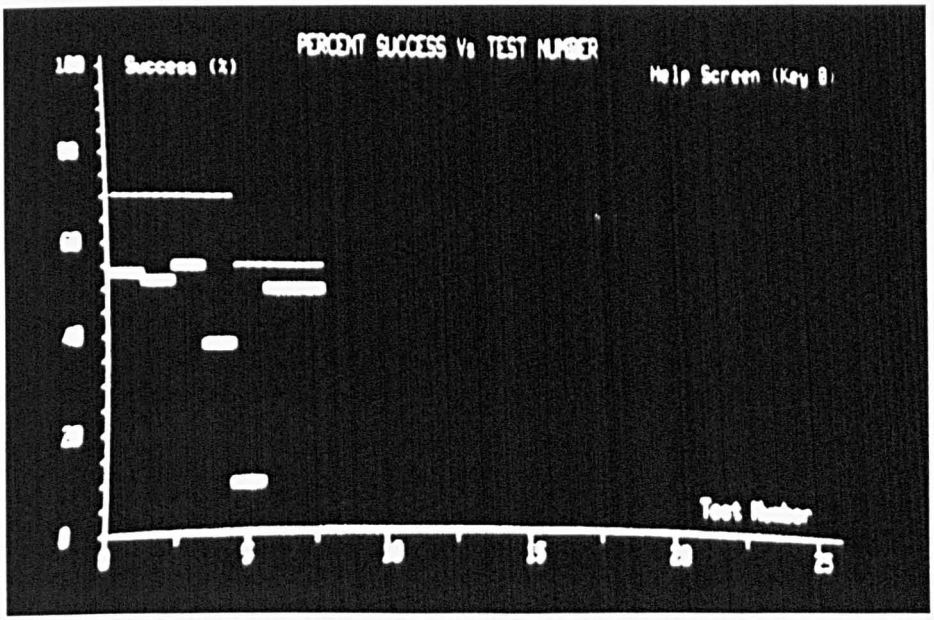

A set of help screens are available to the operator under the control of the software module HELP; the help topics are described in Figure 32. These scrolled screens can be called to overlay any other screen and include the controls for the audio output.

3.1.5 Instrument Fabrication

The Nasal Resonometer design is intended for portable use in clinics, speech laboratories and schools and was therefore fabricated in the most compact manner possible. Figure 40 shows the complete instrument from the front panel which incorporates, microphone and line connections, keyboard, printer and VDU.

The rear panel of the instrument carries the mains connector and fuses. The PLL, Audio, Keyboard and DAS PCB,s shown in Figures 23, 27, 28, 30, 31 are fabricated on eurosize doublesided cards, housed in the PCB cage as shown and connected via 64 way edge connectors to the STE bus mother board at the rear of the card rack. The last two card slots are occupied by the Z80 processor card and the SVC video display card.

The instrument power supply is located in the centre of the internal layout and comprises multi output switched mode power supplies of +5V, 8A and +/- 12V,3A supplies. The front panel printer is hinged for operator access to the paper roll and ribbon change. The instrument is cooled internally by a small fan, mounted adjacent to the PCB card rack , that draws outside air through slots in the side of the case and across the PCBs. The audio loudspeaker is mounted on the slotted side wall of the instrument case.

Figure 40: Nasal Resonometer.

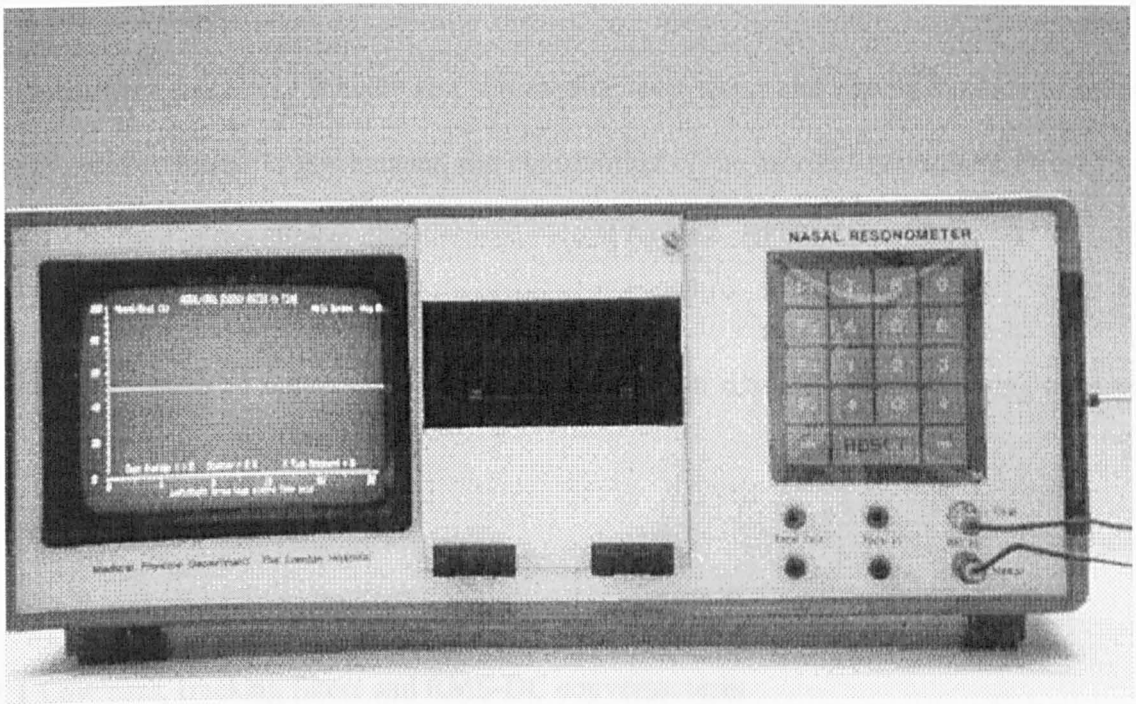

Front Panel.

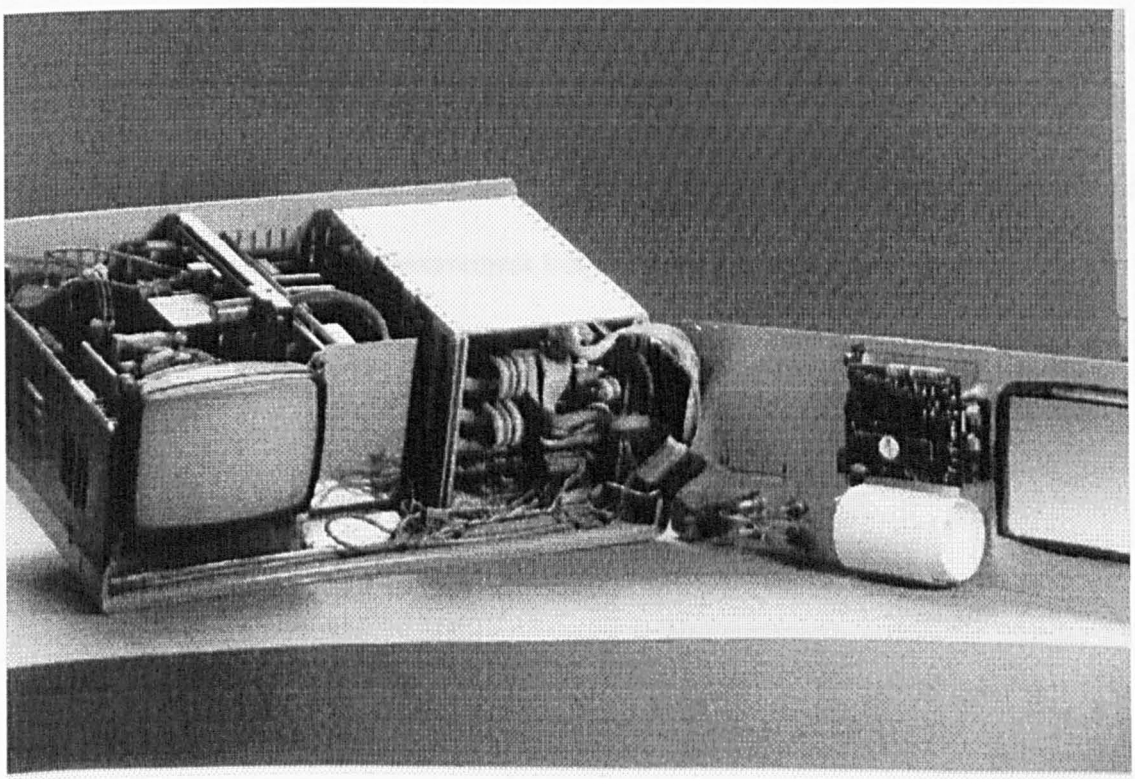

Internal View

3.2 Instrument testing.

The instrument was tested initially at a sub-module level using test signals in place of outputs from the microphones. In this manner, the contribution of the inherent instrument errors to the overall accuracy of the clinical measurements could be assessed.

Referring to Figure 41 which shows the instrument circuit schematic, the following tests were performed.

3.2.1 Low pass, tracking filters and RMS-DC converter tests.

Identical sinusoidal signals of 50mV RMS amplitude and swept frequency were introduced into the x10 gain amplifiers. Measurements from the outputs of the 5kHz low pass filters are shown in Figure 42 and demonstrate that the gain of the filter and amplifiers is typically 12.45 and that the interchannel gains are matched to the extent that the maximum ratiometric error is less than +/- 0.5% within the measurement frequency band.

Figure 41: Instrument Circuit Schematic

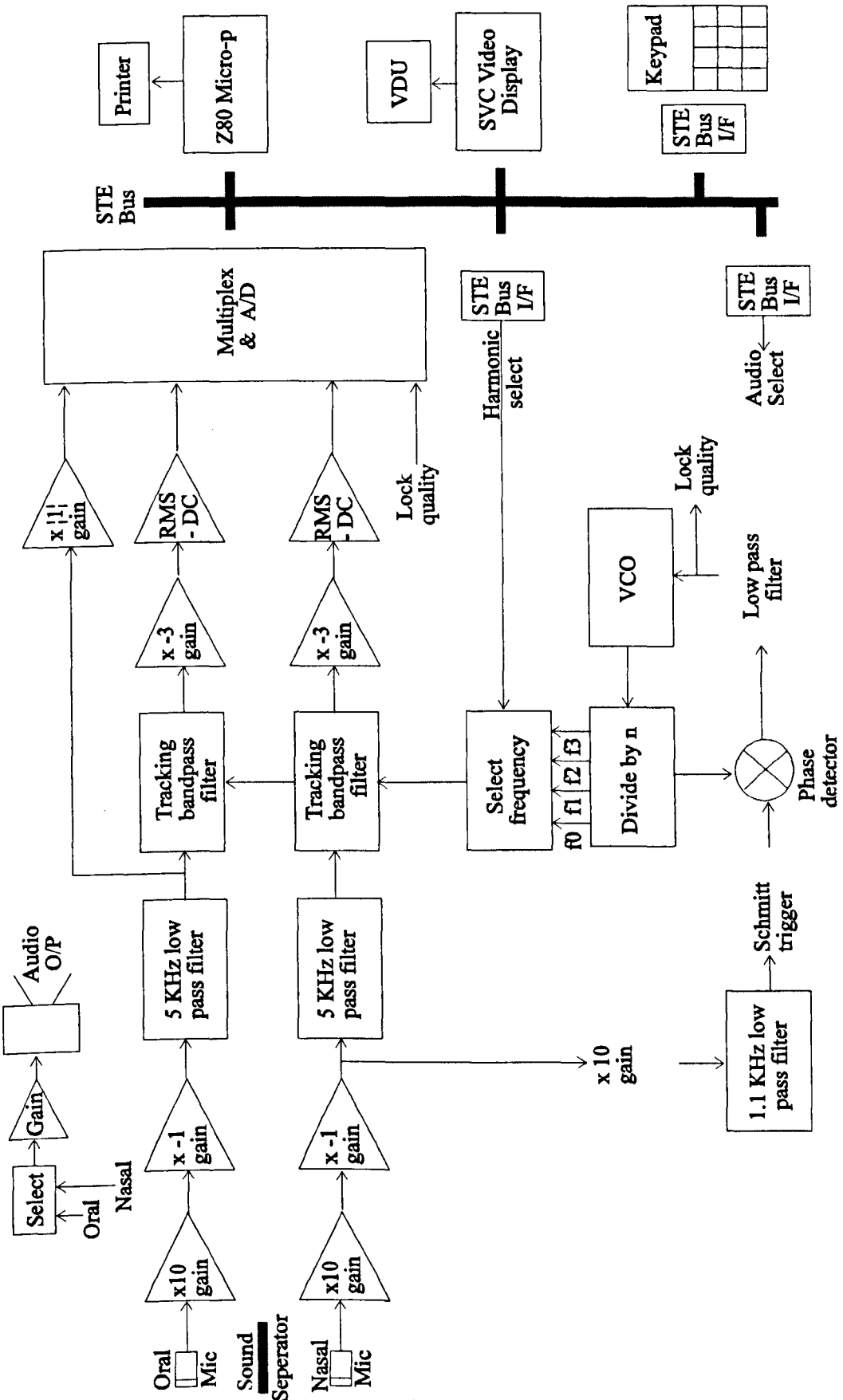

Figure 42: Response of x10, x-1 Amplifiers and 5kHz Low Pass Filters

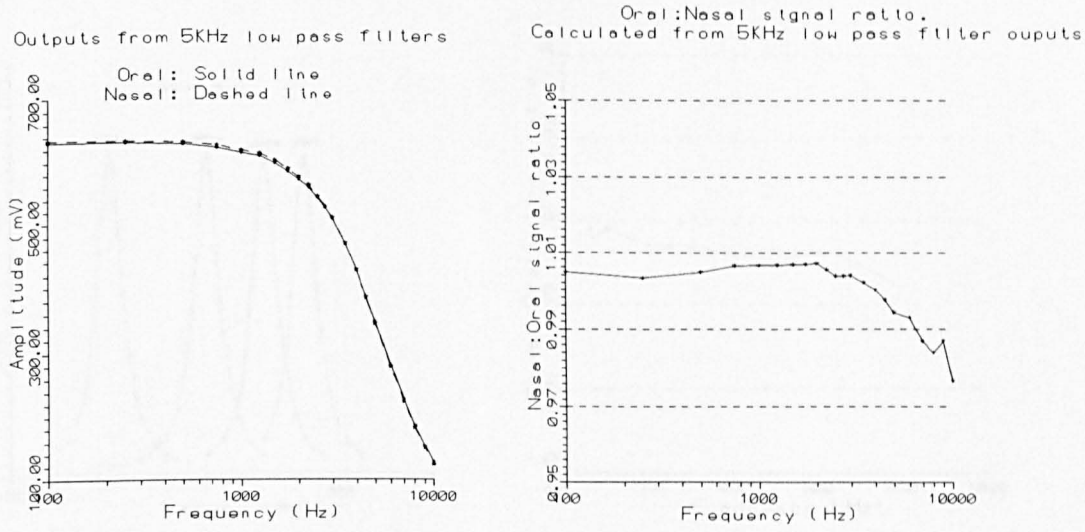

The bandpass characteristic of the tracking filters was tested by placing the centre frequency of the filter at the fixed frequencies of 200,400,600,800 Hz using an external clock signal and for each filter frequency, introducing a swept frequency, constant amplitude signal into the x10 gain amplifiers. Figure 43 shows the outputs from the oral and nasal tracking bandpass filters. The filters have a Q of 5 and a gain at 800 Hz of 1.016. The interchannel gains are matched to the extent that the maximum ratiometric error is less than +0.8%, -0.6% within the frequency range of the first formant. Wider bandwidth measurements show a maximum error of less than +/- 1.0%.

Figure 43: Response of Tracking Bandpass Filters

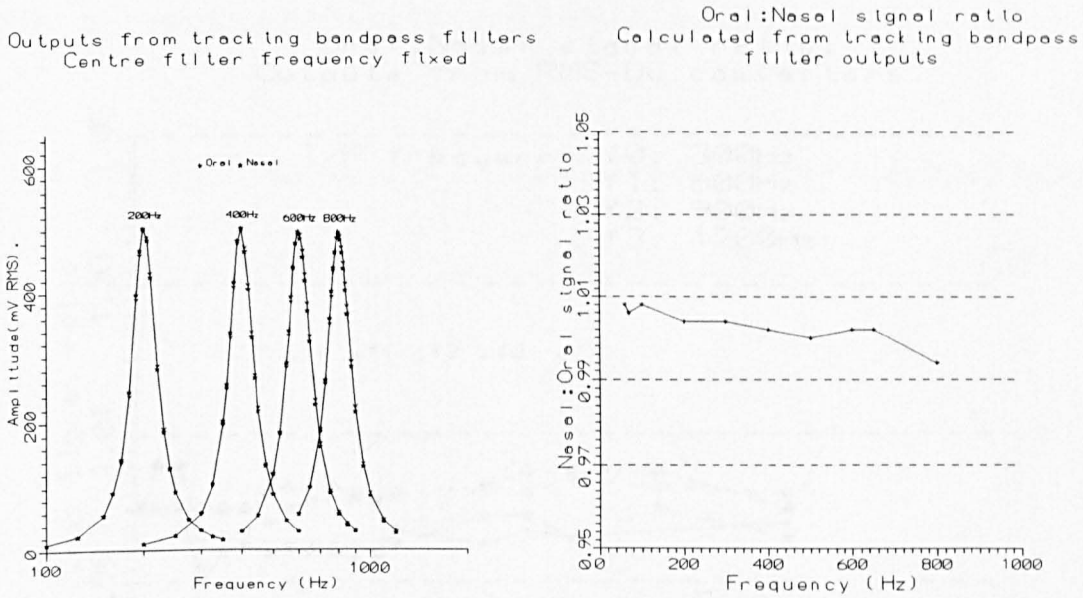

The measurement error of the RMS to DC converters was assessed with the tracking filters centred at fixed frequencies as before and introducing a swept amplitude signal, typical of the microphone output range, into the x10 amplifiers. Figure 44 shows that the ratiometric error, measured at the output of the converters, is less than +/- 1.0%.

These tests lead to the conclusion that the overall ratiometric measurement error, for the low-pass, tracking and RMS-DC converters using clinically typical signal frequencies and amplitudes is less than +/- 1.0%.

Figure 44: Response of RMS-DC Converters

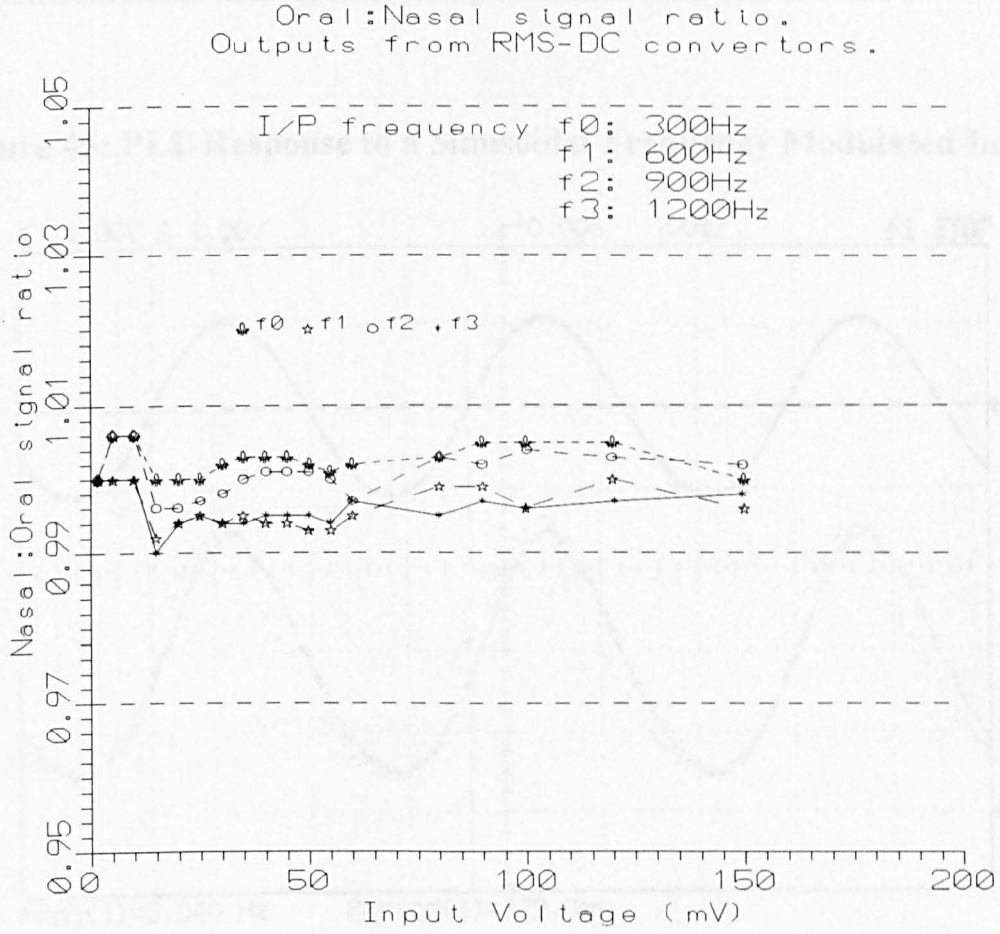

3.2.2 Phase lock loop tests.

The ability of the loop to track changing frequencies was initially tested by introducing a constant amplitude, frequency modulated signal into the nasal x10 amplifier and monitoring the loop's response from the Lock Quality signal. Figure 45 shows the results recorded from an oscilloscope measuring the input frequency modulation envelope on Trace 1 and Lock Quality on Trace 2. The modulation envelope sweeps the input frequency sinusoidally from 65 to 650Hz at a sweep rate of 3Hz. The Lock Quality shows the loop maintaining lock with

the characteristic positive and negative pulses either side of the sinusoid as the phase detector detects a slight deviation from lock with the subsequent servo correction. The loop demonstrated successful tracking of frequency modulations in excess of 15Hz.

Figure 45: PLL Response to a Sinusoidal Frequency Modulated Input

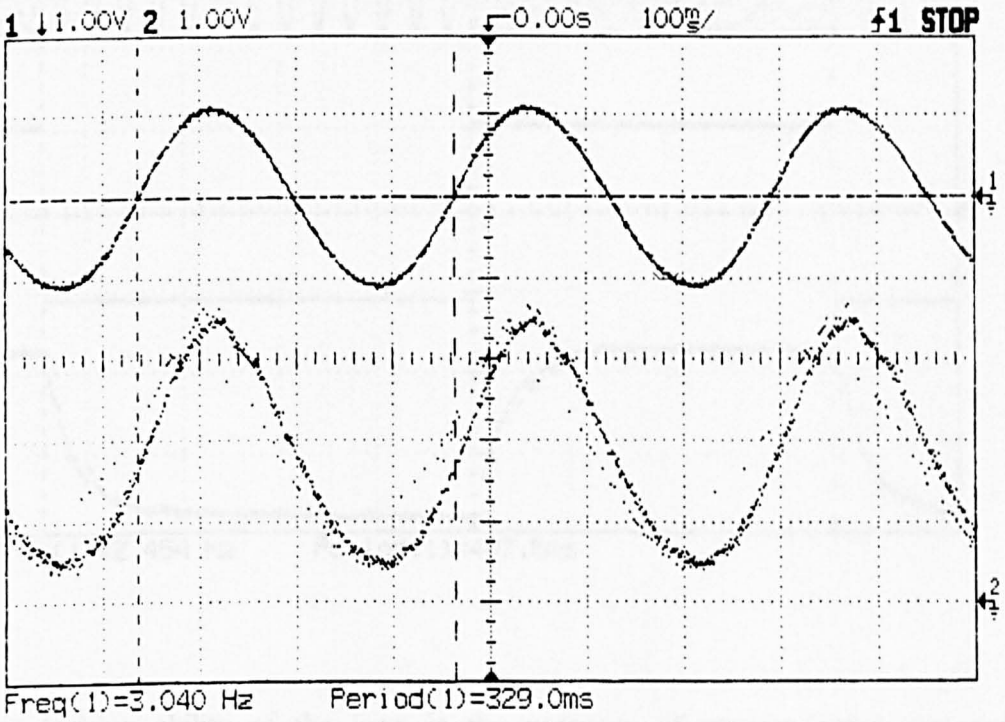

Figure 46 shows a square wave input frequency modulation on Trace 1 and the input frequency on Trace 4 switching between 65 and 650Hz. The Lock Quality shown on Trace 2 demonstrates that the response of the loop is stable when stimulated by this step input. The loop damping, discussed in section 3.1.2.1, gives a time constant of approximately 40 ms as shown by the Lock Quality rise and fall times and therefore a maximum FM bandwidth of 25Hz. The pull-in range of the loop was measured from DC to 1140Hz.

Figure 46: PLL Response to a Square Wave Frequency Modulated Input

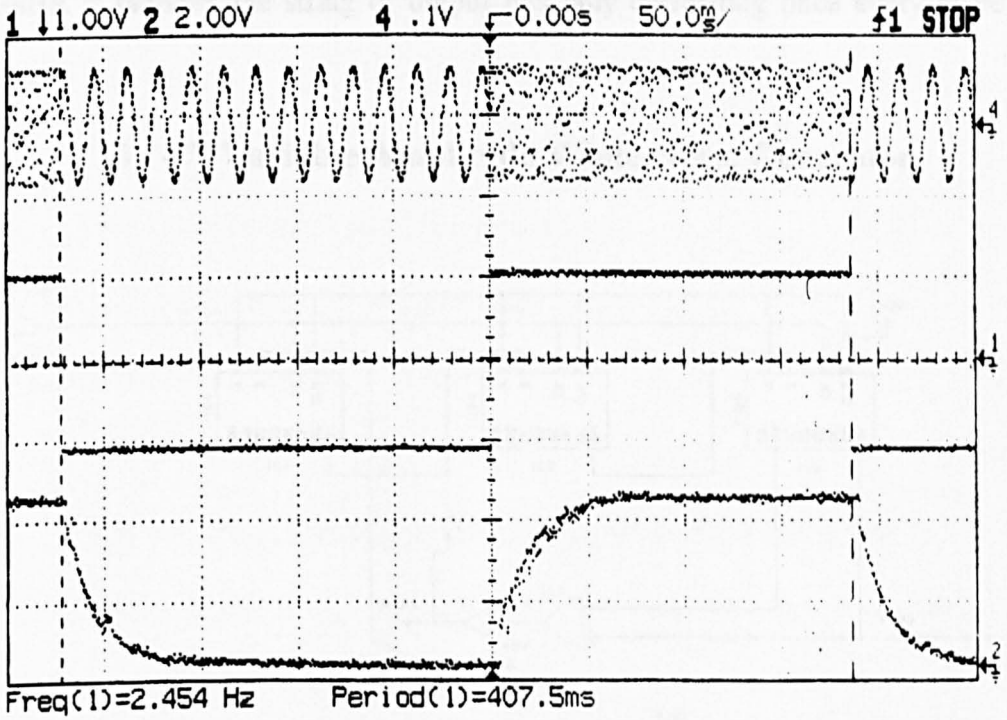

The phase locking ability of the loop in the presence of random noise was tested by introducing a signal of variable signal to noise(s/n) ratio, and then adjusting the s/n ratio until loop lock was lost. This test was achieved by connecting an amplitude and frequency modulated sinusoidal signal to the nasal x10 amplifier input and a variable level noise signal to the nasal Tape In input. The random noise generator, shown in Figure 47, was derived from the lowpass filtering of a pseudo-random bit sequence generator (PRBS) producing band-limited Gaussian white noise. The PSBR consists of ICs1,2,3 that are configured as a 24-bit serial shift register with bits 18 and 23 fedback to the input of an exclusive OR gate, IC4. The output of the exclusive OR gate forms the input to the serial shift register which is clocked at a

fixed rate. This circuit goes through a series of states, defined by the set of bits in the register after each clock pulse, the series eventually repeating itself. The circuit configuration shown, clocked at 160kHz, has a cycle time of approximately 1 minute. Within the cycle, the output of the PSBR is random, the string of output bits only correlating once every cycle for one clock period.

Fig 47: Variable Amplitude White Noise Generator

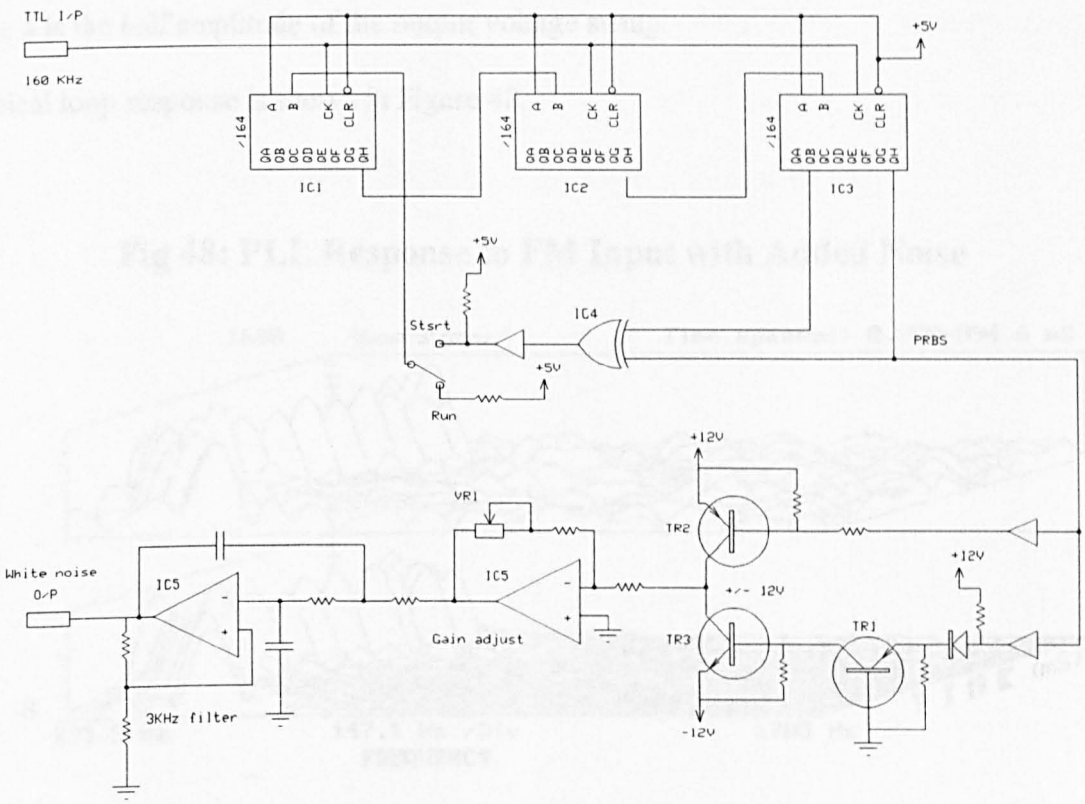

The output spectrum generated by PSBR (70) consists of noise, extending upwards from the cycle frequency with a $(\sin x/x)^2$ envelope; it is flat within +/- 0.1dB up to 12% of clock frequency. The output of the shift register is level shifted from 0/+5 volts to -/+ 12 volts by

TRs1,2,3 and gain adjusted by IC5, a variable gain amplifier. The 2 pole, 3kHz low pass filter formed by IC5, converts the output to a band-limited analogue noise voltage.

The rms noise voltage is represented by the following equation.

$$Vrms = a(2/f_{clock})^{1/2} \quad V/Hz^{1/2} \qquad (3.4)$$

$$\text{Noise bandwidth(2 pole filter)} = 1.11f_{3dB} \qquad (3.5)$$

where a is the half amplitude of the output voltage swing.

A typical loop response is shown in Figure 48.

Fig 48: PLL Response to FM Input with Added Noise

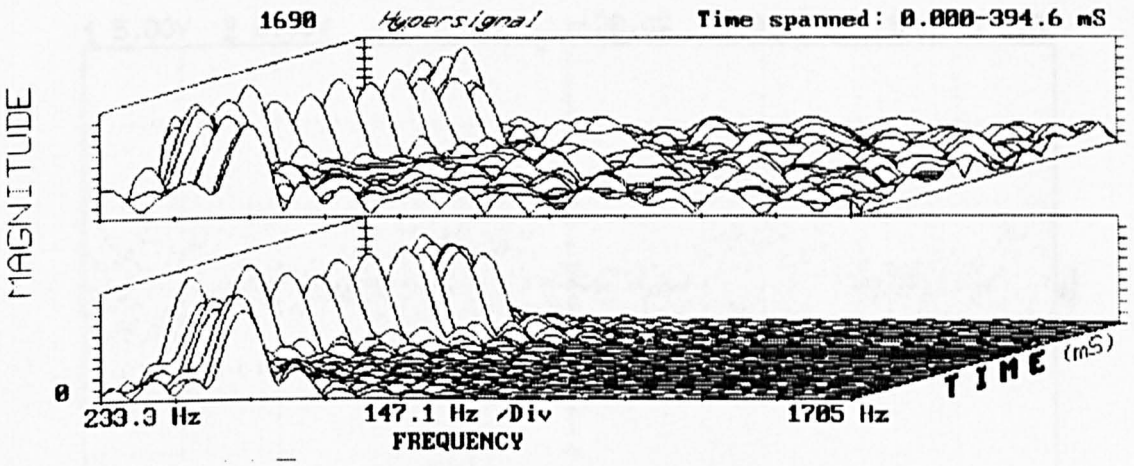

The upper trace shows the spectrum of the input signal to the tracking bandpass filter, consisting of an FM signal with noise added giving a s/n ratio of 0.65dB. The lower trace shows the output of the tracking bandpass filter under control of the phase locked loop. The

centre frequency of the filter tracks the signal frequency accurately in the presence of the input noise and passes only a narrow band noise free signal.

The s/n ratio of the input signal to the loop was adjusted by increasing the depth of amplitude modulation to the signal with a constant noise component added. The unmodulated signal input level was typical of quiet speech. Figure 49 shows, on Trace1, an input signal amplitude modulation of 30% resulting in a s/n ratio modulation of 6.3dB → -4.6dB and, on Trace 2, the Lock Quality maintaining lock throughout the modulation with the momentary exceptions at the instant of change in modulation.

Figure 49: PLL Response to a Noisy Input.

Input Noise Modulation 6.3dB → -4.6dB

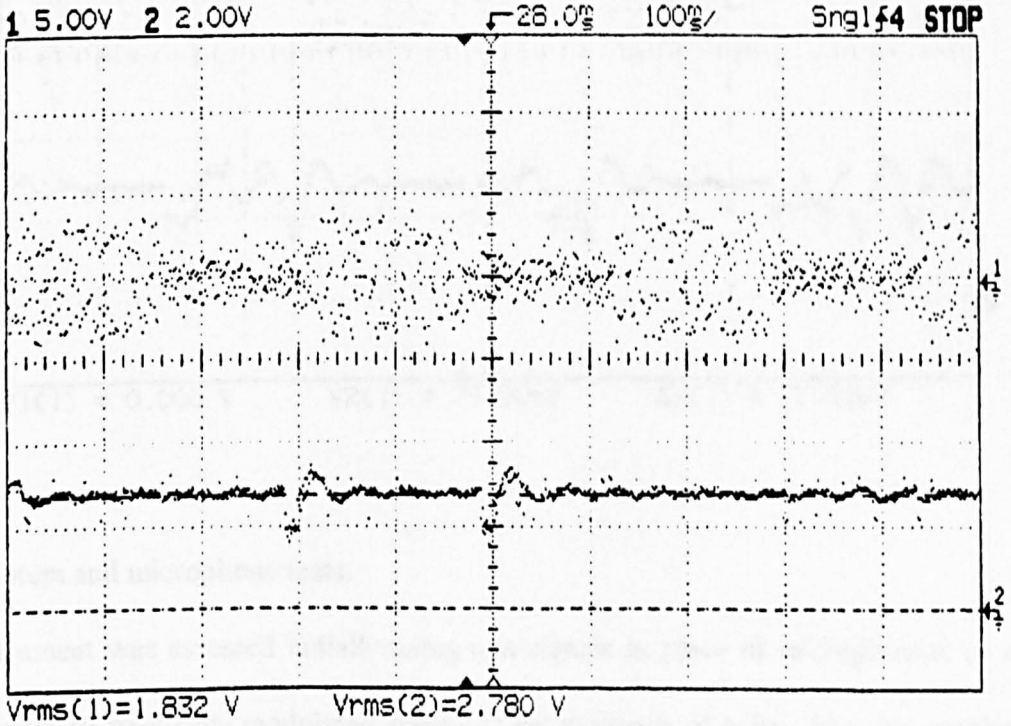

Figure 50 shows, on Trace 1, an input signal modulation of 50% resulting in a s/n ratio modulation of 6.3dB → -8.9dB and, on Trace 2, the Lock Quality losing lock during the lower s/n periods. Further results showed the loop maintaining lock up to a maximum s/n ratio of -8.0dB which was considered to adequately cover the s/n ratio range that would be encountered in clinical practice.

Figure 50: PLL Response to a Noisy Input.

Input Noise Modulation 6.3dB → -8.9dB

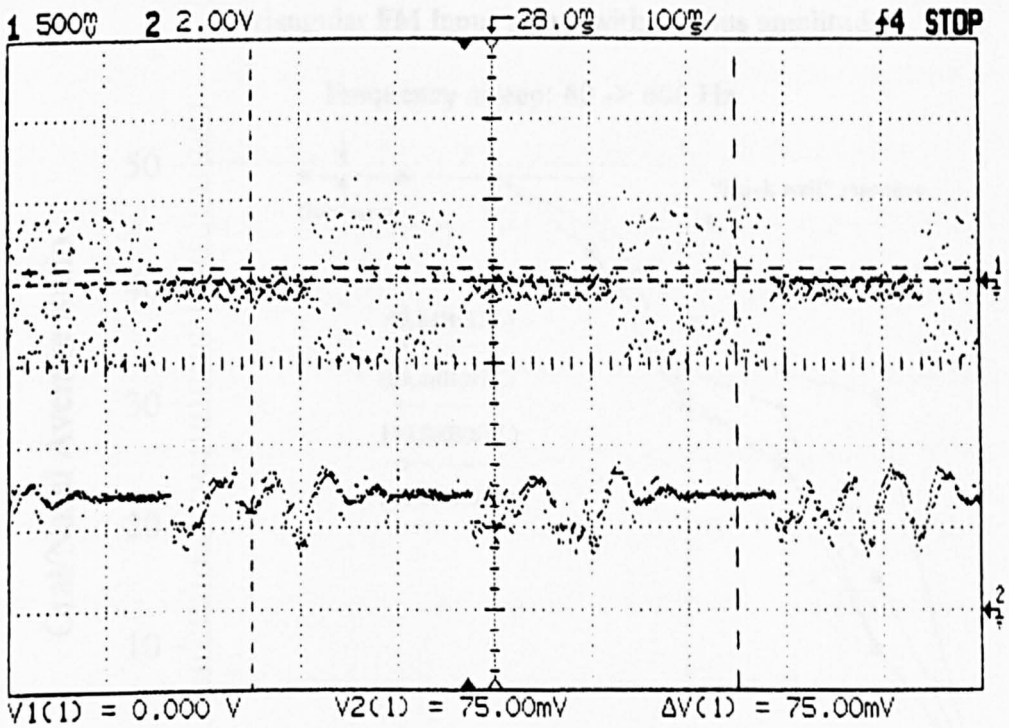

3.2.3 System and microphone tests.

The instrument was assessed initially using test signals in place of microphones, to establish the response to frequency modulated signals in the presence of noise, linearity, resolution and accuracy. The clinical microphones were then assessed in conjunction with the instrument response. Using the instrument in clinical mode, an appraisal of the measurement uncertainty

due to patient movement and position was made. A final instrument specification could then be written.

The system response to frequency modulated, noisy input signals was tested by connecting to the nasal and oral microphone inputs, various clinically typical, amplitude variable FM signals. The results are shown in Figure 51.

Figure 51: System Response to Frequency Modulated Input

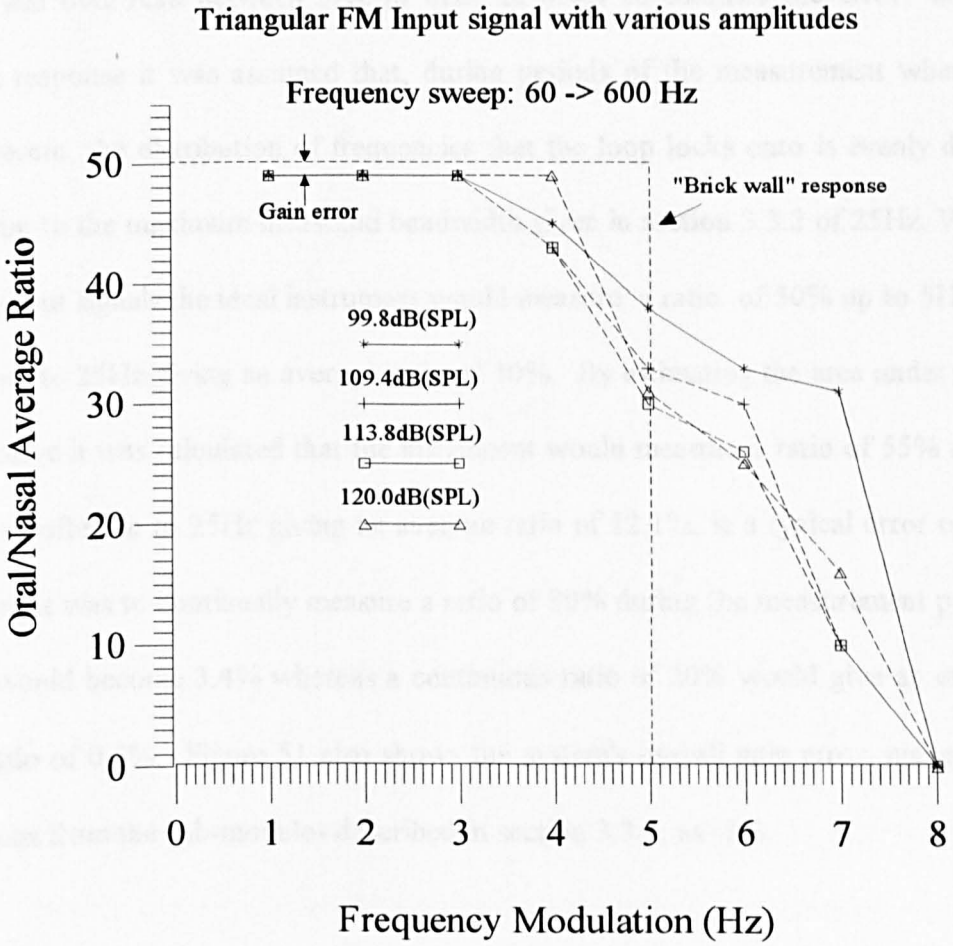

The y-axis shows the magnitude of the average ratio that the instrument measured, during individual measurement periods of 20 seconds with equal amplitude nasal and oral inputs, for the range of input FMs shown on the x-axis. The results show that the instrument clearly discriminates FM signals of 3Hz or less as noise free and thereafter consistently measures the

nasal:oral ratio for a typical set of clinical input amplitudes. FM signals of 8Hz or above are assessed by the instrument as noisy, therefore rejected and no measurements commenced. The graph reveals that, for FM signals between 3Hz and 8Hz, the instrument demonstrates a band of uncertainty that will introduce an error into the measurements. The ideal response for the instrument as discussed in Section 3.1.2.1 would be a "brick-wall" low pass filter, as shown in Figure 51, with the ratio changing instantaneously from maximum to zero at the 5Hz threshold. The actual response however, gives results that will under-read between 3Hz to 5Hz, and will over-read between 5Hz to 8Hz. In order to estimate the error due to this instrument response it was assumed that, during periods of the measurement when random noise is present, the distribution of frequencies that the loop locks onto is evenly distributed from 0Hz up to the maximum measured bandwidth given in section 3.3.2 of 25Hz. With equal amplitude input signals the ideal instrument would measure a ratio of 50% up to 5Hz and 0% thereafter up to 25Hz giving an average ratio of 10%. By estimating the area under the actual response curve it was calculated that the instrument would measure a ratio of 55% up to 8Hz and 0% thereafter up to 25Hz giving an average ratio of 12.1%, ie a typical error of 2.1%. If the instrument was to continually measure a ratio of 80% during the measurement period then the error would become 3.4% whereas a continuous ratio of 20% would give an error in the average ratio of 0.5%. Figure 51 also shows the system's overall gain error, made up of the contributions from the sub-modules described in section 3.3.1, as -1%.

Figure 52 demonstrates the response of the instrument when a random noise signal, as previously described in Section 3.2.2, was added to the nasal signal. The graph shows, in the same manner as the previous test when the signals were perturbed by FM, that a band of uncertainty occurs in the measurement. This arises as the frequency modulations of the loop

lock occupy the band 3Hz to 8Hz which occur, as Figure 52 shows, within a band of s/n ratio of 1dB to 8dB.

Figure 52: System Response to a Variable S/N Ratio Input

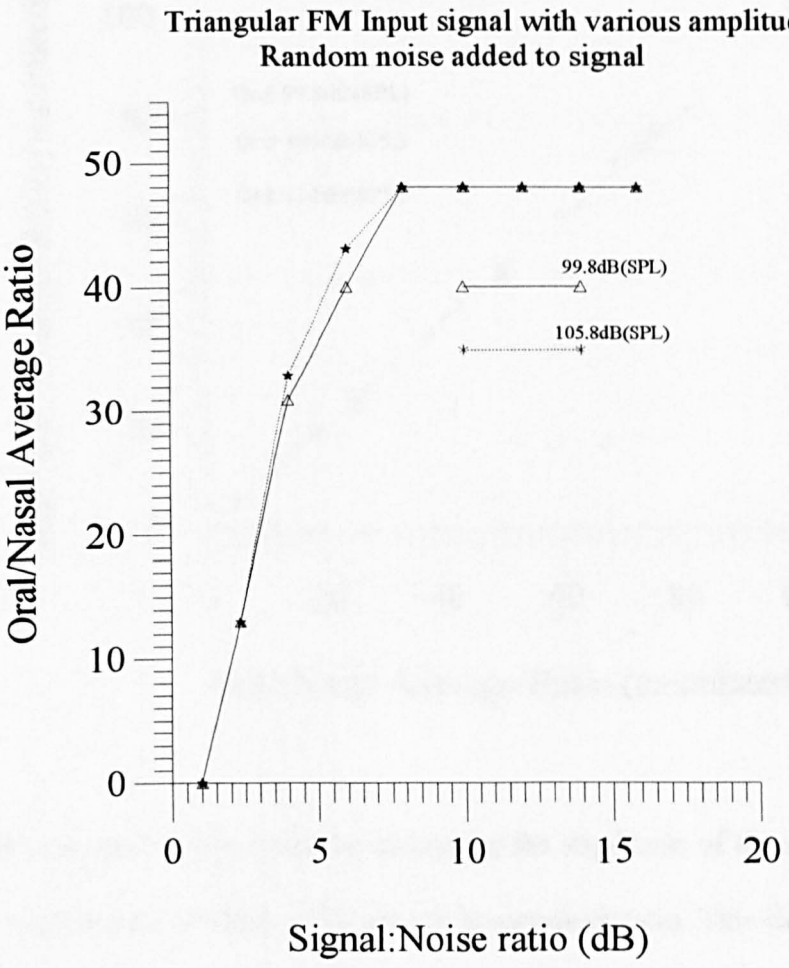

The instrument's linearity and accuracy were tested by introducing FM signals into the oral and nasal channels and then progressively altering the amplitude of the nasal signal through the clinical measurement range. Figure 53 shows the oral:nasal ratio measured by the instrument on the y-axis and the ratio, calculated from the input amplitudes, on the x-axis. Various typical oral amplitudes were tested with swept nasal signal levels. The results showed that the linearity was <1%.

Figure 53: System Linearity

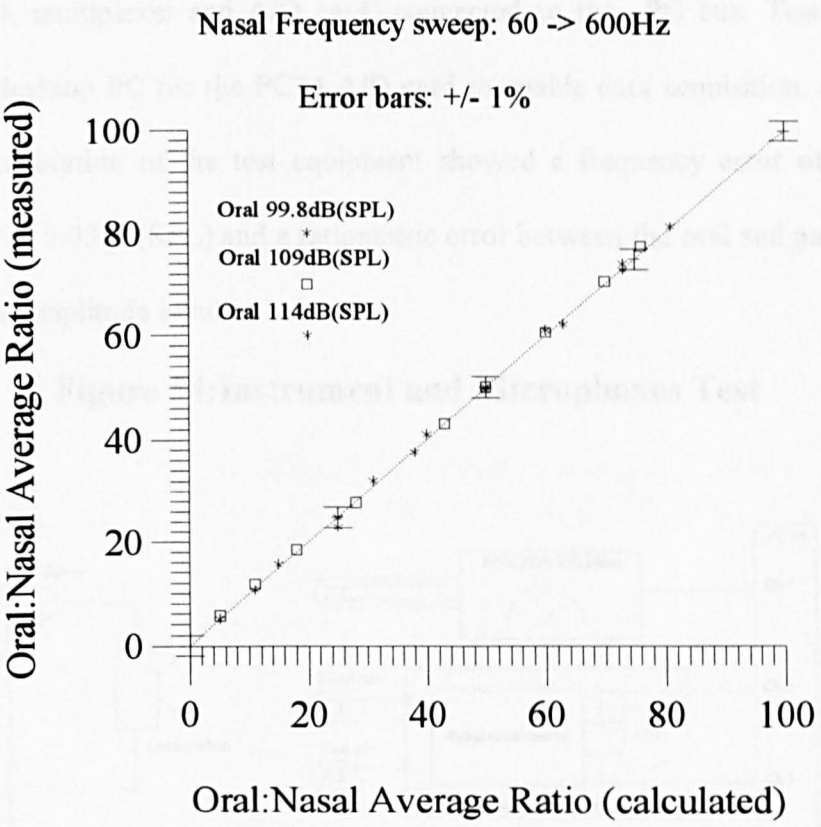

The instrument's resolution was tested by increasing the amplitude of the nasal channel with respect to the oral channel to effect a 1% change in measured ratio. This change corresponded to a sound pressure level of -10dB(SPL) at 1 metre, therefore less than the human hearing threshold.

The clinical microphones were tested in conjunction with the instrument using the test arrangement shown in Figure 54. In the same manner as section 2.2.1, the microphones were placed equidistantly from the sound source and in the same plane as the B&K 2230 sound pressure level meter. The analogue signals from the nasal and oral channels of the instrument,

the SPL meter output, and a voltage from the signal generator indicating FM/AM were analysed on a desktop PC. The digitisation of these signals was accomplished using an Amplicon PC74, multiplexer and A/D card, connected to the PC bus. Test software was written on the desktop PC for the PC74 A/D card to enable data acquisition, calibration and display. The calibration of the test equipment showed a frequency error of +/- 1Hz, an amplitude error of 0.03dB(SPL) and a ratiometric error between the oral and nasal channels of 0.005 with equal amplitude inputs.

Figure 54:Instrument and Microphones Test

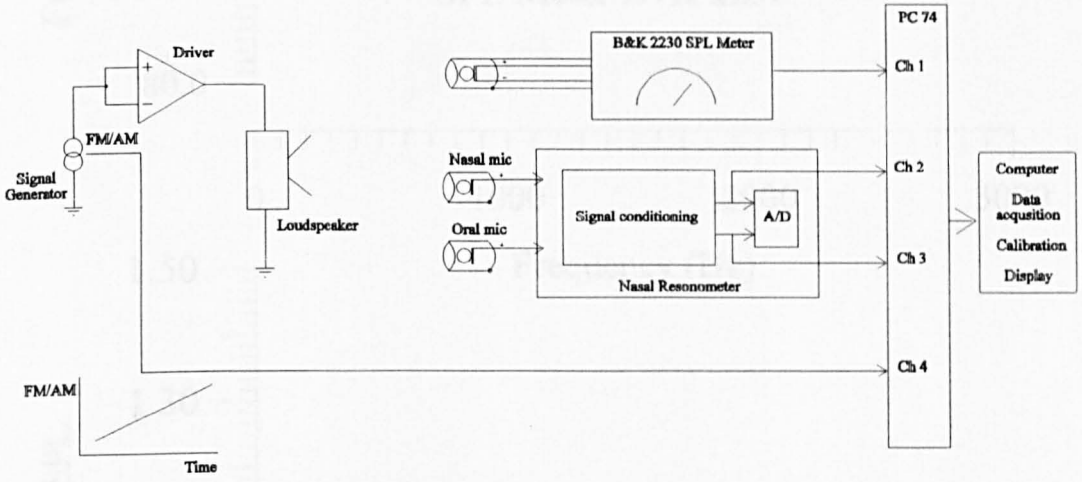

Figure 55 shows the response of the instrument to a variable freefield sound pressure, frequency modulated between 400Hz to 3kHz. The ratiometric error remained <2% throughout the frequency and amplitude range that the instrument was expected to encounter clinically.

Figure 55: Microphones' Response to FM Freefield Sound Pressure

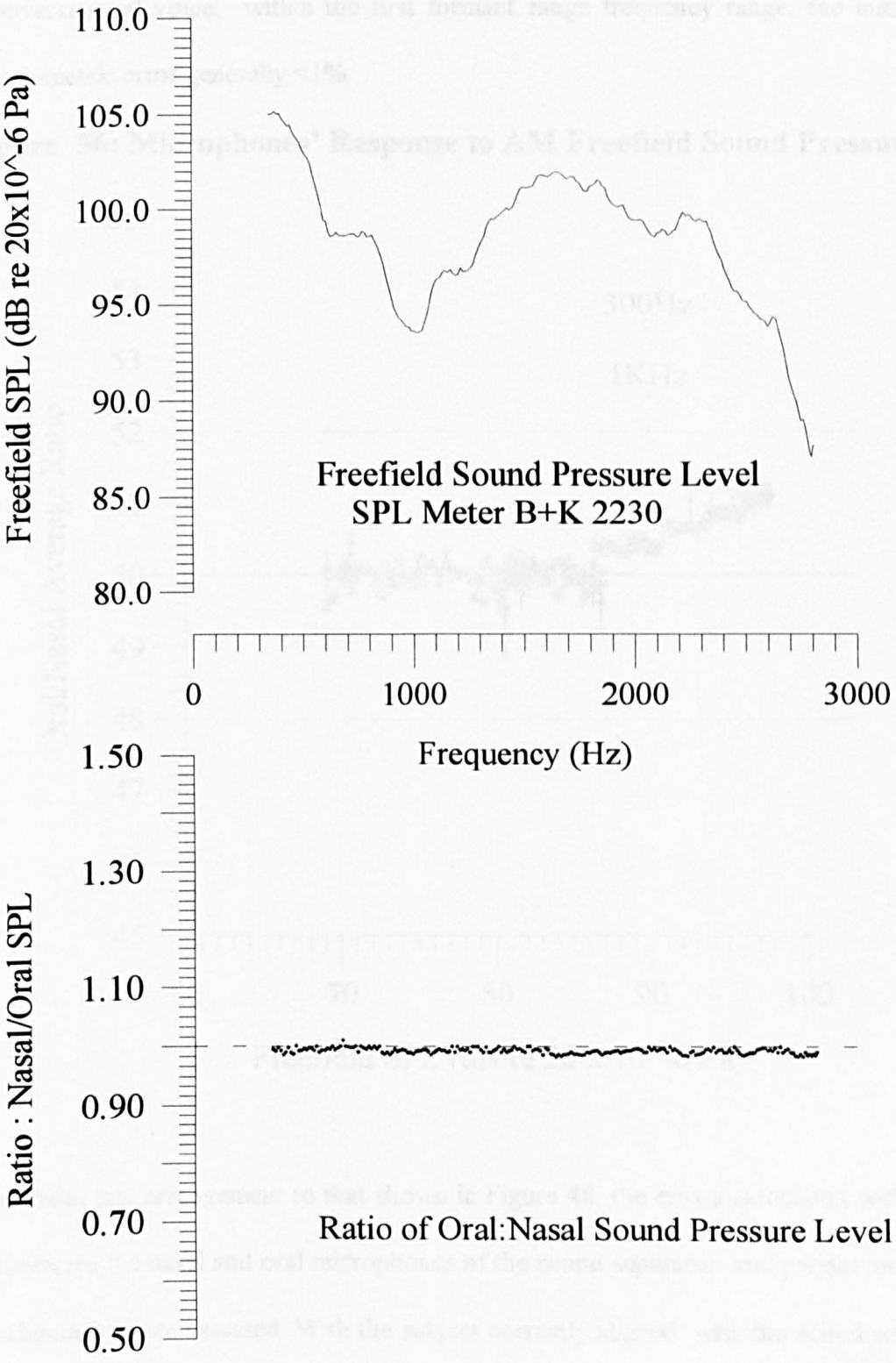

Figure 56 shows that for low amplitude sound, approximately equivalent to a whisper up to a quiet conversational voice, within the first formant range frequency range, the instrument gave a ratiometric error generally <1%.

Figure 56: Microphones' Response to AM Freefield Sound Pressure

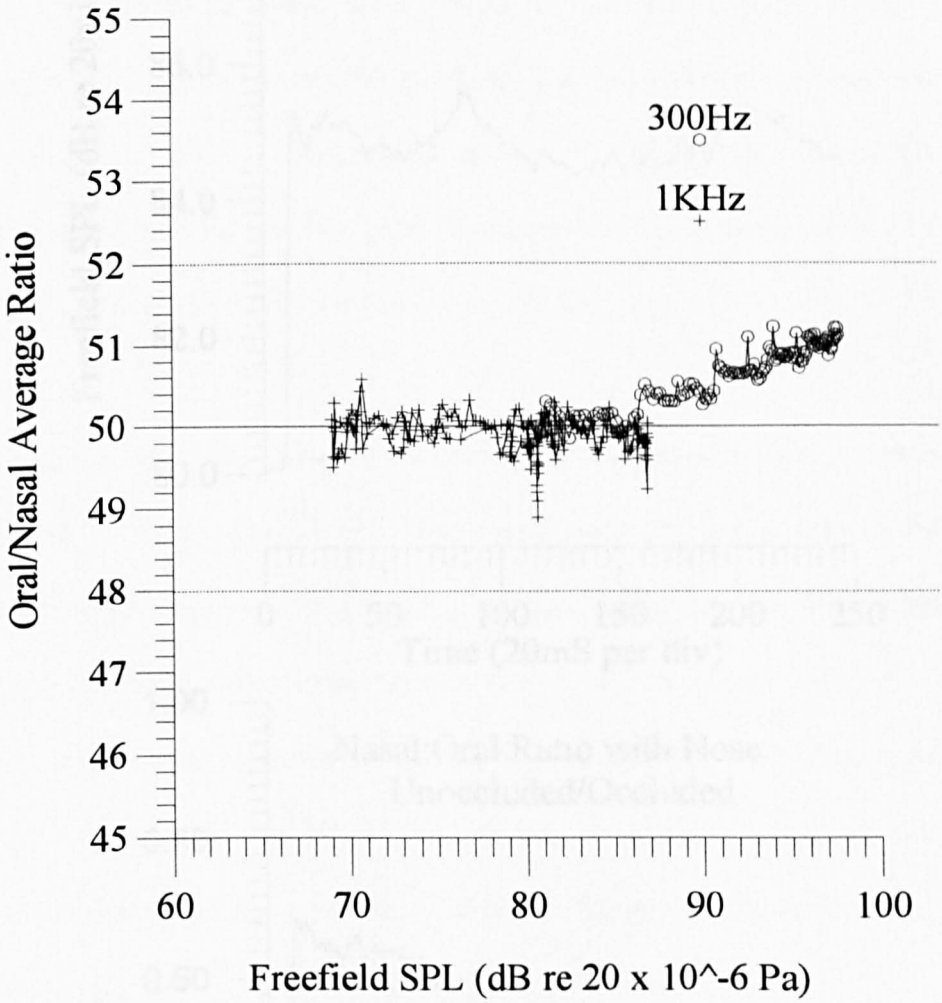

Using a similar test arrangement to that shown in Figure 48, the errors associated with sound leaking between the nasal and oral microphones of the sound separator and patient movement and misalignment were assessed. With the subject correctly aligned with the sound separator, a sustained /i/ vowel was phonated with the nares unoccluded, then occluded by

Figure 57: Sound Separator Leakage Test

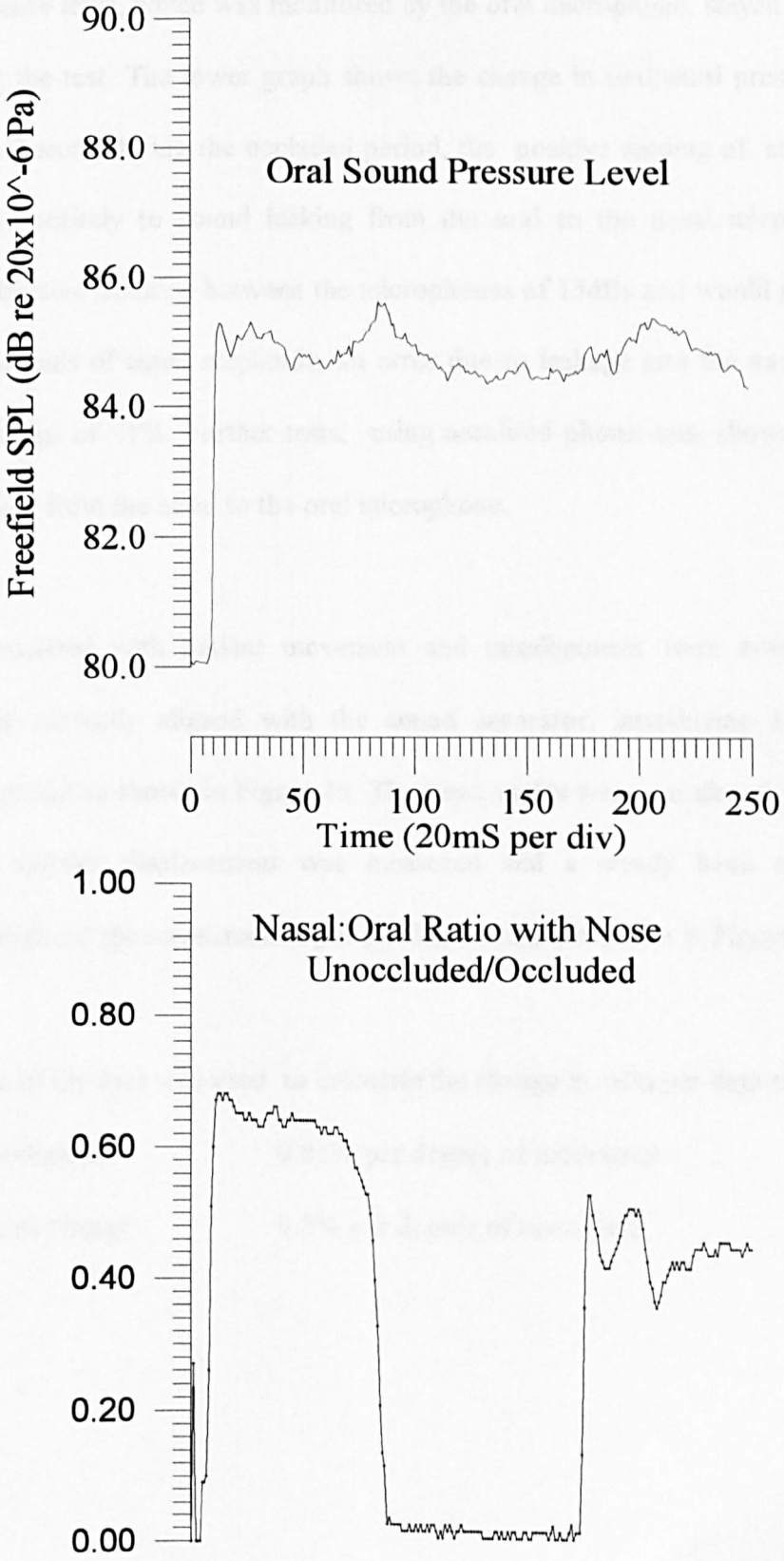

simply pinching the nose and then unoccluded. The upper graph of Figure 57 shows that the oral sound pressure level, which was monitored by the oral microphone, stayed approximately constant during the test. The lower graph shows the change in oral:nasal pressure ratio as a result of the occlusion. During the occluded period, the positive reading of an average ratio of 0.02 is due entirely to sound leaking from the oral to the nasal microphone. This represents an effective isolation between the microphones of 15dBs and would introduce, with oral and nasal signals of equal amplitude, an error due to leakage into the nasal microphone from the oral signal of <1%. Further tests, using nasalised phonations, showed very similar results for leakage from the nasal to the oral microphone.

The errors associated with patient movement and misalignment were assessed with the subject, initially correctly aligned with the sound separator, introducing a horizontal or vertical misalignment as shown in Figure 15. The head angles were not directly monitored but the maximum angular displacement was measured and a steady head movement was maintained throughout the measurement period. The results are shown in Figure 58.

A linear portion of the data was used to calculate the change in ratio per degree as follows.

Vertical change:	0.85% per degree of movement.
Horizontal change:	0.5% per degree of movement.

Figure 58: Measurement Error Due to Head Movement

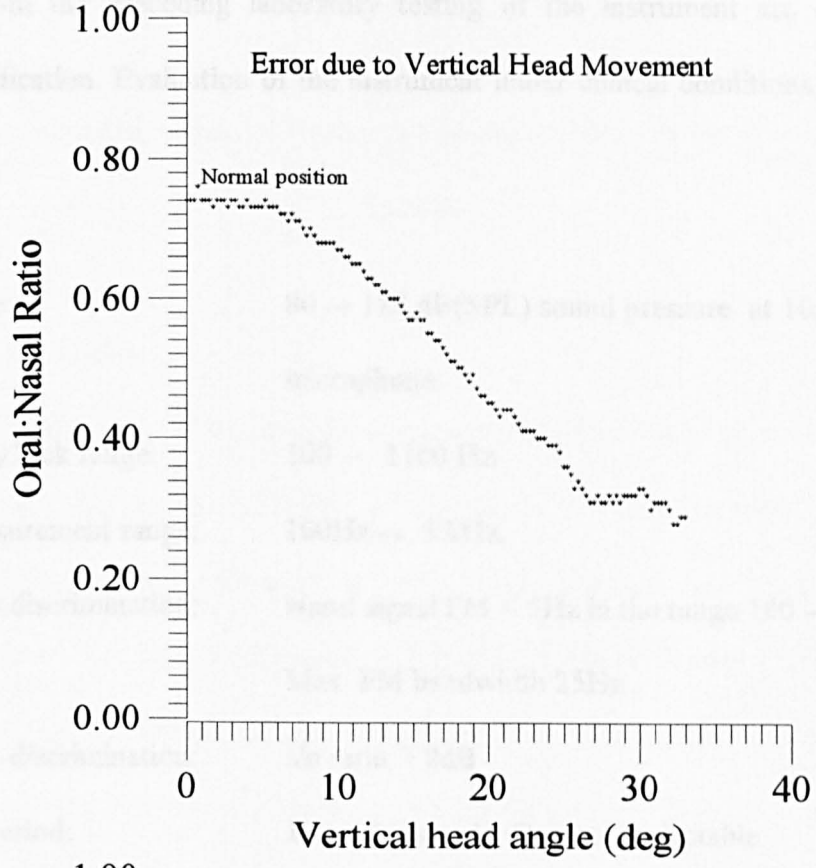

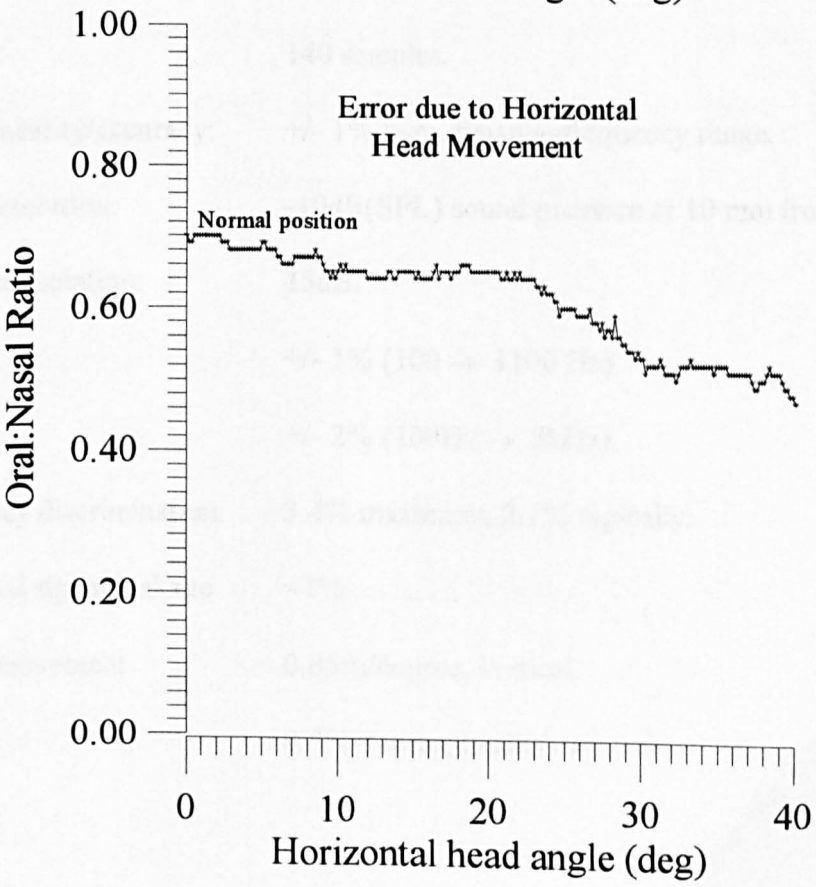

3.2.4 Instrument specification

The results from the preceding laboratory testing of the instrument are collated in the following specification. Evaluation of the instrument under clinical conditions is presented in Chapter 4.

Dynamic Range:	80 → 128 dB(SPL) sound pressure at 10mm from the microphone.
Nasal frequency lock range:	100 → 1100 Hz.
Frequency measurement range:	100Hz → 5 kHz.
Lock frequency discrimination:	Nasal signal FM < 5Hz in the range 100 → 1100 Hz. Max. FM bandwidth 25Hz
Lock amplitude discrimination:	s/n ratio > 8dB
Measurement period:	1 → 20 seconds. Operator selectable.
Samples/period:	140 samples.
Measurement linearity/accuracy:	+/- 1% over dynamic/frequency range.
Measurement resolution:	-10dB(SPL) sound pressure at 10 mm from microphone.
Nasal/Oral signal isolation:	15dB.
Errors: Gain	+/- 1% (100 → 1100 Hz).
	+/- 2% (100Hz → 5kHz).
Frequency discrimination	3.4% maximum, 2.1% typically.
Oral/nasal signal leakage	<1%
Patient movement	0.85%/degree, vertical.
	0.5%/degree, horizontal.

Chapter 4.

Nasal Resonometer. Clinical Evaluation, Measurement Protocol and Clinical Studies

4.1 Clinical Evaluation

The clinical evaluations of the instrument were conducted prior to its introduction for clinical use, in order that the reliability and limitations of the device could be assessed. The formal trials were conducted in the Speech Therapy and Medical Physics Departments of The London Hospital and Highgate Junior School, North London. Several informal evaluations, to test the practical operation of the instrument in it's intended operating environment, were carried out by speech therapists in several local schools and, as a result, various changes were made to the software controlling the operator interface. These modifications did not affect the measurement principles or instrument parameters and therefore, are not detailed herein.

4.1.1 System response to speech

The instrument's response to a variety of audio input signals with known parameters, generated from test equipment, is detailed in Chapter 3. To initially evaluate the response to typical patient phonations, a trained speech therapist emulated the five single vowels sounds, each sequentially containing three elements. The first element

contained normal speech, the second included uncontrolled nasal emmision and the third consisted of a discernible degree of hyper-nasalised speech.

Typical results are shown in Figures 59, 60 and 61 which show the signals, NASAL on channel 1, LOCK QUALITY on channel 2 and A on channel 3. The digital signal A is part of a two bit output from the microprocessor that switches one of the four harmonic frequencies to the tracking bandpass filters. When no phase lock is present the processor continuously monitors the fundamental frequency and A remains high, however when phase lock is detected the instrument begins to acquire data and A is toggled. This signal therefore acts as an indicator that the instrument has "decided" that the signal is noise free and is therefore acquiring data. Figure 62 shows a photograph of the screen during the measurement period when the three phonetic elements are sequentially present.

Figure 59: Vowel sound i (as in feet). Normal speech.

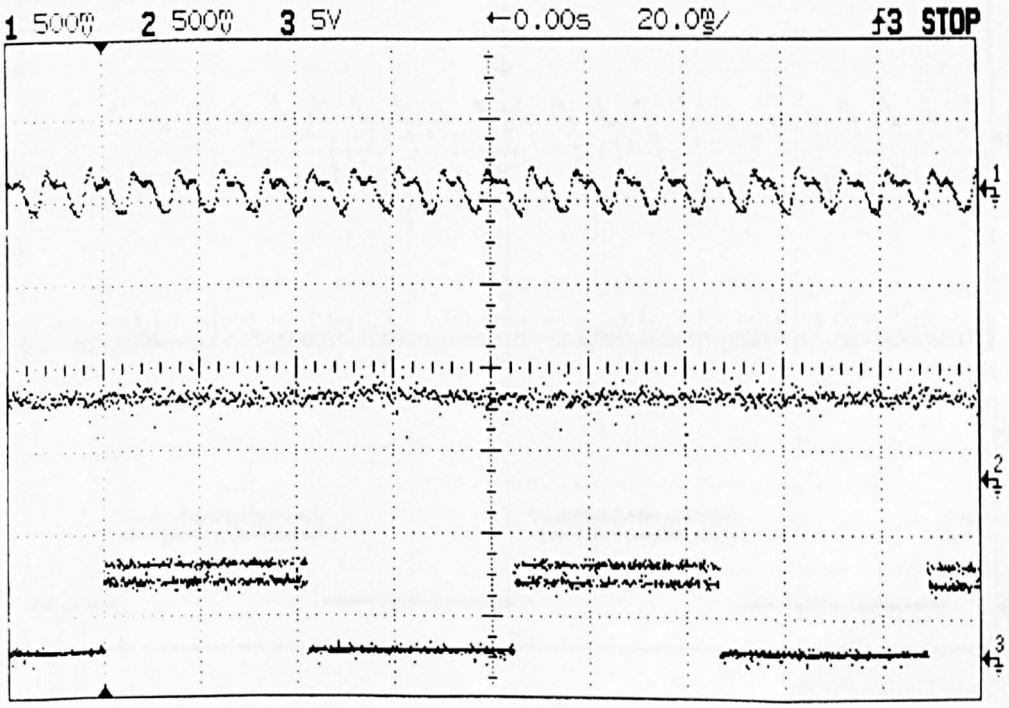

Figure 60: Vowel sound i. Emissive noise present.

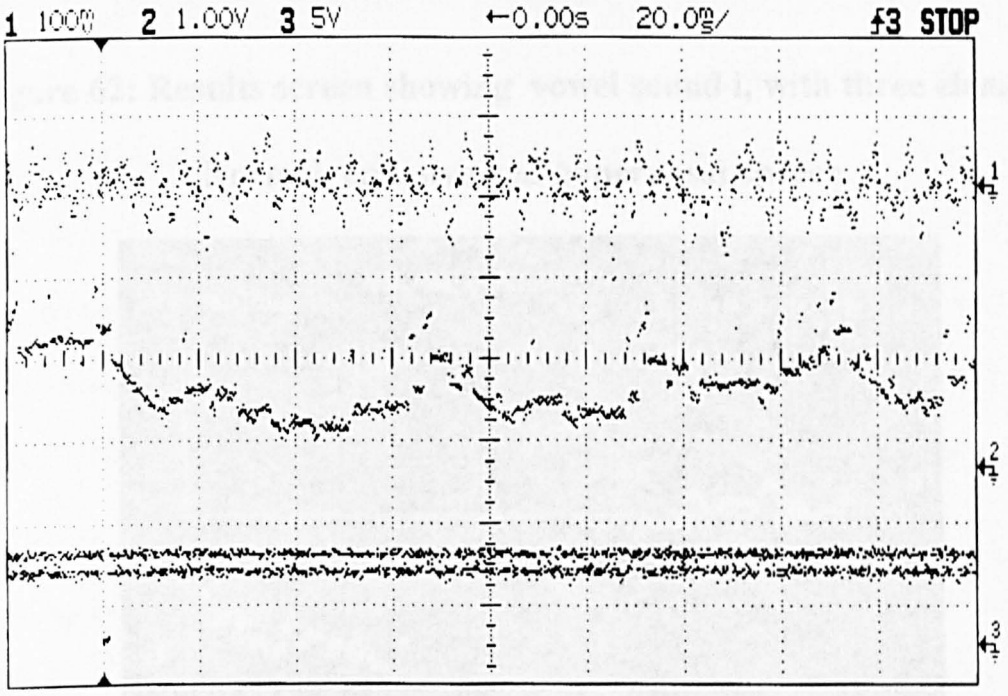

Figure 61: Vowel sound i. Hypernasal speech present.

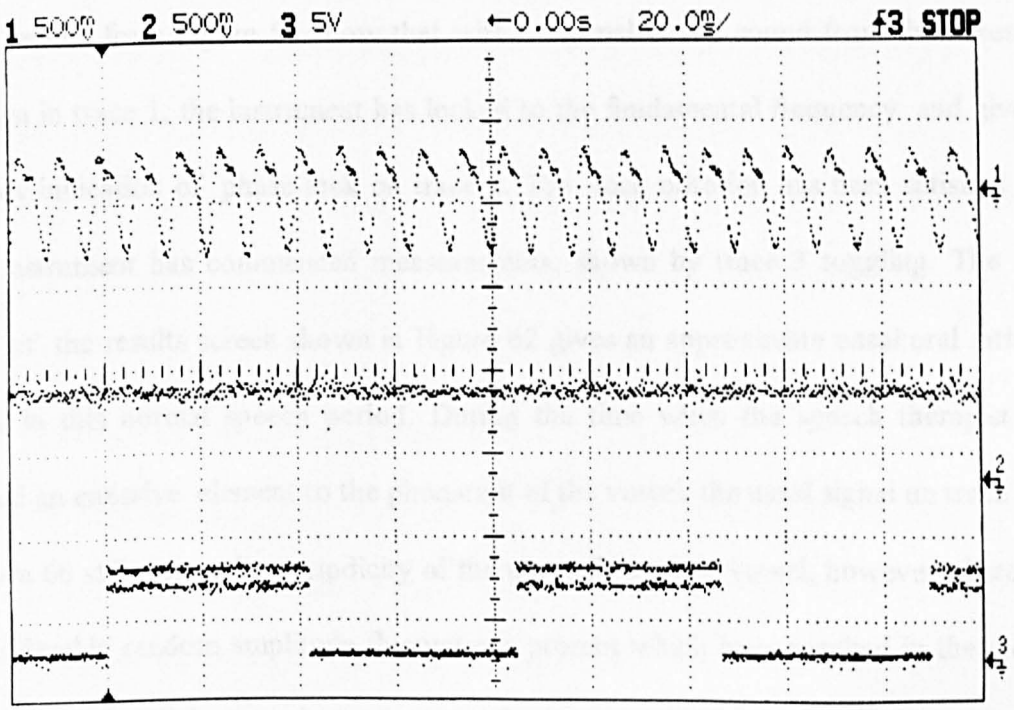

Figure 62: Results screen showing vowel sound i, with three elements. Normal, emissive and hypernasal speech.

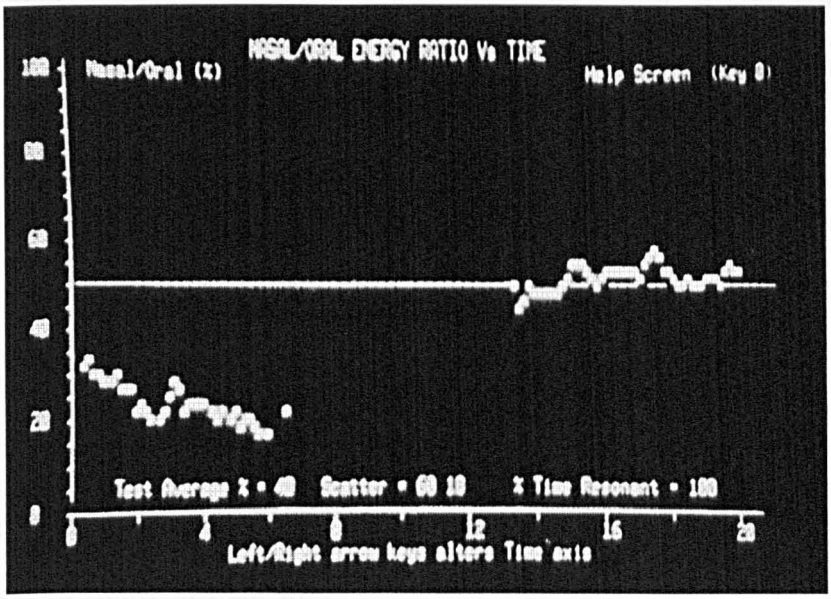

The results from Figure 59 show that with a normal vowel sound from the nares, as shown in trace 1, the instrument has locked to the fundamental frequency and gives a steady indication of phase lock on trace 2. The lock criterion has been satisfied and the instrument has commenced measurements, shown by trace 3 toggling. The first part of the results screen shown in Figure 62 gives an approximate nasal:oral ratio of 20% in this normal speech period. During the time when the speech therapist has added an emissive element to the phonation of the vowel, the nasal signal on trace 1 of Figure 60 still shows the periodicity of the normally spoken vowel; however, there are considerable random amplitude fluctuations present which have resulted in the steady phase lock being lost as shown in trace 2. As a result, the instrument has stopped

measurements, depicted by the DC state of trace 3 and the region of "no readings" in Figure 62. During the third period of phonation when a hyper-nasal element has been added to the vowel, Figure 61 trace 1 shows the periodic waveform has become re-established in the NASAL signal but at a higher amplitude than the normal speech. An increase in sound pressure could be attributed to a change in the overall volume of the test, however the lowering of the velum to emulate hyper-nasal speech would also divert sound energy to the nasal cavity resulting in an increase in nasal sound pressure. Trace 2 shows a steady phase lock with an upward shift in frequency, compared to normal speech, of approximately 50 Hz which is consistent with the predicted behaviour (28) of the first formant with an added degree of nasal coupling . During this period of hyper-nasal speech, trace 3 depicts that the instrument has recommenced measurements as shown in the third time period of Figure 62 where the nasal:oral ratio has risen to approximately 50%.

Results from the remaining four vowel sounds also consistently demonstrated the instrument's ability to discriminate between emissive and hyper-nasal sound. Although not quantitative in nature, these tests indicated that in principle, the instrument worked effectively with signals originating from patients and normal subjects and therefore the assessment of the instrument was broadened to a full clinical evaluation.

4.1.2 Evaluation protocol and measurements

The clinical evaluation of the instrument was based upon the set of phonetic test material shown in Appendix 1, subdivided into the following categories. Vowels, unvoiced fricatives and plosives, non-nasalised single words, nasalised single words, non-nasalised sentences, nasalised sentences and an extended non-nasalised passage.

The construction of the non-nasalised single words was chosen as, *consonant-vowel-consonant* with at least one example each of high, medium and low vowels embedded between both voiced and unvoiced consonants. The nasalised single words were designed so as to include the high, medium and low vowels preceded by a single opening gesture of the velum, as in the case of *m* in *more* and embedded within an open-close-open gesture, as in the case of *m* and *n* in *mean.*

The subjects for the evaluation were subdivided as a group of 18 normal adult females between the ages 22 and 40 years, 15 normal adult males between the ages 24 and 35 years, 36 normal children between the ages 7 and 14 years and a group of 24 hyper-nasal patients between the ages 7 and 40 years. The patient group contained patients with repaired and non repaired clefts of both the hard and soft palate or velopharyngeal insufficiency, such that a degree of hyper-nasality was subjectively detected by a speech therapist.

The phonetic material and the test procedure were carefully described to each subject prior to measurements being taken. The speech therapist would initially prompt the subject with the phonation and thereafter the subject would repeat the test unprompted. In the case of vowel and single words, the subject was instructed to repeat the sound five times, of which only the middle three were measured in order that "end effects" noted on the first and last phonation were excluded. Sentences were repeated twice and the extended passage read through or, in the case of reluctant children, repeated once.

The trial was designed to test several hypotheses as described below.

- The instrument's measurement errors do not introduce a significant variation in results.

- There is no significant variation in measurements within phonetic categories in normal subject groups.
- There is no significant variation in measurements between normal subject groups tested using identical phonations.
- There is a significant variation between the normal groups and the hypernasal group tested using identical phonations.
- The retesting over time does not introduce a significant variation within any subject group.

The trials were designed such that for each hypothesis two or more sets of data, characterised by their sample means χ_i χ_j, were measured and the null hypothesis H_o tested. ie H_o: $\chi_i = \chi_j = \chi$

The statistic considered most appropriate for these tests was the one way analysis of variance. This method of testing the total variation between groups of results, partitions the variation into two components; one analyses the variation *within* the group and the second assesses the variation *between* groups. These two components are then compared by means of a test of significance, the F-test. The procedure of comparing different components of variation is called the analysis of variation.

The within group variation, s^2 or residual variation is given by:

$$s^2 = \sum_{i=1,c} \sum_{j=1,n} (x_{ij}-\chi_i)^2/c(n-1)$$

where c is the total number of groups, i (=1,c) denotes an individual group
n is the number of tests within the group, j (=1,n) denotes an individual test
x_{ij} is an individual test within a group , ie test j within group i
χ_i is the mean of group I

The between group variation, s_B is given by:

$$s_B^2=\sum_{i=1,c} (\chi_i- \chi)^2/(c-1)$$

where χ is the mean of all tests.

If H_o is true then s^2 and s_B^2 will be estimates of the variance and the ratio

$$F = s_B^2 / s^2$$

will follow an F-distribution. However if H_o is not true, s^2 will still be an estimate of the variance but s_B^2 will increase due to differences between the groups and so the F-ratio may be significantly large and H_o is rejected.

The F-distribution is derived from the following. Given two sets of tests, numbering c and n tests , taken from a large normal distribution then the ratio of their variances, s_c^2/s_n^2 would be close to unity. Repeated pairs of samples, of size c and n, will result in a distribution of ratios called the F-distribution. The distribution relies upon the degrees of freedom of s_c^2 and s_n^2 which are given by c-1 and n-1. The significance test is carried out by comparing the measured F-ratio with a figure derived from standard tables that summarise the F-distribution.

The trials were also designed to establish the typical range of nasal:oral ratios within the normal subjects in order that the threshold ratio between normal and hypernasal speech could be established.

- Hypothesis: The instrument's measurement errors do not introduce a significant variation in results.

Test: A single set of phonetic test material containing 20 phonations from a hyper-nasal patient, recorded as part of a subsequent trial, was played and then replayed from tape 41 times into the instrument, giving a total of 820 tests. The results were subdivided into 7 groups, each containing 6 sets of data that were analysed for within group variation and the 7 groups were analysed for between group variation. Results are shown in Tables 5 and 6.

Table 5. Variation in play/replay. $F_{5,36} = 3.59$							
Vowels		Non nasalised words		Non nasalised sentences/passage		Nasalised words/sentences	
	F ratio		F ratio		F ratio		F ratio
i	0.70	Book	0.66	Book	1.00	Man	0.62
u	0.25	Car	2.38	Jigsaw	1.49	Mean	1.89
ae	0.39	Cat	1.20	Ship	0.44		
>	0.39	Hat	0.06	Day	1.30	Bang	1.84
a	1.64	Talk	1.85			'99'	0.70
				Passage	1.36	Many	0.34

Table 6. Play/replay data				
Phonation	**Mean Ratio(χ)**	**Std Dev(σ)**	**95% CI**	**Std Error**
Vowels				
i	75.90	5.56	74.1 → 77.6	0.85
u	38.33	4.95	36.8 → 39.6	0.76
ae	56.74	5.95	54.9 → 58.5	0.91
>	22.05	3.91	20.8 → 23.2	0.60
a	49.79	2.67	48.9 → 50.6	0.41
Non nasalised words				
Book	2.05	4.42	0.35 → 3.78	0.83
Car	39.68	3.19	38.7 → 41.4	0.64
Cat	43.71	5.88	40.3 → 44.7	1.07
Hat	27.18	5.21	25.1 → 29.1	0.98
Talk	9.81	3.66	9.1 → 12.1	0.71
Nasalised words/sentences				
Man	72.88	3.69	71.7 → 74.0	0.57
Mean	86.05	1.65	85.5 → 86.5	0.25
Bang	61.45	6.14	59.5 → 63.3	0.95
99	72.40	5.60	70.6 → 74.1	0.86
Many	67.42	9.22	64.7 → 70.4	1.42
Non nasalised sentences/passage				
Book	9.52	5.35	7.8 → 11.1	0.82
Jigsaw	27.52	4.46	26.1 → 28.9	0.68
Ship	35.17	4.34	33.8 → 36.5	0.67
Days	28.98	5.35	27.3 → 30.6	0.82
Passage	34.93	3.87	33.7 → 36.1	0.59

To test for significant variation within this data containing 6 sets of 7 samples, an F-test with degrees of freedom 5 and 36 (corresponding to n-1 and c-1) was performed, giving a value of 3.59. In all cases the measured F ratios shown in Table 5 are less than this value which demonstrates that variations between each set of samples are not significantly different and therefore the null hypothesis is proven, that is, the instrument's measurement errors do not introduce significant variation into the results.

The 95% CI column given in Table 6 shows the range within which the mean of the results will occur with a confidence level of 95%; that is, the mean will be found in this range 95 times in every 100 tests. Typically the results show a 95% CI of between 3 and 4 % which is in reasonable agreement with the measured instrument errors previously assessed using test signals, summarised in section 3.2.3. The set of test material contained both hyper-nasal and emissive elements which has resulted in higher mean oral:nasal ratios; this would be expected when compared with the normal subject group, described subsequently. The average standard deviation of all 820 tests for this test material was 4.7 compared with an average standard deviation of 2.9 for identical play/replay tests using recordings from a normal subject. This implied that the error introduced by the instrument had increased due to the presence of hyper-nasal and emissive sound as would be expected due to the uncertainties in the measurement described in section 3.2.3.

- Hypothesis: There is no significant variation in measurements within phonetic categories in normal subject groups.

- Test: The three normal subject groups were tested using a set of phonetic material containing 20 tests, subdivided into 5 phonetic categories, totalling 1380 tests. As previously described, for each group an analysis of variance was carried out within each phonetic category. The results are shown in Table 7 and Figure 62.

Table 7: Variation of measurements from 3 Normal Subject groups within 5 Phonetic Categories

Subject Group	Vowels	Non-nasalised words	Non nasalised sentence	Nasalised words	Nasalised sentence
	$F_{4,\infty}= 3.32$	$F_{4,\infty} = 3.32$	$F_{3,\infty} = 3.78$	$F_{1,\infty}= 6.63$	$F_{2,\infty}= 4.61$
Children	1.16	1.11	0.56	18.00	0.98
Adult Males	1.57	1.20	0.71	9.27	0.20
Adult Females	2.56	3.80	0.51	10.51	1.15

The results in Figure 62(a-d) are displayed in the form of box plots where the inter-quartile range is shown as the rectangular shaded areas which are divided into two parts at the median, a line is drawn to the highest and lowest values in each group. Results that lay within 1.5→ 3 boxlengths of the upper box are shown as a '0', extreme results that fall outside 3 boxlengths are shown as a '*'.

The variation within the vowel phonetic category shown in Table 7 and Figure 62a shows no significant difference in measurements in the case of children and adult males however there is a larger variation within the adult female group. The average standard deviation of all groups is 13.2. In the case of vowel sounds there is no significant variation of measurements taken from normal subject groups and the null hypothesis is accepted.

Fig 62a: Variation within Phonetic Categories

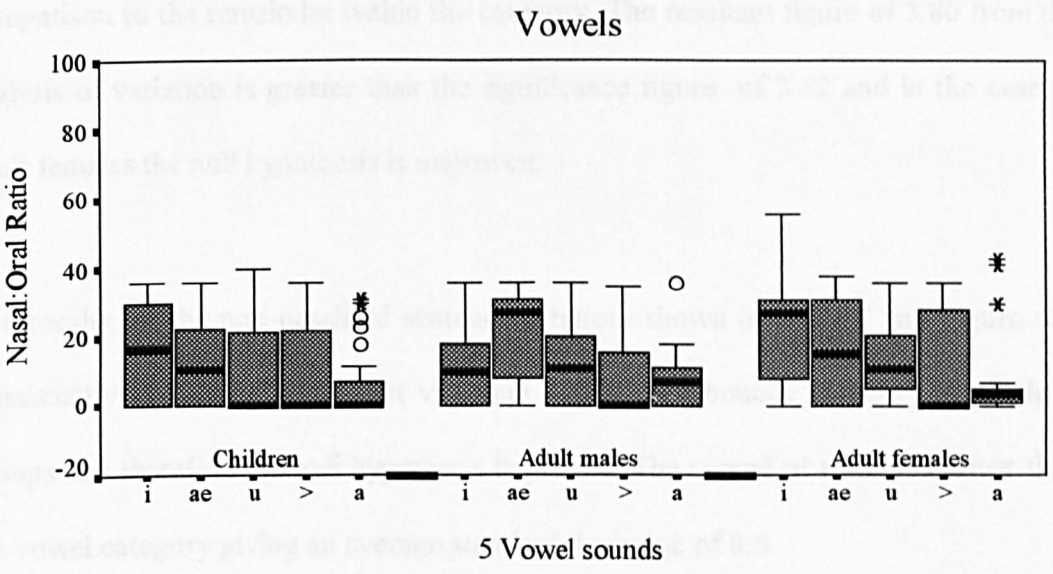

The variation within the non-nasalised words phonetic category is shown in Table 7 and Figure 62b. No significant variation is apparent in the case of children and adult males. These results are similar to the vowel category in terms of variation however the spread of results is smaller which is confirmed by the lower average standard deviation of 8.3.

Fig 62b. Non-nasalised words

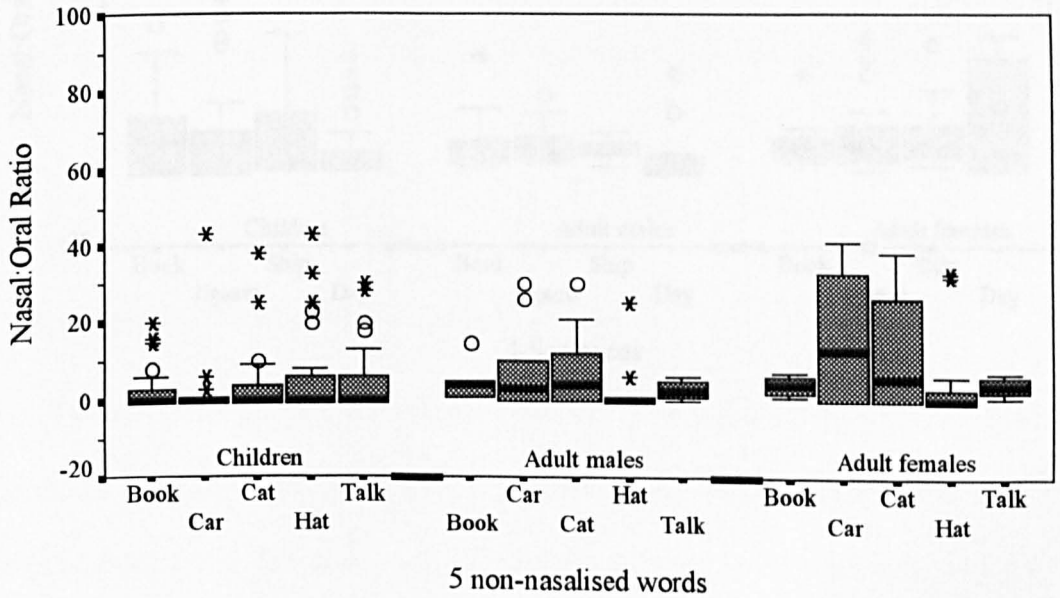

In the case of adult females, the words *car* and *cat* show a striking variation in comparison to the remainder within the category. The resultant figure of 3.80 from the analysis of variation is greater than the significance figure of 3.32 and in the case of adult females the null hypothesis is unproven.

The results for the non-nasalised sentence category shown in Table 7 and Figure 62c consistently reveals no significant variation within the phonetic category in all three groups and therefore the null hypothesis is proven. The spread of results is lower than the vowel category giving an average standard deviation of 8.8.

Fig 62c. Non-nasalised sentences

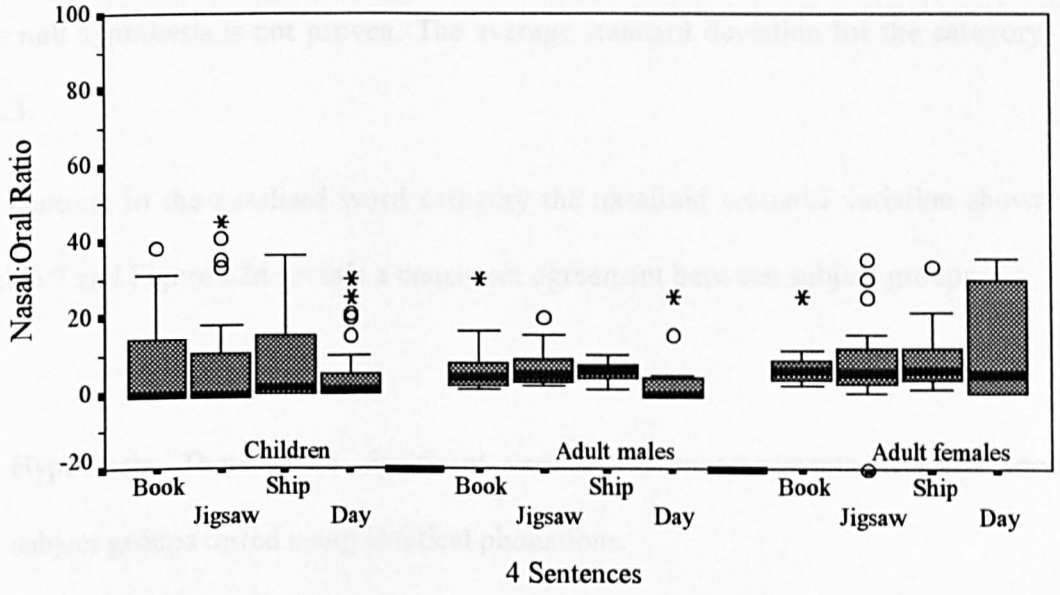

Fig 62d. Nasalised words/sentences

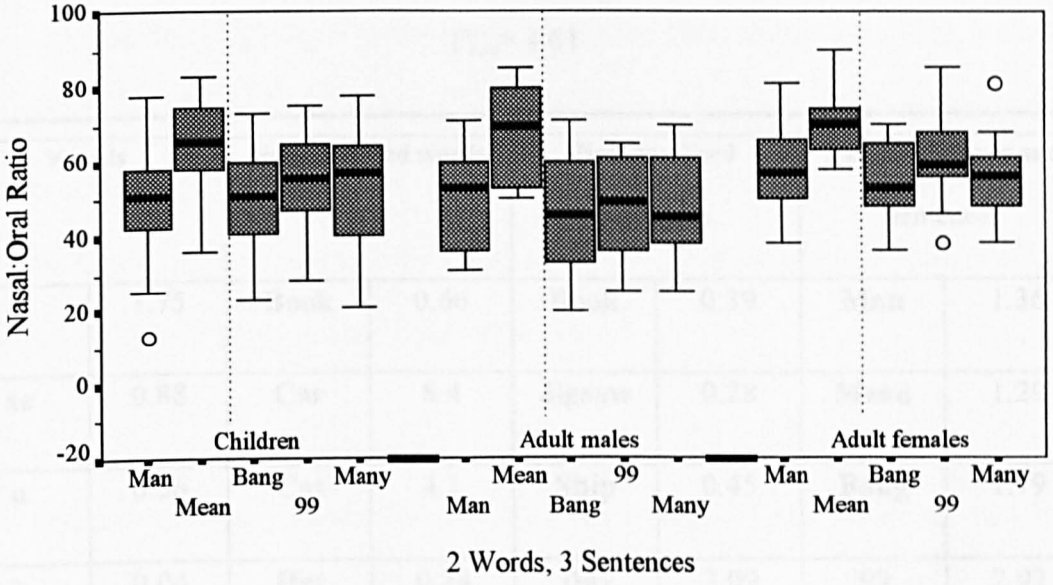

The results for the nasalised words category shown in Table 7 and Figure 62d reveal a significant variation within the phonetic category for all subject groups and therefore the null hypothesis is not proven. The average standard deviation for the category is 12.3.

In contrast to the nasalised word category the nasalised sentence variation shown in Table 7 and Figure 62d reveals a consistent agreement between subject groups

- Hypothesis: There is no significant variation in measurements between normal subject groups tested using identical phonations.

Test: The three normal subject groups were tested using a set of phonetic material containing 20 tests, subdivided into 5 phonetic categories, totalling 1380 tests. As previously described, for each group an analysis of variance was carried out between

Table 8: Variation of measurements within 3 Normal Subject Groups

$F_{2,\infty}$= 4.61

Vowels		Non-nasalised words		Non-nasalised sentences		Nasalised words and sentences	
i	1.75	**Book**	0.66	**Book**	0.39	**Man**	1.36
ae	0.88	**Car**	8.4	**Jigsaw**	0.28	**Mean**	1.29
u	0.56	**Cat**	4.1	**Ship**	0.45	**Bang**	1.79
>	0.04	**Hat**	0.24	**Day**	3.09	**99**	2.92
a	0.30	**Talk**	0.24			**Many**	1.11
All tests	0.17	**All tests**	6.28	**All tests**	2.76	**All tests**	2.03

subject groups for each phonation . The results are shown in Table 8 and Figures 63(a-d).

Fig 63a: Variation within Normal Subject Groups

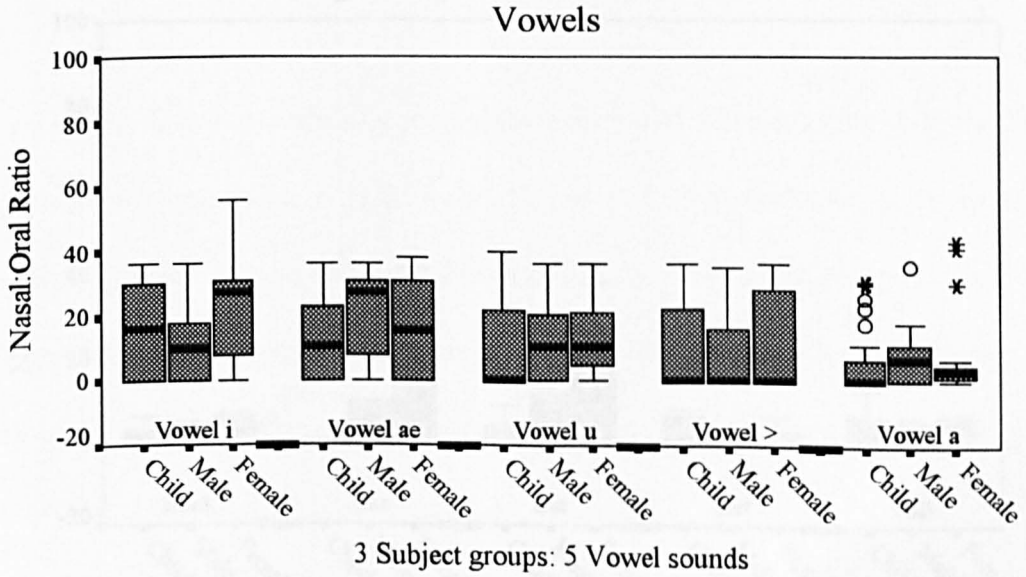

The variation between subject groups tested using identical vowel phonations is shown in Table 8 and Figure 63a. The analysis of variance reveals a consistent agreement between the three normal subject groups in all five individual vowel phonations and also no significant variation was found between groups when analysed across all test phonations. The null hypothesis is therefore proven.

The variation between subject groups tested using identical non-nasalised words is shown in Table 8 and Figure 63b. Significant variation and a wide spread of results is revealed between groups in the case of *car* and *cat* , the adult female group showing the largest standard deviations of 16.0 and 14.8. The remaining three tests show good agreement and in these cases the null hypothesis is proven. There is significant variation between groups measured across all non-nasalised words.

Fig 63b: Non-nasalised Words

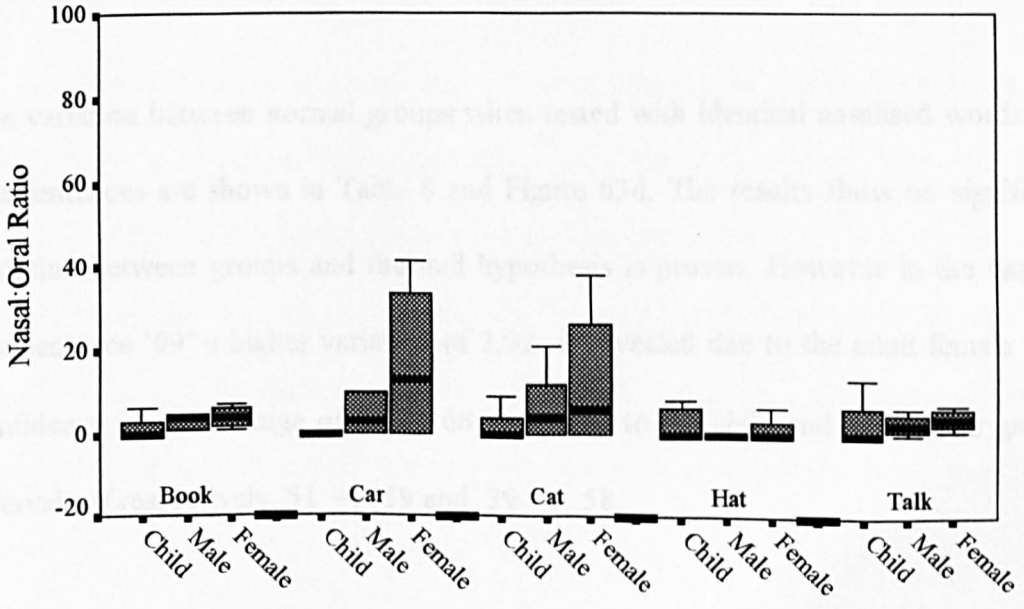

The variation between normal groups when tested with identical non-nasalised sentences is shown in Table 8 and Figure 63c.

Fig 63c: Non-nasalised Sentences

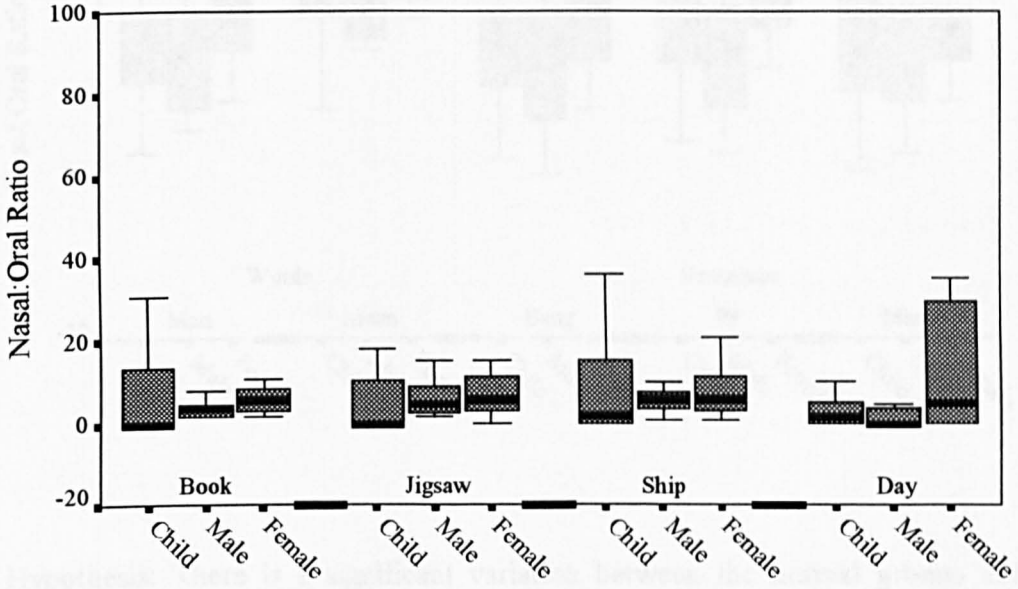

The results show no significant variation and the null hypothesis is proven. In the case of the test sentence 'day' the adult female group has a wider spread of results with a standard deviation of 15.6 compared to 8.2 and 7.8 for the respective, child and adult groups.

The variation between normal groups when tested with identical nasalised words and test sentences are shown in Table 8 and Figure 63d. The results show no significant variation between groups and the null hypothesis is proven. However in the case of test sentence '99' a higher variation of 2.92 is revealed due to the adult female 95% confidence interval range of 54 → 68 compared to the child and adult male groups intervals of respectively, 51 → 59 and 39 → 58.

Fig 63d: Nasalised Words/Sentences

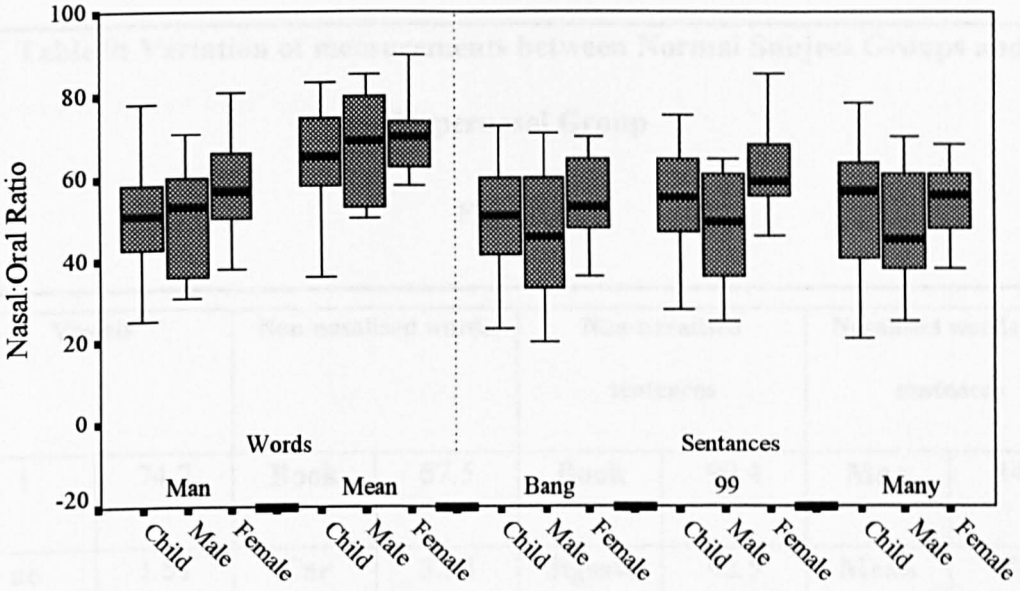

- Hypothesis: There is a significant variation between the normal groups and the hypernasal group within phonetic categories.
- Test: The three normal subject groups and the patient group were tested using phonetic material containing 20 tests, subdivided into 5 phonetic categories, totalling 1860 tests. An analysis of the variation was carried out between the three normal subject group and the hypernasal group.

The variations between measurements of vowel phonations taken from the normal groups and the hypernasal group are shown in Table 9 and Figure 64a. Significant variations are revealed in the cases of the vowels *i,u,<* and *a.* In these cases the hypothesis is proven, that is, a significant variation occurs between the normal and hypernasal groups. In the case of the vowel sound *ae* there is a significant agreement between the measurements taken from the groups and therefore the hypothesis is unproven.

Table 9: Variation of measurements between Normal Subject Groups and Hypernasal Group

$F_{1,\infty}$= 6.63

Vowels		Non-nasalised words		Non-nasalised sentences		Nasalised words and sentences	
i	74.7	**Book**	67.5	**Book**	90.4	**Man**	14.1
ae	1.51	**Car**	32.4	**Jigsaw**	92.5	**Mean**	5.4
u	49.5	**Cat**	49.5	**Ship**	94.9	**Bang**	18.0
<	35.2	**Hat**	83.6	**Day**	105.6	**99**	16.8
a	28.2	**Talk**	86.5	**Passage**	80.6	**Many**	11.6

Fig 64a: Variation between Normal Groups and Hypernasal Group

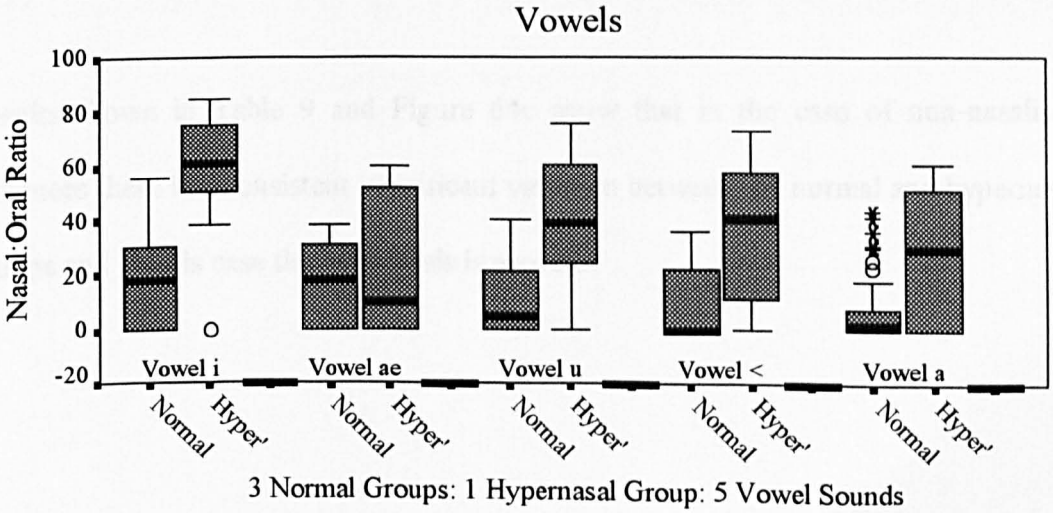

The results shown in Table 9 and Figure 64b show that for non-nasalised words there is a consistent significant variation between the normal and hypernasal groups and in this case the hypothesis is proven.

Fig 64b. Non-nasalised words

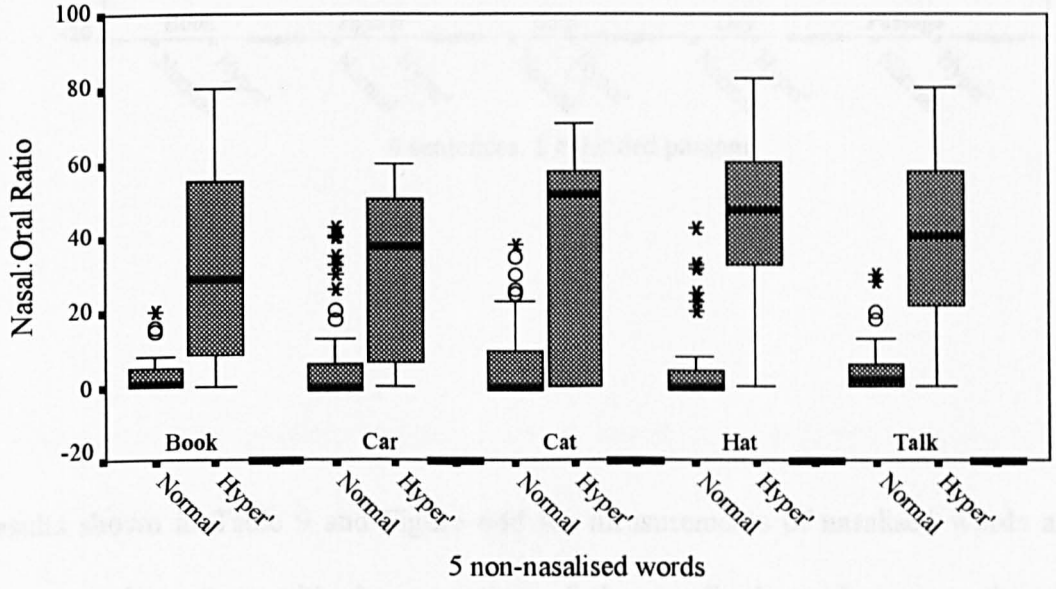

Results shown in Table 9 and Figure 64c show that in the case of non-nasalised sentences there is a consistent significant variation between the normal and hypernasal groups and in this case the hypothesis is proven.

Fig 64c. Non-nasalised sentences

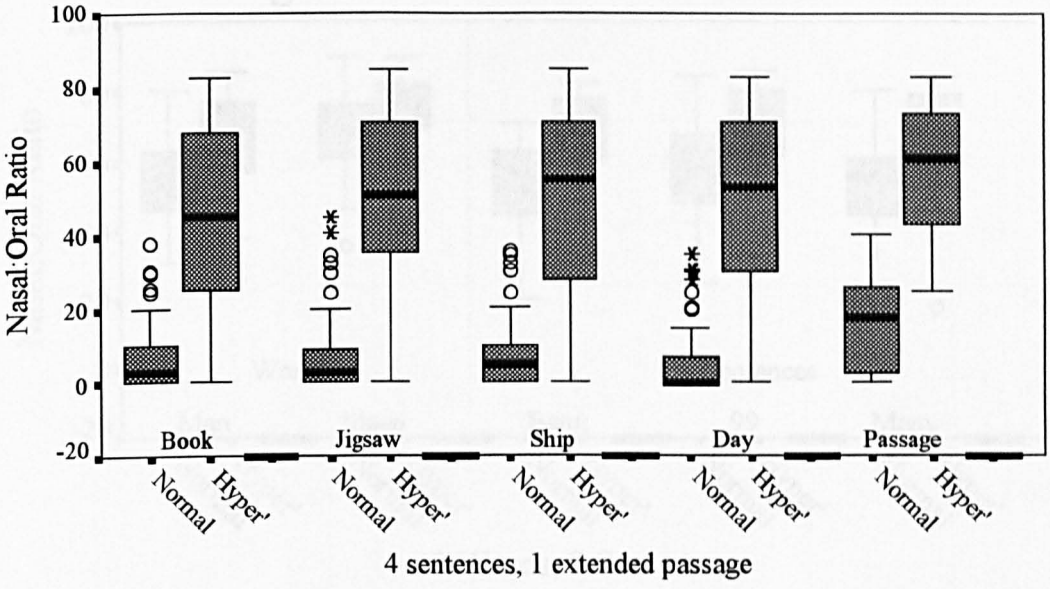

Results shown in Table 9 and Figure 64d for measurements of nasalised words and sentences show that, with the exception of the nasalised word *mean* , there is significant variation between the normal and hypernasal groups and the hypothesis is proven. In the single case of the nasalised word *mean* there is significant agreement between the groups and the hypothesis is unproven.

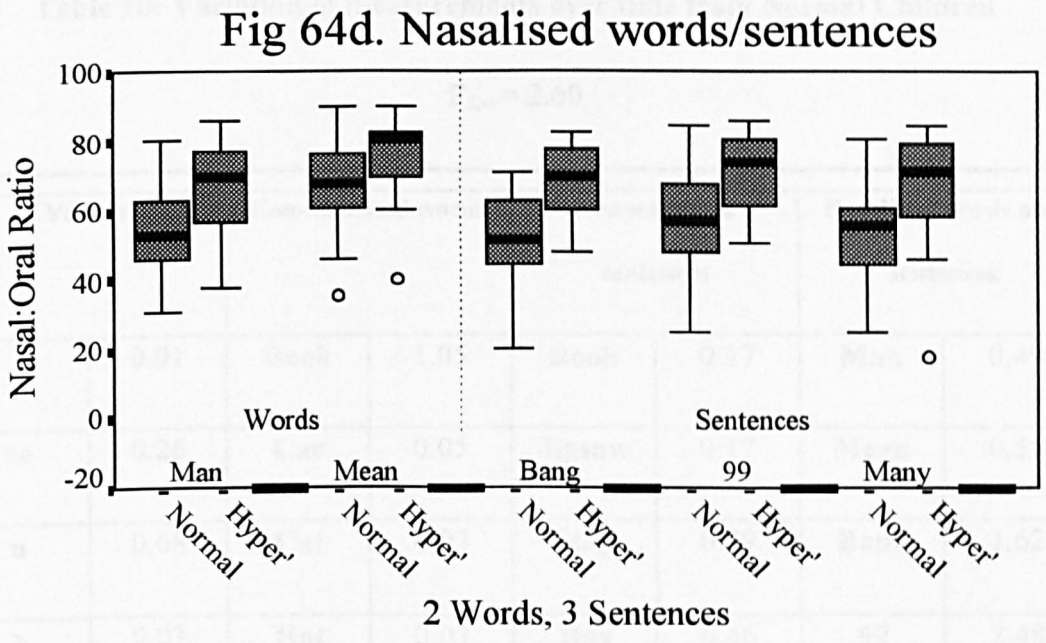

- Hypothesis: The retesting over time does not introduce a significant variation within a normal subject group.

- Test: A sub-group of 8 normal children, randomly chosen from the group of 36, were tested and then retested at weekly intervals for a period of four weeks. The test material comprised as before of 20 tests and 5 phonetic categories, totalling 640 tests. A one way analysis of variance was carried out between the weekly sets of data.

Table 10: Variation of measurements over time from Normal Children

$F_{3,\infty} = 2.60$

Vowels		Non-nasalised words		Non-nasalised sentences		Nasalised words and sentences	
i	0.91	**Book**	1.05	**Book**	0.17	**Man**	0.49
ae	0.26	**Car**	0.05	**Jigsaw**	0.17	**Mean**	0.55
u	0.68	**Cat**	0.03	**Ship**	0.09	**Bang**	1.62
>	0.03	**Hat**	0.03	**Day**	0.46	**99**	2.48
a	0.21	**Talk**	0.21	**Passage**	0.16	**Many**	0.24

The results in Table 10 show that, with the exception of the nasalised sentence *99*, there is no significant variation in measurements taken over a period of time from normal children and the hypothesis is therefore proven. In the exceptional case there is a variation of 2.48 which although less than the F-test value is notably higher than the other results.

The results shown in Tables 11,12,13,14 summarise χ, σ, standard error and 95% confidence intervals for the normal and hypernasal subject groups.

Table 11. 36 Normal Children.				
Phonation	**Mean Ratio(χ)**	**Std Dev(σ)**	**95% CI**	**Std Error**
Vowels				
i	16.9	13.5	12.0 → 21.8	2.4
ae	12.7	13.3	1.6 → 23.8	4.7
u	9.3	13.7	4.4 → 14.2	2.4
>	10.0	13.8	5.0 → 14.9	2.4
a	5.4	9.5	2.1 → 8.8	1.6
Non nasalised words				
Book	2.6	5.2	0.7 → 4.5	0.9
Car	1.9	7.8	0.9 → 4.7	1.4
Cat	3.3	8.0	0.4 → 6.2	1.4
Hat	5.8	11.4	1.7 → 9.8	1.9
Talk	4.5	8.4	1.5 → 7.5	1.5
Nasalised words/sentences				
Man	50.6	14.8	45.1 → 55.2	2.6
Mean	64.8	11.7	60.2 → 69.3	2.0
Bang	50.5	13.2	45.2 → 55.4	2.3
99	55.2	11.6	51.3 → 59.2	2.0
Many	52.7	15.3	47.4 → 58.5	2.7
Non nasalised sentences/passage				
Book	6.6	11.0	2.6 → 10.5	1.9
Jigsaw	7.6	13.9	2.6 → 12.6	2.4
Ship	8.2	11.4	4.1 → 12.3	2.0
Days	5.1	8.2	2.1 → 8.0	1.4
Passage	15.6	12.2	10.9 → 20.2	2.3

Table 12. 15 Normal Adult Males.				
Phonation	**Mean Ratio(χ)**	**Std Dev(σ)**	**95% CI**	**Std Error**
Vowels				
i	11.1	12.7	1.3 → 20.9	4.3
ae	21.3	13.9	11.3 → 31.3	4.4
u	13.1	12.5	3.5 → 22.7	4.1
>	9.0	13.2	0.8 → 18.8	4.3
a	8.9	11.2	0.8 → 16.9	3.5
Non nasalised words				
Book	4.2	4.2	1.2 → 7.2	1.3
Car	8.8	11.7	0.2 → 17.7	3.9
Cat	8.2	10.5	0.6 → 15.7	3.3
Hat	3.1	7.9	2.5 → 8.7	2.5
Talk	2.9	2.0	1.4 → 4.3	0.6
Nasalised words/sentences				
Man	50.1	17.0	41.1 → 59.6	4.1
Mean	67.7	12.7	59.2 → 77.2	4.0
Bang	44.5	17.0	32.5 → 57.4	5.3
99	48.8	13.4	39.5 → 58.4	4.2
Many	47.2	15.0	36.3 → 58.9	4.7
Non nasalised sentences/passage				
Book	4.1	1.9	2.6 → 5.5	0.6
Jigsaw	7.0	6.0	2.7 → 11.3	1.9
Ship	5.7	2.5	4.2 → 7.3	0.7
Days	4.2	7.8	0.7 → 9.2	2.3
Passage	14.7	14.5	4.2 → 25.1	4.6

Table 13. 18 Normal Females.				
Phonation	**Mean Ratio(χ)**	**Std Dev(σ)**	**95% CI**	**Std Error**
Vowels				
i	23.3	17.3	10.9 →35.7	5.5
ae	16.2	14.0	8.0 → 24.3	3.7
u	13.0	12.0	6.3 → 19.6	3.1
>	10.4	14.1	4.1 → 10.7	3.0
a	7.7	12.7	2.0 → 13.3	2.7
Non nasalised words				
Book	3.8	2.1	2.6 → 4.9	0.5
Car	16.5	16.0	6.8 → 26.2	4.4
Cat	12.8	14.8	4.2 → 21.4	3.9
Hat	5.7	12.0	1.5 → 12.9	3.3
Talk	4.1	2.2	2.9 → 5.3	0.6
Nasalised words/sentances				
Man	57.5	12.0	50.2 → 64.7	3.2
Mean	70.5	9.4	65.6 → 76.3	2.4
Bang	54.9	10.1	49.8 → 61.4	2.7
99	60.9	12.5	54.6 → 68.4	3.3
Many	56.0	10.7	50.6 → 62.3	2.8
Non nasalised sentances/passage				
Book	7.4	6.5	3.1 → 11.8	1.9
Jigsaw	10.2	11.0	4.1 → 16.3	2.8
Ship	9.4	9.3	3.8 → 15.3	2.7
Days	13.2	15.6	2.7 → 23.6	4.7
Passage	18.7	9.1	12.5 → 24.9	2.7

Table 14. 24 Hypernasal Patients				
Phonation	**Mean Ratio(χ)**	**Std Dev(σ)**	**95% CI**	**Std Error**
Vowels				
i	56.8	25.4	46.1 → 67.5	5.1
ae	23.5	25.7	12.6 → 34.3	5.2
u	40.2	24.1	29.9 → 50.4	4.9
>	35.0	24.6	24.1 → 45.9	5.2
a	27.3	25.1	16.2 → 38.5	5.3
Non nasalised words				
Book	39.6	26.9	20.6 → 52.6	6.1
Car	43.2	25.7	31.5 → 55.0	5.6
Cat	39.2	28.2	24.2 → 54.2	7.0
Hat	30.7	23.0	19.6 → 41.9	5.2
Talk	32.8	26.5	20.4 → 45.2	5.9
Nasalised words/sentances				
Man	67.5	12.9	61.4 → 73.6	2.9
Mean	75.8	11.3	70.3 → 81.3	2.6
Bang	68.2	12.6	61.9 → 74.5	2.9
99	71.2	11.2	65.9 → 76.5	2.5
Many	67.5	16.5	59.7 → 75.3	3.7
Non nasalised sentances/passage				
Book	46.1	26.7	33.2→ 58.9	6.1
Jigsaw	50.8	26.4	38.0 → 63.5	6.0
Ship	47.8	26.5	35.7 → 59.9	5.7
Days	49.0	25.9	37.2 → 60.8	5.6
Passage	56.2	18.5	46.6 → 65.7	4.5

4.1.3 Evaluation conclusions and clinical measurement protocol.

The overall conclusion from the extensive clinical trials was very positive. The instrument demonstrated that the measurement errors that had been predicted during the laboratory trials were not significant and that the uncertainty present in clinical measurements, quantified in section 4.1.2 as a worst case error of 4% within a 95% confidence interval, was acceptably small and meets the instrument specification given in Section 3.2.3.

The response of Resonometer to the normal subject groups tested using 5 phonetic categories has demonstrated in the case of vowels that the variation between subject groups within this phonetic category is strikingly consistent. The average standard deviation of 13.2, measured across all vowels, confirms the view outlined in Section 1.2 that the acoustic effect of the velum is not binary in nature but that the degree of coupling of the oral and nasal cavities varies between normal subjects. The variation between vowel sounds shown in Figure 63a reveal that the low vowel *a* has a comparatively lower spread of results and lower absolute nasal:oral ratio in all three subject groups. This is consistent with a lower tongue position producing a less sensitive effect on the acoustic impedance of the oral cavity. The different tongue positions between subjects exerts a less pronounced change in velum posture which results in a lower variation in resonant balance. Table 8 and Figure 63a reveal that the agreement in variation for each vowel sound between groups is highly significant and suggests that normal subjects produce a consistent range of nasal:oral balance that is dependant on the phonation, not on the subject group. This conclusion is further supported, by comparison of the results from Tables 7 and 8, in the case of the

nasalised words phonetic category. Table 7 shows that the variation between different phonations within each subject group is significant however, the variation between subject groups for the same nasalised word, shown in Table 8, reveals a consistent agreement. The same conclusion can be drawn by examination of the variation between groups for non-nasalised words, in the case of adult females there is a notable difference; with the other subject groups however there is no significant variation when the individual phonations are compared in Table 8. There is an exception to this conclusion in the case of the word *car*. The presence of the low vowel *a* in this phonation would tend to predict a small variation in results as is the case of the individual vowel sound *a*. However the preceding consonant requires a high tongue position against the hard palate to form an effective pressure seal during the formation of the unvoiced sound. This may lead to an effectively higher acoustic impedance with a resultant wider than predicted variation in results.

The measurement response of the instrument to the normal subject and the hypernasal patient group is conclusively demonstrated by the consistent high significant variations shown in Table 10. A clear delineation between the groups in all non nasalised phonations is evident in Figures 64(a-c) with the exception of the vowel *ae*. With the exception of the vowel *ae*, the results shown in Tables 11,12,13 and 14 show that in all non nasalised phonations the normal group, with respect to the hypernasal group, has the following properties;

- a significantly lower mean value.
- a significantly lower standard deviation.

- no overlap between the upper limit of the normal results range and the lower limit of the hypernasal results range within the 95% confidence intervals.

These properties point to the confident clinical use of the instrument in achieving its main design criterion of delineating the normal and hypernasal case. The wide standard deviation of the hypernasal group enables a further differentiation of the degree of hypernasality.

Table 9 and Figure 64d demonstrate that for the nasalised words and sentences category the normal group, with respect to the hypernasal group, has the following properties;

- a consistently lower mean value.
- no significant difference in standard deviations.
- a slight degree of overlap between the upper limit of the normal results range and the lower limit of the hypernasal results range within the 95% confidence intervals.

The inclusion into the test material of nasalised phonations was designed to evaluate the effectiveness of the instrument in detecting the hyponasal case. The absence of hyponasal patients during these trials has meant that a conclusion on the effectiveness of the instrument when used with this group remains untested. However the measurements have revealed that, to an extent, the Resonometer has differentiated the hypernasal group from the normal group when using nasalised test phonations. This tends to suggest that the hyponasal group would be further delineated and that the results would be clinically significant.

Repeated sets of measurements over time taken from the normal children group reveal that no significant variation occurs in any phonetic category. This leads to a further confirmation of the conclusion that the instrument's measurement errors do not introduce any significant variations in results. The conclusion that the measurement uncertainty in clinical results taken over time is acceptable, enables application of the instrument in assessing the efficacy or otherwise of patients undergoing a course of speech therapy.

The conclusion of the trial in establishing a typical range of nasal:oral ratios for normal subjects was to adopt the ranges within the 95% confidence intervals shown in Tables 11,12,13. In the context of differentiating the normal and hypernasal groups the exceptional case of the vowel sound *ae* was noted.

The subjective assessment of the severity of hyper- and hyponasality by speech therapists has traditionally been classified as normal, mild, moderate and severe. Objective nasal:oral ratio measurements from the Nasal Resonometer range from 0 → 100% and have been subdivided as follows;

Normal	Lower limit normal range → upper limit normal range
Mild	Upper limit, normal range → lower limit interquartile patient range
Moderate	Lower limit interquartile patient range → upper limit interquartile patient range
Severe	Upper limit interquartile patient range → upper limit

The overall conclusion of the clinical trials was that the Nasal Resonometer successfully met the initial clinical design specification outlined in Section 2.3 and that the technical specification achieved, summarised in Section 3.2.3, did not require major modifications. It was concluded that as the uncertainties in the measurements were sufficiently understood, provided the instrument's applications were carefully kept within the protocol of the clinical trial, the clinical use of the Nasal Resonometer could commence.

4.2 Clinical Studies

The first clinical study was on a group of orthodontic patients under the care of one consultant prosthodontist at the Department of Prosthetic Dentistry, Guys Hospital.

4.2.1 Orthodontic Study

The Prosthodontist is called upon to produce a variety of obturators and speech aids which may be specifically designed to help improve the quality of speech or may do so incidentally. Historically a plethora of claims (75,76,77) have been made regarding the efficacy of such applications and accompanied by a range of explanations as to how they may work. The use of x-ray imaging has enabled greater objectivity in the interpretation of the influence of the appliance on the palatopharyngeal musculature while the quantification of airflow and pressure has been achieved using anemometry. The application of the Nasal Resonometer to this patient group would bring about an

objective assessment of the alteration of resonant balance due to the occlusion of palatal deficiencies by prosthetic means.

Five adult male patients with an acquired palatal deformity involving massive fistulae of the anterior palate through either trauma or illness, had their nasal:oral resonant balance measured objectively by the Nasal Resonometer followed by subjective assessment of hypernasality and speech intelligibility by a highly experienced Speech Therapist. All patients had worn palatal obturators for many years, designed and fitted by the same prosthodontist. The patients were tested, firstly with their obturators in place, using the material and method described in Section 4.1.2, and then retested in an identical manner with their appliances removed.

The results shown below are classified in terms of normal, mild, moderate and severe hypernasality for the purpose of comparison between the speech therapist rating and instrument measurement. The delineation criterion of measurement results into these terms is given in Section 4.1.3.

Patient A. Male 57 years.		
Subjective rating.	**Obturated**	**Open fistula**
Resonant balance	Normal	Severe hyponasal
Emission	Normal	Severe
Intelligibility	Normal	Poor
Resonometer Measurement		
Vowels	Normal	Mild hypernasal
Non nasalised words	Mild hypernasal	Moderate hypernasal
Non nasalised sentences	Mild hypernasal	Moderate hypernasal
Nasalised words/sentences	Normal	Hyponasal
Patient B. Male 52 years.		
Subjective rating.	**Obturated**	**Open fistula**
Resonant balance	Normal	Severe hypernasal
Emission	Mild	Severe
Intelligibility	Normal	Unintelligible
Resonometer Measurement		
Vowels	Normal	Normal
Non nasalised words	Normal	Mild hyponasal
Non nasalised sentences	Normal	Normal
Nasalised words/sentences	Normal	Hyponasal

Patient C. Male 60 years.		
Subjective rating.	**Obturated**	**Open fistula**
Resonant balance	Normal	Severe hypernasal
Emission	Normal	Severe
Intelligibility	Normal	Unintelligible
Resonometer Measurement		
Vowels	Normal	Mild hypernasal
Non nasalised words	Normal	Mild hypernasal
Non nasalised sentences	Normal	Moderate hypernasal
Nasalised words/sentences	Normal	Hyponasal

Patient D. Male 55 years.		
Subjective rating.	**Obturated**	**Open fistula**
Resonant balance	Normal	Severe hypernasal
Emission	Normal	Severe
Intelligibility	Normal	Unintelligible
Resonometer Measurement		
Vowels	Mild hypernasal	Moderate hypernasal
Non nasalised words	Mild hypernasal	Moderate hypernasal
Non nasalised sentences	Mild hypernasal	Moderate hypernasal
Nasalised words/sentences	Mild hypernasal	Hyponasal

Patient E. Male 63 years.		
Subjective rating.	**Obturated**	**Open fistula**
Resonant balance	Normal	Severe hypernasal
Emission	Normal	Severe
Intelligibility	Normal	Unintelligible
Resonometer Measurement		
Vowels	Normal	Normal
Non nasalised words	Normal	Mild hypernasal
Non nasalised sentences	Normal	Mild hypernasal
Nasalised words/sentences	Normal	Hyponasal

The subjective results consistently show that following the obturator removal a decrease in the intelligibility of speech to unintelligible occurs in all cases except patient A who also showed a notable deterioration in speech quality.

The speech therapists' assessment also revealed that, without the prosthesis, all patients underwent a dramatic increase in nasal emission and a perceived severe increase in hypernasality occurred in all cases except patient A where the presence of severe hyponasality was detected.

The patients all reported the greatest sensation was complete loss of intra-oral pressure on removal of the obturator and consequent inability to articulate without the greatest effort.

The Nasal Resonometer measurements show that in the case of non-nasalised phonations a general mild increase in hypernasality, of the order of 30%, occurred when the obturator was removed except in the case of patient B who showed notably little change from the obdurated readings.

In the case of nasalised words and sentences there is evidence of a marked consistent denasalisation in all patients.

Comparison of the two assessment methods shows that the speech therapists awareness of a gross degree of nasal tone following obturator removal in all patients was inconsistent with the instrument's readings.

With the exception of patient A the speech therapist did not perceive the presence of hyponasality with the fistula open in contrast to the Nasal Resonometer results that show a consist denasalisation during nasalised phonations.

The conclusion of the study from the prosthodontist point of view was that the presence of the obturators had obviously helped all the patients achieve a normal degree of speech intelligibility.

Contrary to expectations, according to the Nasal Resonometer readings, the patients exhibited only a mild increase in hypernasality following the removal of their obturators. If the measurements are accepted, this would appear to indicate that the loss of clarity of speech in the unobdurated case is in fact due to the obturator's ability to help improve the patient's control of oral air pressure. This conclusion is supported by the patients' reports and the consistent observations of increased nasal emission by the clinician. This aim for the use of a oral obturator would be contrary to the traditional prosthodontist's approach which is to ensure that the clarity of speech is not impaired by nasal resonance(75).

The contrast in the perceived degree of hypernasality and the measurement results could have resulted from a systematic difference in the classification of the severity ranges of the instrument compared to the speech therapist ratings. However the results do not appear to consistently support this possibility as shown in the case of patient B where remarkably little change in measured nasal:oral ratio in the unobdurated case coincided with a perceived severe increase in hypernasality.

The perception of apparent severe hypernasality may be associated with several variables which would not produce a commensurate increase in the nasal:oral ratio measured by the instrument.

- Imprecise articulation resulting from the reduction in oral air pressure.
- The presence of hyponasality.
- The presence of acoustic noise due to uncontrolled emission.

The consistent indication from the instrument of hyponasality during nasalised phonation would appear to be counter intuitive to the notion of the fistula enabling a permanent acoustic pathway to the nasal cavity. However, in the context of the cylindrical vocal tract model as described in Section 2.1, the presence of the fistula would be represented by an additional set of complex impedances that would have a marked effect on the *total* filter transfer function of the *complete* acoustic system. The permanent addition of this filter characteristic would appear to have a marked damping effect that has produced an unexpected presence of hyponasality during nasalised phonations and a suprisingly low degree of hypernasality during non-nasalised test material.

Section 4.2.2 Cleft palate and velopharyngeal insufficiency studies

The Nasal Resonometer was used for clinical measurements in conjuction with other measurement techniques during routine cleft and palatal investigations. The clinical results presented in this section relate to a comparison of results from two surgical techniques and an example of pre and post -operative data from an individual patient.

A further study of pre and post-operative data measured from a patient who had undergone a palate re-repair is presented in Section 6.1.

The results in Table 15 show a comparison between four subject groups who had undergone measurements using the Nasal Resonometer as described in Section 4.1.2. The normal subject group results are taken from Table 11. The remaining three subject groups contain data measured from patients attending one of ten cleft clinics during a two year period. All patients in the following categories were included.

The pre-operative group had all undergone primary repair of clefts of lip and palate and been referred for subsequent assessment. The conclusion of the investigation had been that a further surgical procedure was required to correct for hypernasal speech.

The two post-operative groups had undergone a further surgical procedure. One group underwent a procedure known as palate rerepair and the other group underwent a procedure known as a Hynes pharygoplasty. Both these methods were carried out by the same surgeon, to correct for hypernasal speech or velopharyngeal insufficiency. These procedures are described briefly in Section 6.2 and in detail elsewhere (65).

Table 15. Comparison of normal, pre and post-operative results

Vowels

	Normals(36)	Pre-ops(9)		Re-repairs(11)		Pharyng'(6)	
Phonation	95% CI	χ	σ	χ	σ	χ	σ
i	12.0 → 21.8	52.7	13.4	44.6	11.4	57.4	9.7
ae	1.6 → 23.8	49.2	15.6	34.4	19.5	37.8	28.7
u	4.4 → 14.2	47.7	13.8	35.7	10.4	37.6	17.4
>	5.0 → 14.9	56.3	20.6	34.6	21.7	51.6	27.5
a	2.1 → 8.8	50.0	17.0	34.1	20.5	28.8	19.3

Non nasalised words

	Normals(36)	Pre-ops(9)		Re-repairs(11)		Pharyng'(6)	
Phonation	95% CI	χ	σ	χ	σ	χ	σ
Talk	1.5 → 7.5	42.3	12.6	35.9	15.9	41.8	19.0
Cat	0.4 → 6.2	42.7	16.9	29.5	23.4	40.0	26.6
Car	0.9 → 4.7	39.8	22.5	29.6	12.2	36.8	30.3

Nasalised words/sentences

	Normals(36)	Pre-ops(9)		Re-repairs(11)		Pharyng'(6)	
Phonation		χ	σ	χ	σ	χ	σ
Man	45.1 → 55.2	68.3	13.2	63.2	18.8	70.8	14.1
Mean	60.2 → 69.3	77.2	15.8	68.9	13.5	73.0	16.3
99	51.3 → 59.2	67.8	15.2	62.8	18.1	70.2	20.1
Many	47.4 → 58.5	65.0	16.0	63.6	13.4	67.0	15.4

Non nasalised sentences/passage

	Normals(36)	Pre-ops(9)		Re-repairs(11)		Pharyng'(6)	
Phonation	95% CI	χ	σ	χ	σ	χ	σ
Day	2.1 → 8.0	58.3	11.4	34.1	13.2	57.2	24.2
Book	2.6 → 10.5	51.2	13.0	37.6	14.5	45.4	23.7
Ship	4.1 → 12.3	51.3	9.7	37.4	17.1	54.0	22.5
Passage	10.9 → 20.2	51.8	12.9	41.4	13.2	50.4	24.1

where χ is the mean, σ is the standard deviation, 95% CI is the 95% confidence interval and figures in brackets represent the subject numbers.

The pre and post operative results in Table 15 are not directly comparable because they involved separate patient groups and therefore a much larger group of patients would be necessary to make definitive conclusions. However the results do allow some tentative points to be made as follows.

- The pre-operative mean is consistently considerably higher than the normal group. Indicating that the Nasal Resonometer measurements are consistent with the subjective assessments.
- Both the mean of the re-repair and Hynes pharyngoplasty techniques show a consistent reduction in nasal:oral ratio for all phonations compared to the pre-operative group.
- The mean of the re-repair group consistently shows a larger reduction in nasal:oral ratio for all phonations compared to the pharyngoplasty group.
- Neither of the post-operative groups attain the mean of the normal group for any phonation.
- The re-repair group have consistently lower standard deviations for all phonations than the pharyngoplasty group.
- The means of both groups show no evidence of hypo-nasality for the nasalised phonations.

A specific case study is presented of a 34 year old male who had suffered a severe head injury resulting in a variety of problems including dysarthria and a degree of dysphonia.

A right sided palatal palsy had led to an anatomical velo-pharyngeal incompetence and co-ordination disorder. The patient had been fitted with a palatal lift aid in an attempt to correct for the palatal irregularity.

Pre-operative examination by a speech therapist had concluded the following.

- There was a consistent nasal escape and hypernasality throughout speech
- There appeared to be very little difference in his speech with and without the palatal lift in place.
- With the palatal lift in place his articulation became more exaggerated and the patient also reported difficulties in swallowing saliva.

Examination by plastic surgeon concluded the following.

- Lateral video fluoroscopy revealed that without the palatal lift device the palate hung down almost vertically. During speech there was good palatal lift and extensibility. With the palatal device, the palate resting position was significantly raised but no change in palatal mobility during speech was noted.
- Nasendoscopy revealed that without the palatal lifting device there was a large velopharyngeal opening. During speech the velum appeared to achieve near closure on the left side while a small persistent defect remained on the right side. With the palatal device in place there was an obvious change in the resting position of the velum however a smaller right side defect persisted during speech.

The conclusion of the investigation was that a Hynes pharyngoplasty should be performed on the right side of the post pharyngeal wall.

Pre and post-operative measurements were carried out using the Nasal Resonometer as described in Section 4.1.2, the results are shown in Table 16.

Table 16. Nasal Resonometer Results: Pre and Post Operative Pharyngoplasty

Phonation	Pre Op (without palatal lift) 13/2/92	Pre Op (with palatal lift) 13/2/92	Post Op (with palatal lift) 28/1/93	Normals 95% CI
Vowels				
i	56	51	36	1.3 → 20.9
u	33	38	10	11.3 → 31.3
ae	61	41	38	3.5 → 22.7
>	45	40	31	0.8 → 18.8
a	23	35	10	0.8 → 16.9
Non nasalised words				
Book	x	x	x	1.2 → 7.2
Car	56	58	51	0.2 → 17.7
Cat	68	61	55	0.6 → 15.7
Hat	x	x	x	2.5 → 8.7
Talk	73	68	25	1.4 → 4.3
Nasalised words/sentences				
Man	81	66	63	41.1 → 59.6
Mean	80	80	80	59.2 → 77.2
Bang	x	x	x	32.5 → 57.4
99	75	75	78	39.5 → 58.4
Many	76	78	75	36.3 → 58.9
Non nasalised sentences/passage				
Book	56	56	33	2.6 → 5.5
Jigsaw	x	x	x	2.7 → 11.3
Ship	60	60	25	4.2 → 7.3
Days	65	65	26	0.7 → 9.2
Passage	46	53	50	4.2 → 25.1

The pre-operative results tend to confirm the speech therapist's assessment in relation to the apparent ineffectiveness of the palate lift device. No systematic improvement in either short or long duration phonations is shown with the palate device in place.

The post operative results show a consistent reduction in the nasal:oral ratio for all phonations with the exception of the extended passage. The results for vowel sounds *ae* and > are within the normal range for adult males. The three vowels *i,u* and *a* all lay in the lower quartile of the hypernasal group as shown in Figure 64a. With the exception of the non-nasalised words *car* and *cat,* all results lay in the lower quartile of the hypernasal group as shown in Figures 64b and 64c. The average improvement in nasal:oral ratio for all non-nasalised tests was 21.8% with a standard deviation of 13.7% and a range of -4 % → 48%. In the case of the extended passage the post-operative nasal:oral ratio had increased very slightly. There was no significant change noted for the nasalised tests and no evidence of post-operative hypo-nasality.

Post-operative speech assessment concluded the following.

- He achieved a good oral nasal resonance balance.
- Slight hypernasality was present during connected speech.
- He could achieve good intra-oral pressure with a considerable reduction in nasal emission.
- His speech intelligibility was considerably improved.

Examination by plastic surgeon concluded the following.

- Nasendoscopy revealed that palatal movement remained only on the left side. However with the support of the additional flap on the right side, he was achieving consistent velopharyngeal closure with only occasional bubbling.

From the patient's point of view the pharyngoplasty had resulted in a considerable improvement in the quality of his speech although slight hypernasality was still present during connected speech. The post-operative clinical assessment concluded that the presence of the pharyngeal flap enabled the patient to improve the control of his intraoral pressure during phonations, thus allowing him to produce much longer phrases with one breath.

Conclusions from the Nasal Resonometer results tended to confirm the speech assessment findings both pre and post-operatively. The results from the tests using nasalised phonations revealed no evidence of hypo-nasality. This is an important fact to establish following a pharyngoplasty because the fixed presence of additional tissue in the velopharyngeal cavity may cause a permanent increase in acoustic impedance in the acoustic pathway to the nares. The slight post-operative increase in nasal:oral ratio for the extended passage test tends to confirm that a degree of hypernasality is still present during lengthy connected speech.

Final conclusions and future applications of the Nasal Resonometer are presented in Chapter 7.

Chapter 5.

Velopharyngeal movement measurements.

5.1 Current measurement techniques.

The movement of the velum has to date been investigated principally using optical and radiological techniques. These methods involve the direct viewing of the palate or its x-ray image and they remain the standard method of investigation. The more recent advent of magnetic resonant imaging has, at the time of writing, yet to make an appearance into the range of velopharyngeal tests available to the clinician.

Indirect measurement methods of measuring velopharyngeal movement using acoustic (73), aerodynamic (8, 14, 16) and optical (74) techniques have yet to be accepted as a reliable alternative to direct viewing of the palate. Indeed current developments are tending towards the real time display of indirect measurements mixed with optical or x-ray images of the moving palate.

Direct investigations of velum movement using optical techniques rely upon the introduction of a source of light and a light detector into either or both the oral and nasal cavities. In the case of endoscopy the light detector is usually a flexible fibre optic that enables the image of the soft palate and pharyngeal cavity to be illuminated and viewed directly during phonation. As mentioned in section 1.3.3, this technique is limited in its ability to produce reliable measurements of soft palate position and movement, directly from the optical image. However the reflection of light from the soft palate or the transmission of light across the velopharyngeal port can be measured

(74). The movement of the velum occludes the light transmission path between transmitter and receiver, and hence the modulation of the detected light amplitude is a function of the soft palate movement and position. The principle disadvantages of these indirect measurement techniques are the invasive nature of the method, the specialist equipment required and the difficulty of clinically interpreting the results in terms of velopharyngeal movement.

The use of x-ray examination of velopharyngeal function during phonation has been extensively described (1, 3, 41, 45, 46, 47, 48, 51, 52, 57, 58, 60, 62, 63, 65, 68,71). The principal advantage of x-ray examination by fluoroscopic screening is the ability to view all the major articulators of the upper vocal tract during unimpeded phonations. Furthermore the geometric distortions in optical viewing systems are not present in the x-ray images which can easily be calibrated for measurements of absolute size (71). Ratiometric measurements (48, 52) which are described in section 5.2 allow dimensionless measurements to be made of palate movements and port closure. This enables the direct inter-patient comparison of these parameters. The principal disadvantage of the use of x-ray remains the risk associated with ionizing radiation. However during typical velopharyngeal videofluoroscopy investigations, the absorbed x-ray dose to sensitive organs and the total radiation load have been shown (51) to be relatively low compared to standard x-ray techniques.

Lateral videofluoroscopy is commonly used in the assessment of cleft palate repair and various methods (3,41,47,72,73,74) for extracting measurements from x-ray images have been used. An international working committee (52) have proposed a set of standard measurement protocols based upon ratiometric methods. The second part of

this thesis introduces an extension to this methodology. By successively capturing videofluoroscopic frames from x-ray screening of lateral velopharyngeal movement into a digital form, the resultant image can be processed by a clinician using standard computer equipment. The digital images can be successively examined with the resultant dynamic sequence showing the stages of port closure during the velar cycle. Furthermore, the rate of closure of the velum can be easily compared pre- and post-operatively and comparison of velopharyngeal measurements from normal and patient groups can be made. Furthermore any relationship between measurements of movement and closure can be related to clinical observation, underlying physiology, and other measurement techniques.

5.2 Measurement protocol and system specification.

The standardized protocol (52) for measurement of velopharyngeal closure in the lateral plane is shown diagrammatically in Figure 65. The protocol states:

'The vector of velar movement along it's trajectory is used for analysis because it corresponds to the perceived plane of closure on endoscopic examination. The point on the velum *closest to the posterior pharyngeal wall* at maximum constriction is then identified (in Fig 65a this is the point marked a). A line drawn from that point to *the same point* (in Fig 65b this is the point b) on the velum at rest (preferably during nasal inspiration) defines the vector of the movement. When this line is extended to intersect the posterior pharyngeal wall or adenoid at rest it serves as the reference line. The point at which the reference line intersects the velum at rest is defined as 0.0 on a ratio scale. Where the reference line intersects the posterior pharyngeal wall at rest is

Fig 65: Lateral View Videofluoroscopy.
Measurement Protocol

$$\text{Index} = 1 - \frac{a\text{-}a'}{b\text{-}b'}$$

where 1 = complete closure
0 = maximal opening

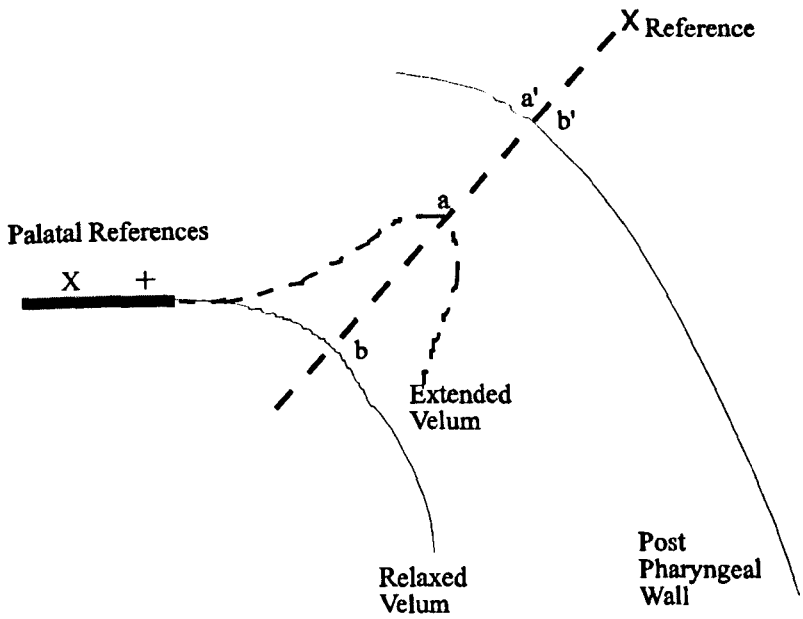

Fig 65a: Velopharyngeal measurement

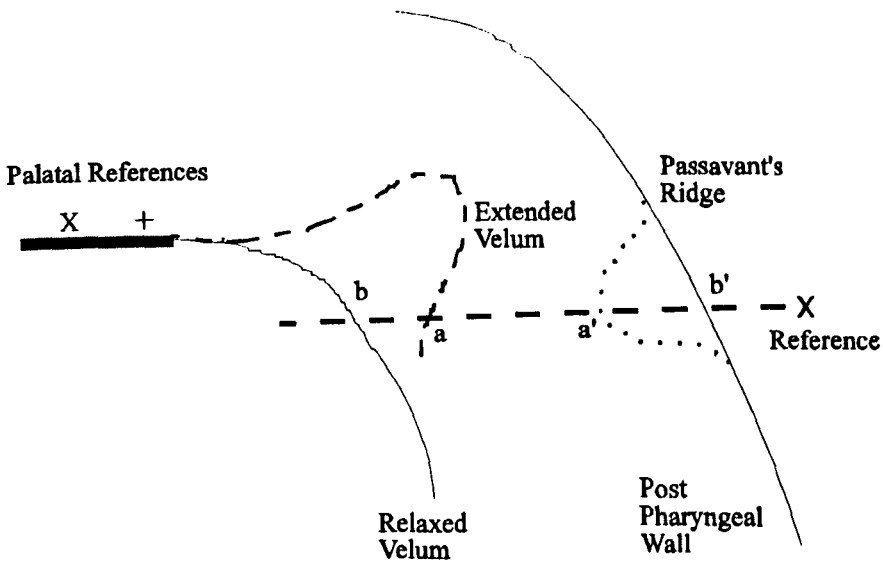

Fig 65b: Passavant's ridge measurement

defined as 1.0. The point of maximum movement of the velum along the reference line establishes the degree of velar displacement relative to points 0.0 and 1.0'

Where there is a Passavant ridge present the protocol suggests:

'The midpoint of Passavant's ridge at maximum constriction is identified (in Fig 65b this is the point marked a') and the location of the same point on the posterior pharyngeal wall (in Fig 65b this is the point b') at rest is defined as 0.0 on a ratio scale. These two points that identify the trajectory of movement should be connected to form a reference line'

Figure 65a shows how the degree of velopharyngeal port closure, measured as a ratio, is calculated from two measurements of absolute distance. The first is taken across the velopharyngeal port with the velum relaxed in the nasal breathing position (giving the maximum open port dimension), and the second is taken from a subsequent image with the velum extended. From the ratio of these two measurements (b-b' and a-a'), a simple index between 0 and 1, of port closure between maximal opening (0) and complete closure (1) can be calculated. The equation for this calculation is shown in Figure 65. The advantages of this ratiometric approach are the minimization of errors in the imaging system (due to, for example, image distortion), nulling of systematic magnification factors and a resultant index that is dimensionless, enabling comparison of patients of different absolute port size.

The measurement system was designed to meet the following requirements.

- Enable the digitization of successive images of the velar cycle from either an x-ray image intensifier or VCR.

- Display, store and retrieve images without loss of resolution.
- Enable measurement of the image according to standard protocol (52) or similar measurement techniques.
- Enable measurements to be carried out on images of the moving velum.
- Enable the comparison of pre and post operative results in graphical format.
- Enable the comparison of measurements from patient groups to be compared with normative data.
- Enable the calculation of rate of closure of the velum.
- Enable measurements to be carried out with sufficient accuracy on standard computer equipment.

5.3 Velopharyngeal measurement system

The principal components of the measurement system are shown in Figure 66. The imaging system is shown as an x-ray tube and image intensifier although the measurement system is capable of capturing images from any standard video composite signal. An initial short exposure is made to produce a standard image of a spherical object of known dimensions for the purposes of geometric calibration. The patient is set up in a standing position with their head horizontal with the aid of a head positioning device (71) which also acts to screen the orbits of the eyes from x-rays. During x-ray screening the patient repeats a short series of sounds that include the vowels *a* and *i*, sibilants *s* and *z*, plosives *b* and *k*, and a count from one to ten. The images produced by the intensifier camera are stored either by video cassette recorder (VCR) or digitised directly for subsequent analysis.

5.3.1 Hardware and software design

Referring to Figure 66, x-ray images of the moving velum are captured by the frame grabber card either directly from the image intensifier camera during x-ray examination or subsequently from VCR.

Figure 66: Principal hardware components

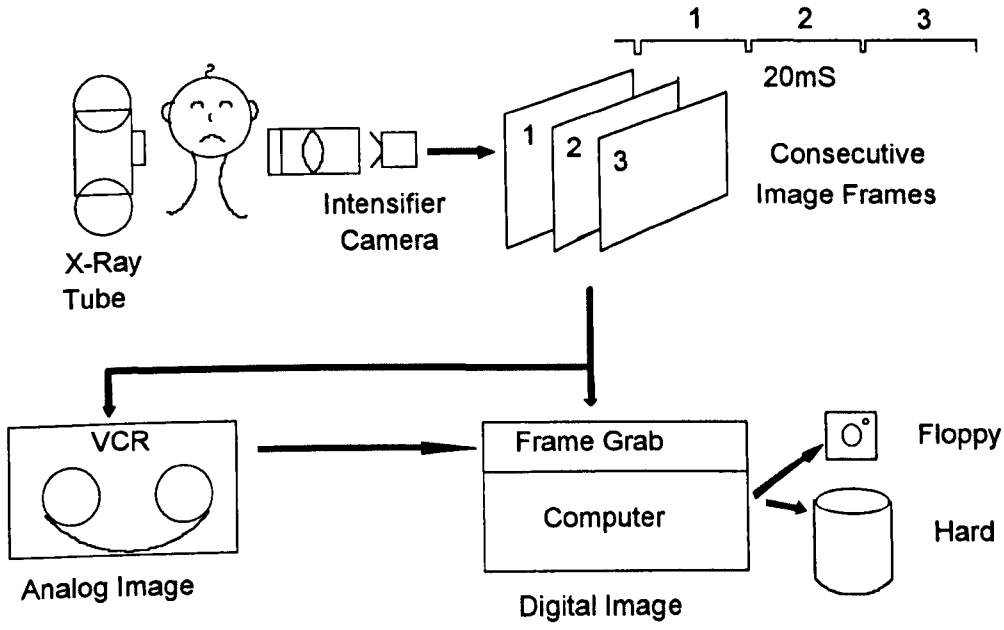

The frame grabber card chosen was a Data Translation DT3851 which is directly compatible with the host IBM PC system bus and is physically located in one of the empty card slots. The DT3851 can accept standard video composite signals from up to four sources enabling future expansion of the measurement system to include base and Townes views of the velopharyngeal port. The card digitizes consecutive frames as 768 x 512 square pixels with 8 bits of grey scale depth. A composite video frame from the intensifier camera or VCR is made up of two fields, called the odd and even

fields, that are displayed contiguously to make up the image on the monitor. The DT3851 captures both fields thus providing a sequence of images of the moving velum at 20ms intervals that are then available for off-line analysis. The DT3851 has 8 Megabytes of RAM available for image storage. The measurement system software enables the operator to capture on odd, even or both video fields in an adjustable image window centered on the region of interest. In this way the image sampling rate is maximized, memory overheads are minimized and adequate digital recording time is available. The images are stored and subsequently analyzed on a standard IBM compatible 486 running at 66 MHz with a 100Mbyte hard disc. The specification for the Panasonic VCR is given in Appendix 2.

The software design for the measurement system was based upon the inter-active requirement of the operator and the image capture, analysis and display processes. The operators' control of the system was therefore based on a menu driven software structure. This enabled the user to simply 'point and click' the mouse to call any appropriate function from the menu structure. The main functions required of the software are given below and shown within the menu structure in Fig 67.

- Image capture
- File handling
- Image manipulation and calibration
- Image measurements and analysis.

The software is written in Microsoft C and in Intel 486 assembly language. The image capturing routines call various hardware drivers from the Data Translation library provided with the frame grabber card.

The Image Capture and File Handling functions shown in Figure 67 are self explanatory. The process of making ratiometric measurements requires further explanation. The operator recalls a captured image to the computer screen using the File Handling function. Using the mouse pointer and the Image Calibration menu, the operator places two reference points in close proximity to one another on bony details of the upper surface of the hard palate. These are shown in Figure 65 as the Palatal References. When these palatal references have been set satisfactorily, Set Image Axis is selected and a software generated line joining these two points and a bisecting line forms the palatal reference axis. All subsequent images are referenced by the operator in the same manner, resulting in a common axis throughout the sequence. There is also a menu option called Absolute Calibration which enables calibration of the image in absolute units of distance. This involves placing two reference points onto an object in the image of known dimensions and calibrating by entering the distance into the computer.

With the images based on a common axis, direct inter-comparison is made possible. Using the Image Analysis menu, the operator places a third anatomical reference point on the posterior side of the post pharyngeal wall that coincides with, either the vector of movement as previously described or a fixed reference point. In the case of the palate re-repair study in Section 6.2, this was chosen as a point inferior to the auditory meatus. This meatus reference was chosen as it related to the normal

Figure 67 Schematic of Menu Structure

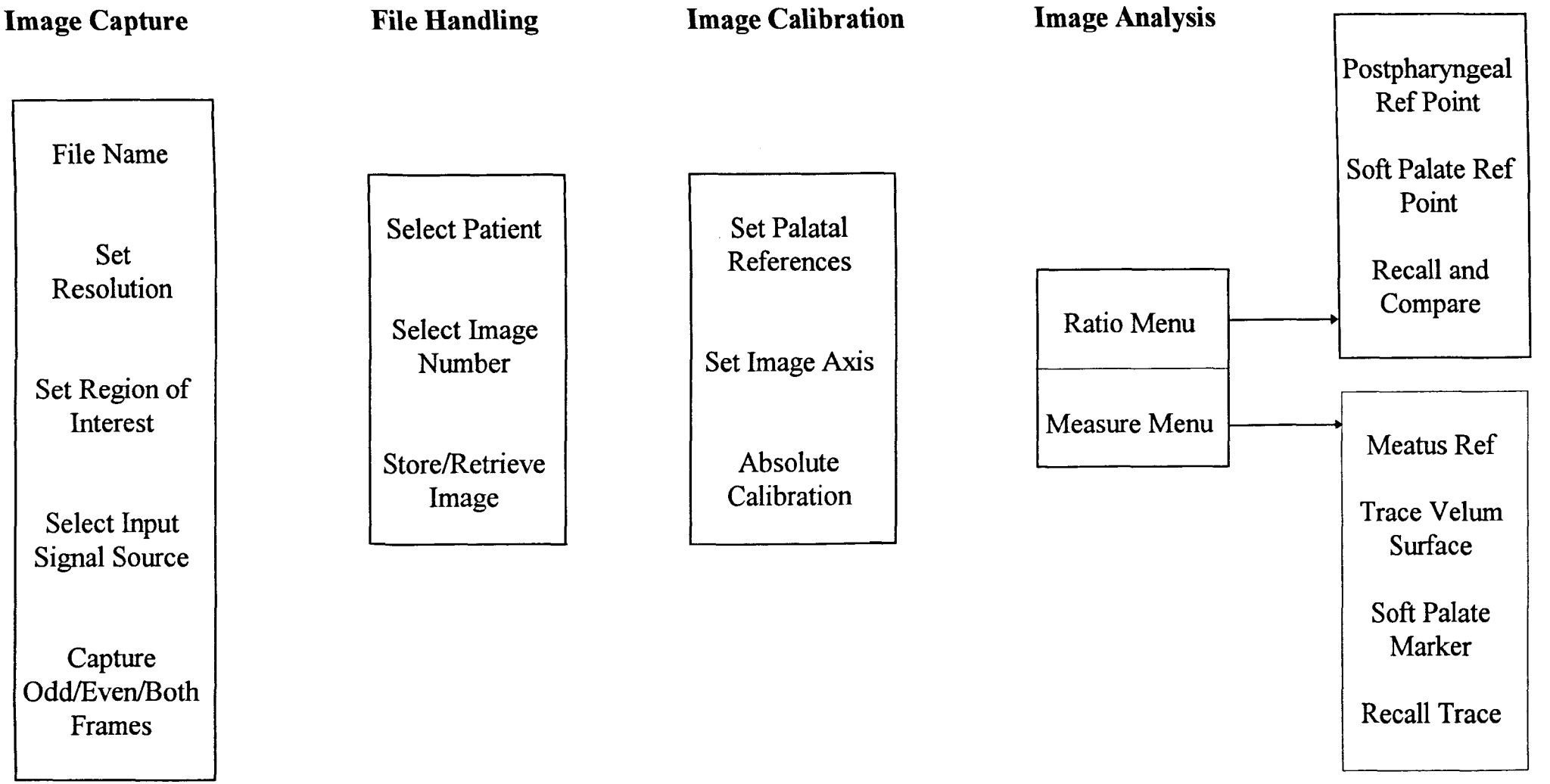

origin of the levator muscles and is the point towards which the velum would normally move. The superior surface of the velum is then traced and using the menu option Soft Palate Mark, the computer calculates the shortest line from the meatus reference point to the superior surface of the velum, this point is marked as the Soft Palate Ref Point. The intersection of this line and the posterior pharyngeal wall is marked with the Postpharyngeal Ref Point and thereby the distance a-a' as shown in Figure 65 is measured. On a subsequent image, the palatal references are again marked. The two images to be compared are then aligned by the software rotating and translating the frames until the palatal reference axis set in the two images coincide. This process is shown schematically in Figure 68. This occurs during the measurement when the operator, using the Recall and Compare menu option, recalls a patient image for comparison with a reference image which is normally the view of the nasal breathing position. Therefore with a common reference axis, the position of the meatus reference can be transferred to the second and all subsequent images.

Figure 68. Aligment of Palatal Reference Axis

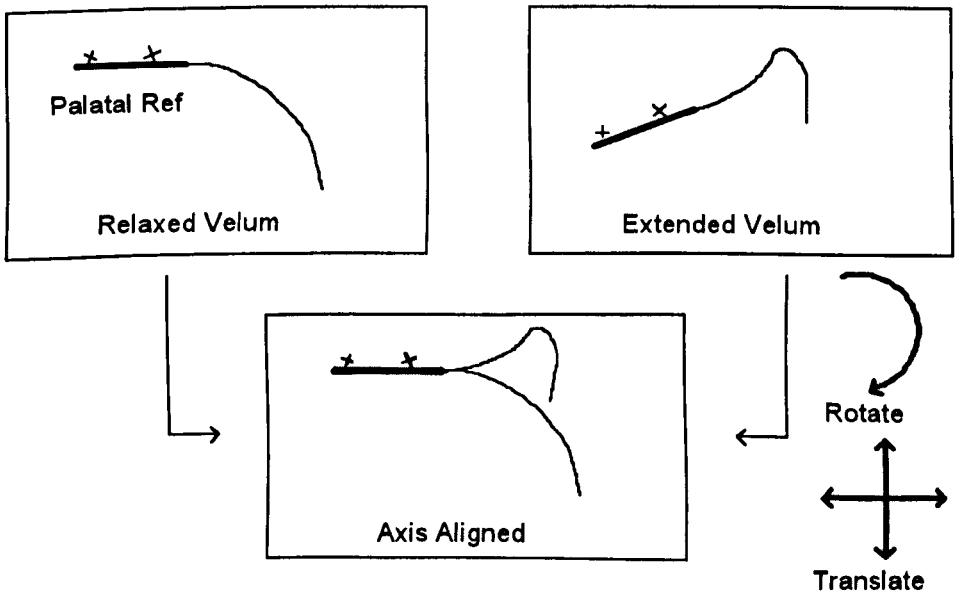

The extended velum surface is traced and the distance b-b', measured between the meatus reference and the extended velum is ascertained for the next image. The ratio on a-a' and b-b' is calculated and forms an index of velum closure as described in Figure 65. In this way measurement uncertainty due to inter-frame movement in the mid-saggital plane is minimized.

Figure 69: Velum Closure Index vs. Time

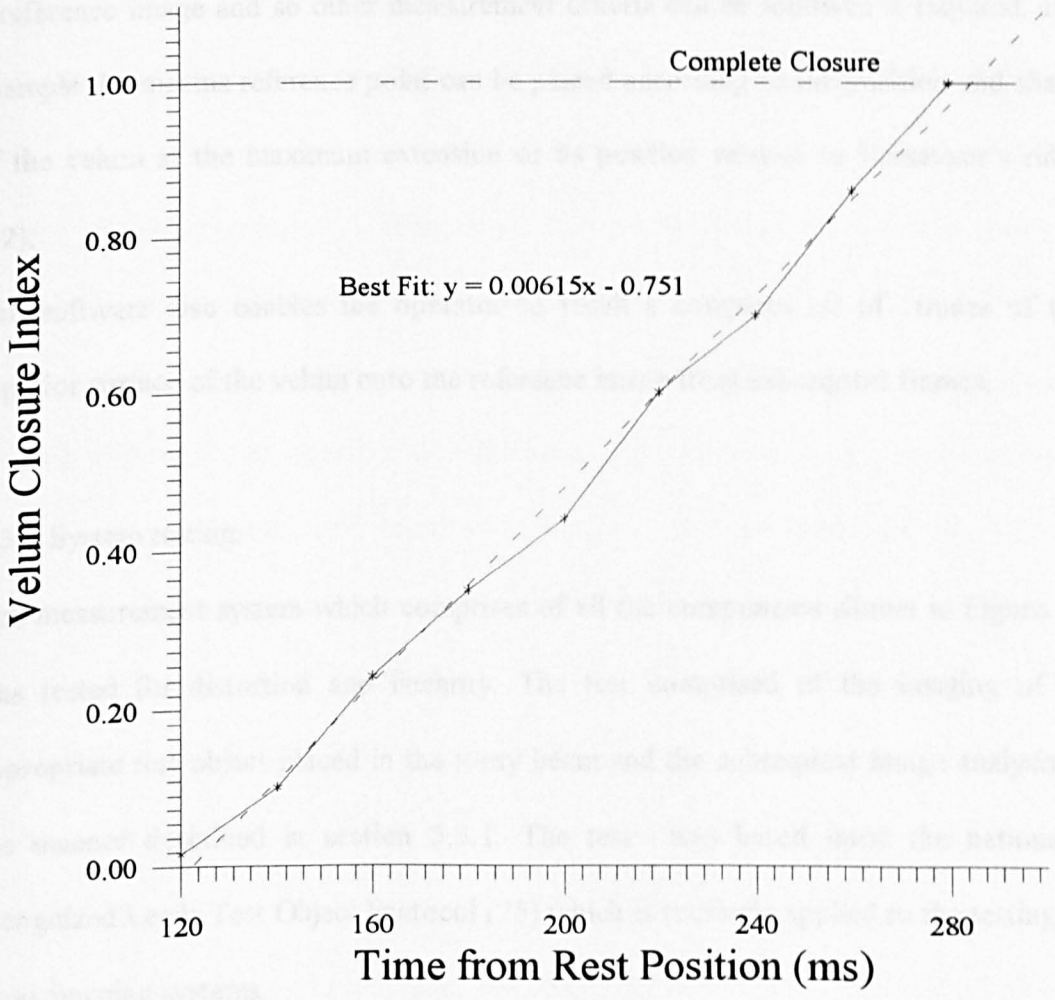

A complete set of ratiometric values, which lie in the range 0 to 1, is derived from the consecutive images of velopharyngeal movement. As shown in Figure 69, this data is

plotted on the y-axis as the velum closure index. The frame number and hence the time elapsed since the nasal breathing frame is plotted on the x-axis. The rate of closure m, is calculated using a simple $y = mc + c$ fit to the data points taken between the first excursion from the nasal breathing position to the point of maximum extension of the palate across the port.

The palatal and meatus reference points can be placed at any point in the image to form a reference image and so other measurement criteria can be followed if required. For example the meatus reference point can be placed according to the position and shape of the velum at the maximum extension or its position relative to Passavant's ridge (52).

The software also enables the operator to recall a complete set of traces of the superior surface of the velum onto the reference image from subsequent frames.

5.3.2 System testing.

The measurement system which comprises of all the components shown in Figure 66 was tested for distortion and linearity. The test comprised of the imaging of an appropriate test object placed in the x-ray beam and the subsequent image analysis in the manner described in section 5.3.1. The test was based upon the nationally recognized Leeds Test Object Protocol (75) which is routinely applied to the testing of x-ray imaging systems.

The image from the test object comprises of a regular grid of known dimensions. The worst case ratiometric error found from measurements of any two equal dimensions within the central portion of the image was < 1%. The worst case errors occurred

when measurements were taken from orthogonal line features. In practice this would not occur because the lines joining the clinical features would always form an acute angle and hence further minimize the ratiometric error.

5.3.3 Clinical evaluation.

Evaluation of the reliability and validity of the procedure proposed (52) has not been undertaken and therefore a specific study of measurement errors associated with measurements of velopharyngeal movement using this system was undertaken. The methods, results and conclusions from this investigation are extensively described (63) elsewhere. Briefly, the measurement system was used by two trained observers to analyze 10 velopharyngeal examinations. The examinations were chosen, using a random list of numbers generated by computer, from a set of 23 videofluoroscopic investigations of post operative re-repaired soft palates. Each examination consisted of 7 video frames of data showing the velopharyngeal movement of the vowel sound *i*. The ratiometric measurements described in Section 5.3.1 were carried out twice by the observers in a random order giving a total of 280 image frames measured.

Analysis of variance as described in Section 4.1.2 was used to measure the uncertainties. One way analysis of variance detected no significant variation between-observer variation which suggests that the measurements were consistent between the two observers.

The analysis of variance of gap size gave a significant result ($p < 0.01$) for the variation between images. The within-image standard deviation was 7.6% with a 95% confidence interval between 6.2% and 8.9%, which suggests that with the same image measured by the same observer the measurement uncertainty was about 7.6%. The

maximum difference that could occur between two successive measurements of the same image was calculated using the repeatability coefficient and shown to be 21%. An identical method of measurement and analysis carried out on images of the velopharyngeal movement during the phonation of the low vowel *a* showed no significant differences with the above results.

The conclusion of the clinical evaluation and the system testing was that the measurement system met the requirements outlined in Section 5.2. It was further concluded that the investigation into the clinical measurement uncertainties were sufficiently understood and therefore the system could be applied to clinical studies.

Chapter 6

Velopharyngeal Measurement System. Clinical Applications.

6.1 Clinical applications.

The measurement system was applied to lateral x-ray video fluoroscopy results taken from patients attending cleft palate and general clinics at The St. Andrews Centre for Plastic Surgery, Essex.

6.1.1 Normative and patient results, example data

Data from a group of six normal adults was collected on an ad-hoc basis during routine cleft palate clinics using the test material and measurement protocol described in Sections 5.2 and 5.3. Results are shown in Figure 70 and Table 17.

Fig 70: Velum Closure in 6 Normal Adults

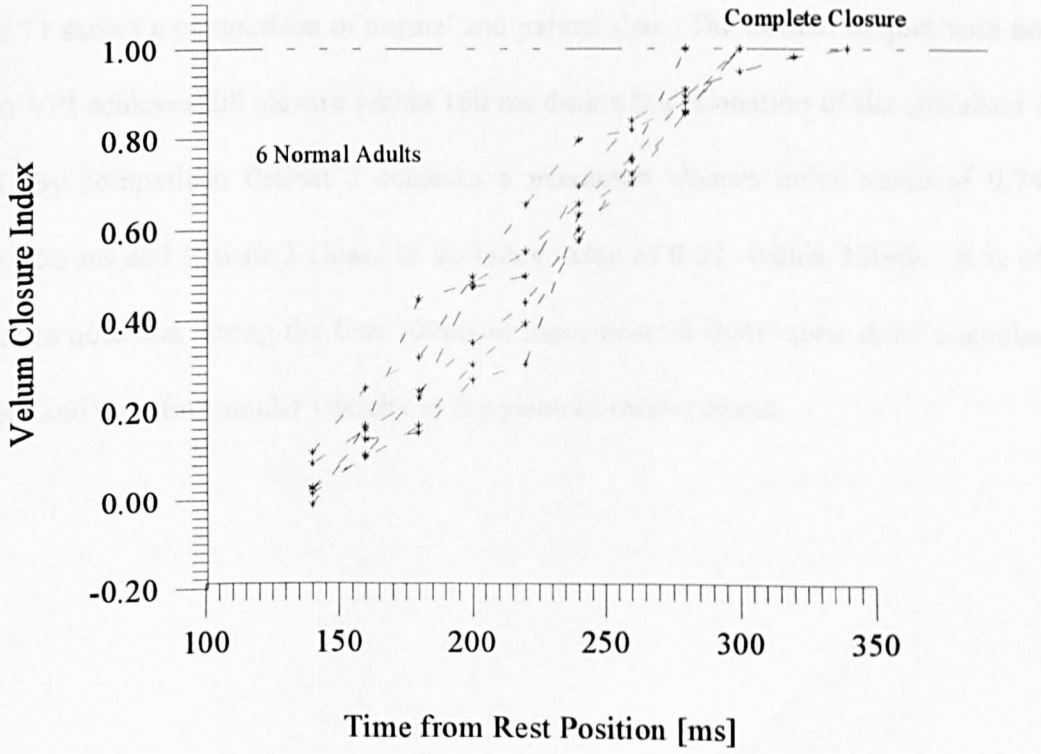

The results, at the time of writing, are too few in number to be considered normative however they are included for reference. As might be expected, this group consistently achieves a high degree of closure and also shows a remarkably constant time of closure. Comparison of these six results with another study of two normals (47) show

Table 17: Velum Closure in 6 Normals and Comparative data

	Mean	Std Dev (σ)	
Degree of Closure	0.98	0.05	
Time of Closure(ms)	135	15	
Degree range	0.86 → 1.00		Comparative data (47)
Time range	113 → 161		109 → 124

good agreement although the group of six has a slightly higher upper time of closure value. However this difference should be treated with caution as the numbers in both studies are too small to be considered normative and the phonetic material used in each group was not equivalent.

Figure 71 shows a comparison of normal and patient data. The normal subject with no known VPI achieves full closure within 160 ms during the phonation of the sustained *i* vowel. By comparison Patient 1 achieves a maximum closure index value of 0.74 within 156 ms and Patient 2 closes to an index value of 0.32 within 120ms. It is of interest to note that during the first 100ms of movement all three cases show a similar gradient and therefore similar velocity in the plane of measurement.

Fig 71: Comparison of Normal and Patient Data

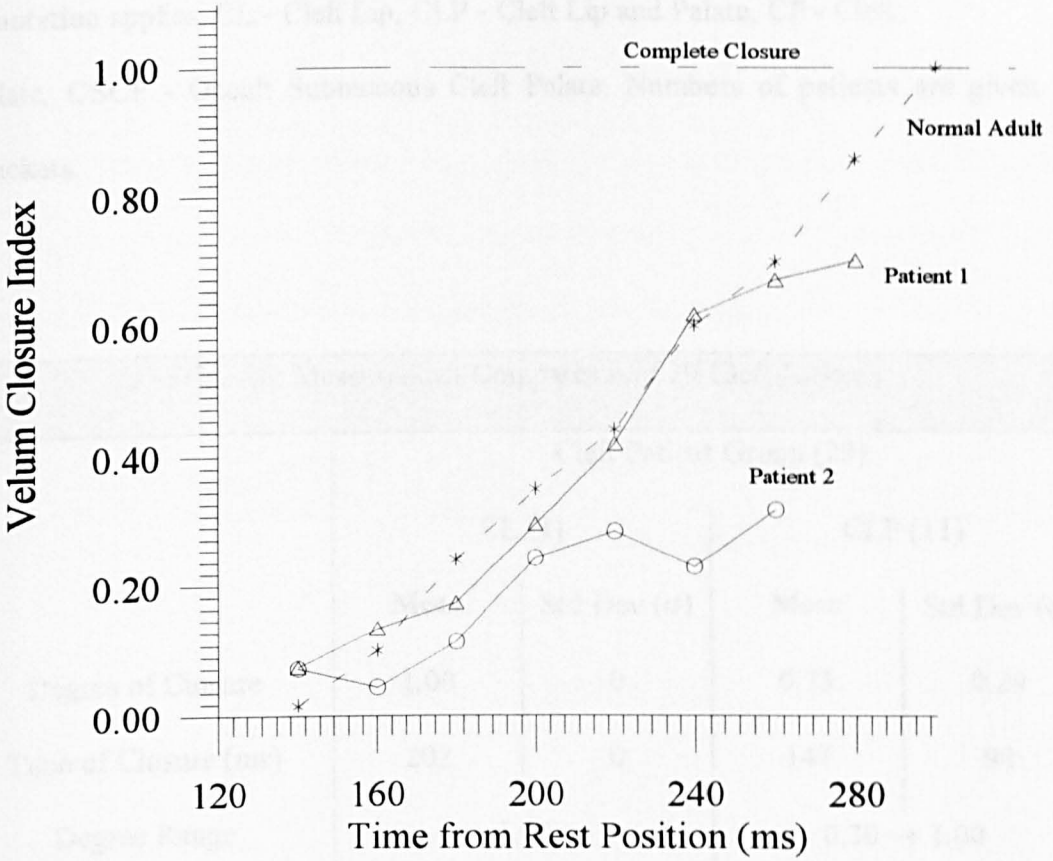

6.1.2 General clinical results.

The fluoroscopic screenings of lateral velopharyngeal movement from a group of 41 patients were analyzed in the same manner as previously described. The patients were attending routine cleft clinics with various clinical conditions associated with impaired articulation.

Times of closure in the case of patients not achieving full closure were calculated using a $y = mx + c$ fit to the data and calculating x for y = 1. The resultant extrapolated closure times could then be compared against the data taken from patients achieving full closure.

Table 16 shows measurement comparisons from 29 cleft patients. The following annotation applies, CL - Cleft Lip, CLP - Cleft Lip and Palate, CP - Cleft Palate, OSCP - Occult Submucous Cleft Palate. Numbers of patients are given in brackets.

Table 16: Measurement Comparison of 29 Cleft Patients				
	Cleft Patient Group (29)			
	CL (1)		CLP (11)	
	Mean	Std Dev (σ)	Mean	Std Dev (σ)
Degree of Closure	1.00	0	0.75	0.29
Time of Closure (ms)	202	0	147	94
Degree Range	1.00		0.30 → 1.00	
Time Range (ms)	202		122 → 362	

Table 16: (continued) Measurement Comparison of 29 Cleft Patients				
	Cleft Patient Group (29)			
	CP (11)		OSCP/SCP (6)	
	Mean	Std Dev (σ)	Mean	Std Dev (σ)
Degree of Closure	0.66	0.25	0.74	0.22
Time of Closure (ms)	273	156	258	89
Degree Range	0.27 → 1.00		0.44 → 1.00	
Time Range (ms)	122 → 575		116 → 360	

Table 17 shows measurements taken from 12 non-cleft patients. The following annotation applies. PPD - Palato-Pharyngeal Disproportion, TC - Treacher Collins Syndrome, VPI - Velopharyngeal Incompetence, D - Dysarthria.

Table 17: Measurement Comparison of 12 Non-Cleft Patients

	Non- cleft Patient Group (12)			
	PPD (3)		TC (2)	
	Mean	Std Dev (σ)	Mean	Std Dev (σ)
Degree of Closure	0.84	0.16	0.38	0.01
Time of Closure (ms)	142	20	138	164
Degree Range	0.68 → 1.00		0.37 → 0.38	
Time Range (ms)	122 → 161		152 → 402	

Table 17: (continued) Measurement Comparison of 12 Non - Cleft Patients

	Non - Cleft Patient Group (12)			
	VPI (5)		D (2)	
	Mean	Std Dev (σ)	Mean	Std Dev (σ)
Degree of Closure	0.54	0.13	0.58	0.07
Time of Closure (ms)	190	90	216	25
Degree Range	0.35 → 0.67		0.51 → 0.65	
Time Range (ms)	113 → 367		191 → 241	

The comparison of the patient groups with the normal group reveals a consistently lower degree of closure amongst patients, however the degree of closure range results show that a number of cleft cases achieve closure. This is in contrast to the non-cleft group where, with the exception of the PPD patients, closure is not achieved.

Comparison between the cleft and non-cleft groups show a consistently higher mean degree of closure from the cleft patients but with a larger standard deviation. This is further demonstrated by the overlapping between cleft and non-cleft groups in the degree range.

Comparisons of the time of closure for the patient and normal groups reveal a consistently longer time of closure for the patient group. The standard deviation of the time of closure results in the normal group is also significantly lower than the patient groups with the exception of the PPD patients.

Comparison of time of closure between the cleft and non-cleft groups shows a wide range of results in both means and standard deviations.

6.1.3 A specific case study of a pre and post-operative cleft palate re-repair.

A sixteen year old female having undergone surgery as a young child for the primary repair of a cleft lip and palate was referred, due to the presence of severe hypernasal speech, to the Cleft Lip and Palate Service, St. Andrews Hospital , Essex.

Pre-operative examination during November 1991 by a speech therapist concluded the following.

- A persistent severe hypernasality was subjectively detected and confirmed using the Nasal Resonometer, results are shown in Table 18 .

- Occasional uncontrolled nasal emission was subjectively detected and confirmed using nasal annenometry.
- The overall sound system was prone to inaccuracy with a resultant poor intelligibility.

Examination by a plastic surgeon using oral examination, nasal endoscopy and lateral video-fluoroscopy concluded the following.

- Extensibility of the velum was poor.
- No contact was made between the superior surface of the velum and the post pharyngeal wall during phonation of the vowels *i* and *a*.
- The origin of the levators emerged from the velum in a noticeably more anterior position than normal.

The conclusion of the preoperative examination was that a surgical procedure known as palate rerepair would be carried out. This procedure is described in detail elsewhere (65). In brief, the operation involves the separation of the levator muscles from the aponeurosis just posterior to the hard palate thus enabling the subsequent dissection of the muscle. The levator is then retropositioned by re-uniting the muscle and velum aiming to create a sling in the middle third of the velum or behind. The procedure seeks, by this process of radical muscle dissection and repositioning, to restore as near as possible the normal anatomy of the nasopharynx.

Figure 72 shows the index of velum closure pre and post operatively for the vowel sound *i*.

Fig 72: Pre and Post Operative Comparison of Palate Re-repair

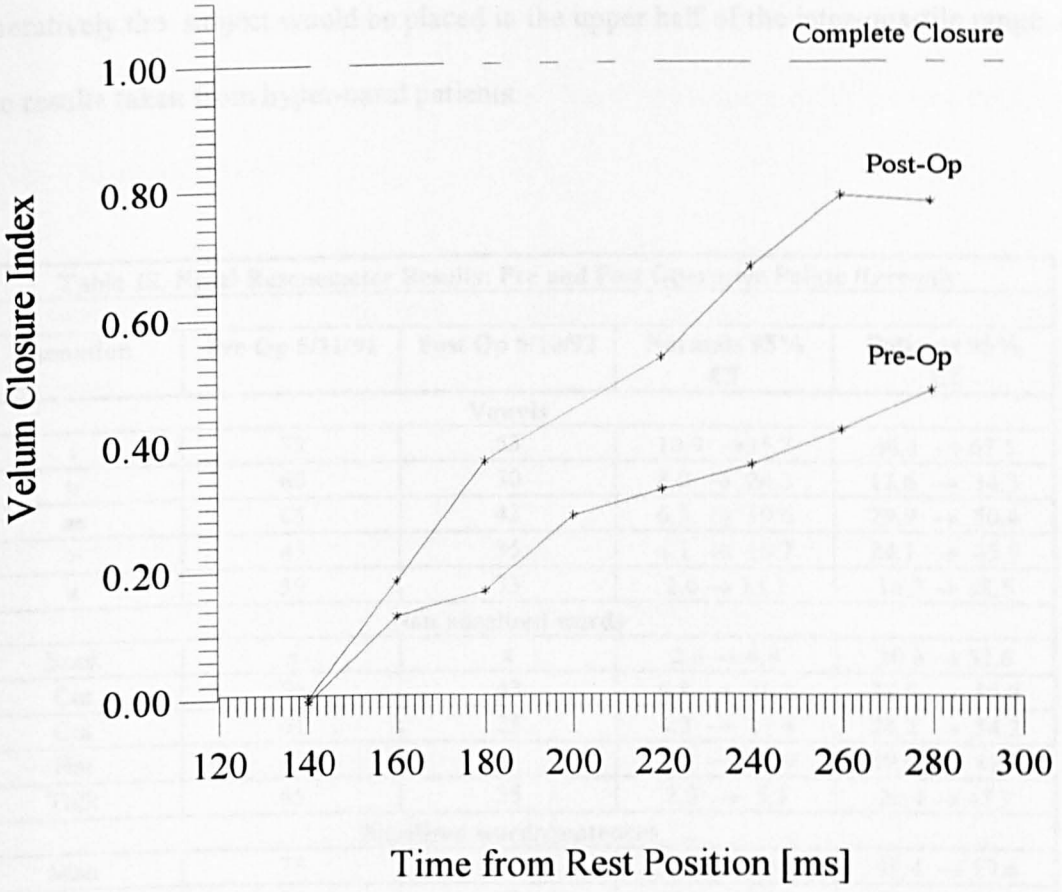

Figure 72 shows that the post-operative velum closure index had increased to 0.8 compared to a pre-operative value of 0.48. The time to reach full extension had decreased post-operatively to 100ms compared to a pre-operative figure of 140ms. Extrapolation of these results to full closure gives a post-operative time to closure of 125 ms, which compares favourably with the group of 6 normals shown in Table 15. The pre-operative time to closure measures as 291ms.

Comparison between the subject's pre-operative measurements taken using the Nasal Resonometer and the normal group given in Table 18 show a consistently high pre-operative result. Referring to the box plots of Figures 64a-d reveals that pre-operatively the subject would be placed in the upper half of the inter-quartile range of the results taken from hyper-nasal patients.

Table 18. Nasal Resonometer Results: Pre and Post Operative Palate Rerepair

Phonation	Pre Op 5/11/91	Post Op 6/10/92	Normals 95% CI	Patients 95% CI
Vowels				
i	78	53	10.9 →35.7	46.1 → 67.5
u	60	30	8.0 → 24.3	12.6 → 34.3
ae	65	43	6.3 → 19.6	29.9 → 50.4
>	45	35	4.1 → 10.7	24.1 → 45.9
a	50	33	2.0 → 13.3	16.2 → 38.5
Non nasalised words				
Book	x	x	2.6 → 4.9	20.6 → 52.6
Car	55	43	6.8 → 26.2	31.5 → 55.0
Cat	61	25	4.2 → 21.4	24.2 → 54.2
Hat	x	x	1.5 → 12.9	19.6 → 41.9
Talk	65	35	2.9 → 5.3	20.4 → 45.2
Nasalised words/sentences				
Man	75	68	50.2 → 64.7	61.4 → 73.6
Mean	85	73	65.6 → 76.3	70.3 → 81.3
Bang	x	x	49.8 → 61.4	61.9 → 74.5
99	80	58	54.6 → 68.4	65.9 → 76.5
Many	76	63	50.6 → 62.3	59.7 → 75.3
Non nasalised sentences/passage				
Book	51	45	3.1 → 11.8	33.2→ 58.9
Jigsaw	x	x	4.1 → 16.3	38.0 → 63.5
Ship	65	30	3.8 → 15.3	35.7 → 59.9
Days	66	48	2.7 → 23.6	37.2 → 60.8
Passage	73	48	12.5 → 24.9	46.6 → 65.7

x - no reading taken.

The post-operative Nasal Resonometer results show a consistent reduction in the ratio of nasal to oral balance when compared against the pre-operative readings. The

average change in nasal:oral ratio was 22.5% with a standard deviation of 9.3%. The range of nasal:oral ratio change was 6 → 36 %. An improvement in the nasal:oral ratio was measured for all phonations including the nasalised tests. Comparison of the subject's post-operative results with Figures 59a-d reveal that in most cases the subject score was either within the upper quartile of the normal range or in the lower quartile of the hypernasal group.

Post-operative clinical assessment by speech therapist reached the following conclusions.

- The subject had much improved nasal:oral resonant balance.
- In connected speech there remained a slight hyper-nasality and nasal emission.
- Her sound system was accurate and had normal intelligibility.

Post operative examination by plastic surgeon concluded the following.

- Oral examination showed levators very posterior with a good high velum lift.
- Lateral video-fluoroscopy showed a slightly short velum with levators inserted posterior to the middle of the soft palate. Soft palate extensibility was estimated as 50%.
- Contact was just made between the superior surface of the velum and the post pharyngeal wall during the phonation of the vowels *i* and *a*.

The contribution of the measurement techniques can be noted as follows.

- Quantification of speech improvement in terms of the change in nasal:oral ratio.
- Comparative nasal:oral ration measurements against normative data.

- Quantification of the improvement post-operative velopharyngeal closure.
- Quantification of the improvement in post-operative time of velopharyngeal closure.

From the patient's point of view the palate re-repair has provided a very pleasing result with measurable increase in palatal function and a marked improvement in her speech

6.2 Assessment of palate re-repair.

The velopharyngeal measurement system was employed as one of several assessment techniques used during a clinical and radiographic study of 32 cleft palate re-repair cases. The object of the study was to test the hypothesis that, *re-repair of the cleft, involving radical muscle correction as a secondary procedure following primary cleft repair, could produce measurable improvement in velar function.* The procedure is suggested by the plastic surgeon as an alternative to the more traditional surgical management of cleft palate patients which would involve the technique of pharyngoplasty. Pharyngoplasty has several forms however they all involve the physical part occlusion of the nasopharynx using additional tissue. However this procedure carries significant possible morbidity in the forms of hyponasality, chronic mouth breathing, catarrh and sleep apnea. This is in comparison to the benefit of the re-repair technique, as postulated by the surgeon, in which normal anatomy is restored with very little morbidity. The surgical technique, the methodology, results from the accompanying measurement techniques and the conclusions of the study are given in detail elsewhere (65).

Brief details of the study are as follows.

Thirty two patients, 21 males, 11 females with an age range of 4 to 37 years, mean age 14.4 years were studied. All patients had undergone primary cleft repair without radical muscle dissection or retropositioning, three had bilateral cleft lip and palate, nine with unilateral cleft lip and palate and twenty with isolated cleft palate. Indications for palate re-repair were consistent clinical, radiographic and nasoendoscopic indications of velopharyngeal incompetence.

Three main pre and post-operative assessment methods of velar function were employed.

- Clinical assessment of speech was made by a panel of speech therapists. Videotape samples of single words, automatic speech and spontaneous speech were viewed in random order and the degree of hypernasality and nasal emission scored on a scale of 0-3 representing a range of normal (0), mild (1), moderate (2) and grossly abnormal (3).
- Radiographic measurement of velopharyngeal movement. The measurement of degree of closure and rate of closure was carried out for the vowel sounds *i* and *a* as described in Section 5.2.
- Nasendoscopy examinations were performed and the resultant video recordings analyzed in random order by a consultant plastic surgeon. Assessment and recording of results were in accordance with the recommendations of the international working group (52).

Results from the velopharyngeal measurement system are shown in Figs 73, 74, 75 and Tables 19, 20, 21.

The results in Figures 73, 74 and 75 are presented in the form of a pre and post-operative comparison of degree of closure, rate of closure and time of closure, respectively. The data is presented with the pre-operative result plotted on the y-axis against the post-operative results on the x-axis. Results that have shown no change pre and post operatively will lay on the diagonal dotted line.

To statistically test the hypothesis, *has palate re-repair improved velar function*, the results from the variables, degree of closure, rate of closure and time of closure were tested using Students paired two tailed t-test and one way analysis of variance. Means and standard deviations were also calculated. The results are given in Tables 19, 20 , 21.

Results for the degree of closure shown in Figure 73 and Table 19 show a statistically significant change between pre and post-operative measurements. Referring to Figure 73, any results that lay to the right of the dividing diagonal line indicate an increase in the post-operative degree of closure and conversely any results that lay to the left of the line indicate a decrease in post-operative closure. Clearly there has been a measurable improvement in the majority of cases. Four results, laying close to the dividing line show no significant improvement. Three results appear on the left of the line, however in one of these cases the pre-operative closure was just greater than 0.9 and the commensurate post-operative closure was just less than 0.9. All remaining measurements show an increase in the degree of post-operative closure. Table 19 reflects this trend by showing that the mean of the results has improved from 0.56 to 0.75 with no significant change in standard deviation. The one way analysis of variance

and the t-test both test the hypothesis that, *there is no significant difference between the pre and post-operative results.* The variance tests the inter and intra-group variation as explained in Section 4.1.2 , the well known paired t-test tests the difference between individual pairs of results. Both results show that there is a significant difference between the pre and post-operative measurements.

Results from the rate of closure measurements shown in Figure 74 and Table 20 show a statistically significant change between pre and post-operative measurements. Figure 74 shows that the majority of post-operative rates have increased. Nine results are to the left of the dividing line of which two show virtually no change. One result shows a noticeable decrease in the rate of closure changing from a pre-operative rate of 465 units/sec to a post-operative rate of 234 units/sec, the remaining six measurements show a decrease in the range 161 units/sec to 85 units/sec. The mean rate of closure has increased from 441.9 units/sec to 587.0 units/sec with a slight increase in standard deviation. The hypothesis that, *there is no significant difference in the rate of closure between pre and post-operative results,* is shown to be not true by the analysis of variance and the t-test. Both results show that there is a significant difference between the pre and post-operative measurements.

Fig 73: Palate Re-repair Study. 23 Patients.

Comparison of Pre and Post Operative Degree of Closure

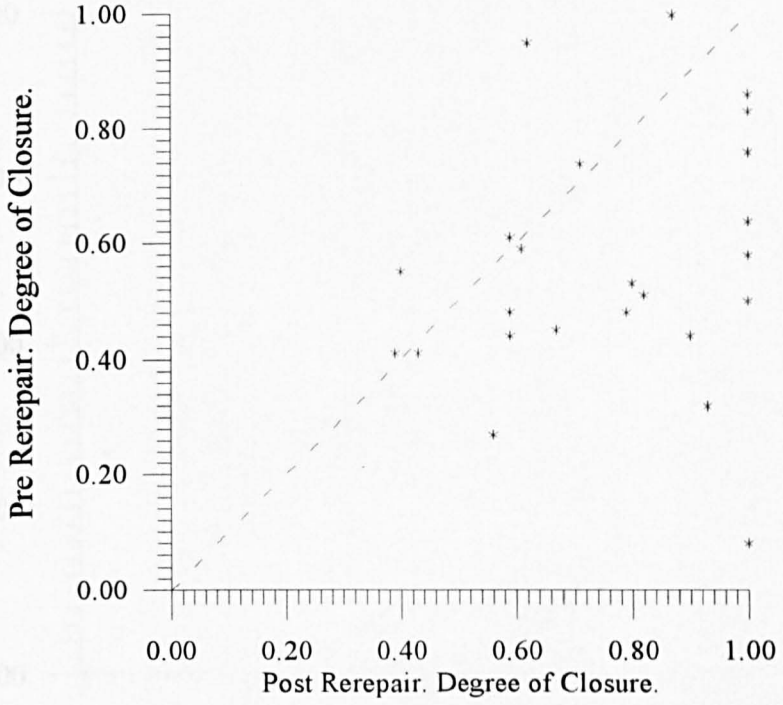

Table 19: Degree of Closure

	Mean	Std Dev (σ)	Std Error
Pre-operative	0.56	0.22	0.042
Post-operative	0.75	0.21	0.039

Pre and Post-operative One Way Analysis of Variance

Degrees of Freedom	$F_{1,46}$ ratio	$F_{1,60}$ test	Significance
55	10.57	7.08	0.01

Pre and Post-operative Paired Students t-test

Mean Difference	t_{46} value	$t_{60,0.005}$ test	95% CI, Difference
-0.19	-3.25	2.66	-0.30 → -0.07

Fig 74: Palate Re-repair Study. 23 Patients.

Comparison of Pre and Post Operative Rate of Closure

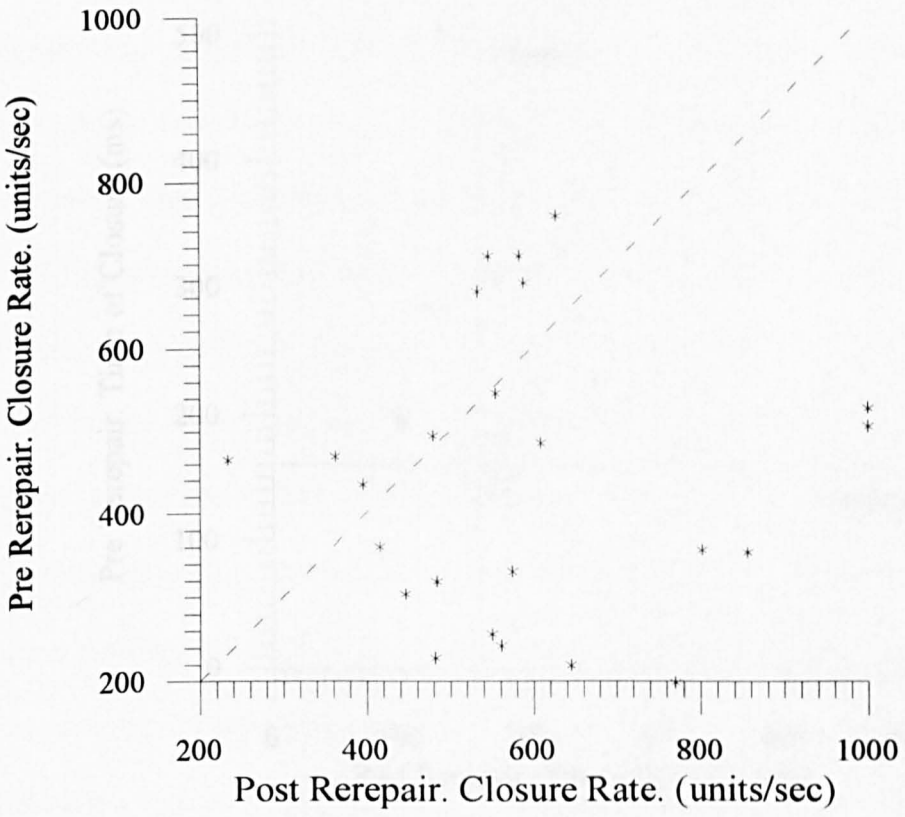

Table 20: Rate of Closure

	Mean	Std Dev (σ)	Std Error
Pre-operative	441.9	170.7	34.8
Post-operative	587.9	186.5	38.1

Pre and Post-operative One Way Analysis of Variance

Degrees of Freedom	$F_{1,46}$ ratio	$F_{1,60}$ test	Significance
47	8.00	7.08	0.01

Pre and Post-operative Paired Students t-test

Mean Difference	t_{46} value	$t_{60,0.005}$ test	95% CI of Difference
-146	-2.83	2.66	-249.9 → -42.1

Fig 75: Palate Rerepair Study. 23 Patients.

Comparison of Pre and Post Operative Time of Closure

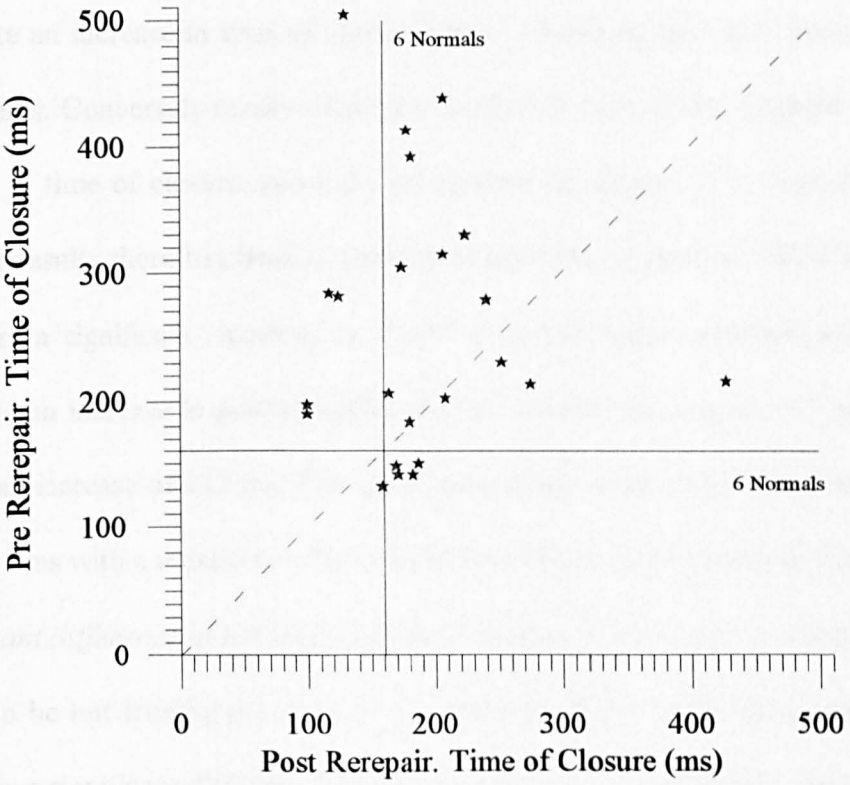

Table 21: Time of Closure

	Mean (ms)	Std Dev (σ)	Std Error
Pre-operative	264.7	110.5	22.5
Post-operative	188.1	67.7	13.8

Pre and Post-operative One Way Analysis of Variance

Degrees of Freedom	$F_{1,46}$ ratio	$F_{1,60}$ test	Significance
47	8.40	7.08	0.01

Pre and Post-operative Paired Students t-test

Mean Difference	t_{46} value	$t_{60,0.005}$ test	95% CI of Difference
76.7	2.90	2.66	23.4 → 129.9

Results from the time of closure measurement shown in Table 21 and Figure 75 show a statistically significant change between pre and post-operative measurements. Referring to Figure 75, any results occurring to the right of the dividing line demonstrate an increase in time of closure when comparing pre and post-operative measurements. Conversely results which lay on the left side of the diagonal line show a decrease in time of closure, pre and post-operatively. Figure 75 reveals that in the majority of results there has been a decrease in the time to closure. There are seven cases where a significant increase in closure time has been measured, six of these results have an increase in post-operative closure time in the range 21 to 42 ms, one result has an increase of 212 ms. The mean time of closure has decreased from 264.7 ms to 188.1 ms with a reduction in the standard deviation. The hypothesis that, *there is no significant difference in the time of closure between pre and post-operative results,* is shown to be not true by the analysis of variance and the t-test. Both results show that there is a significant difference between the pre and post-operative measurements. It is also of interest to note that the post-operative mean time of closure is very similar to the upper limit of the range of results measured from six normal subjects in Section 6.1. Figure 75 also reveals that a significantly greater number of results are close to this upper limit from six normal subjects when compared to the pre-operative measurements.

6.3 Comparison between velopharyngeal and acoustic measurements.

In order to compare results from the measurement of nasal:oral ratio from the Nasal Resonometer and the measurement of degree of closure from velopharyngeal

measurements, data from 40 patients was studied. The data was gathered over three years from patients attending cleft clinics with a variety of velopharyngeal insufficiencies. The study was designed to test the hypothesis that, *results from the two methods are directly comparable,* on the basis that an insufficient velopharyngeal closure would be directly related to the presence and degree of hyper-nasality.

The statistic chosen to test this hypothesis was the Students t-test applied to paired samples. The statistic enables the comparison of two methods by analyzing data from pairs of results, one from each method, taken from many samples. The basis of the statistic is that the mean of the difference between pairs of results will tend to zero if the methods are comparable. The advantage to using the difference between results is that the samples can be dissimilar, in this case different patients, without effecting the comparison of the two methods.

Nasal Resonometer and velopharyngeal measurements from 40 patients were taken for the phonations of the vowels *i* and *a.* The closure data has a range of 1 → 0 which notionally corresponds to the nasal:oral ratio range 0 → 100%. Therefore to enable the comparison the closure data was adjusted by the simple formula, (Closure -1) x -100, to give a closure range 0 → 100%. Results are shown in Table 22.

Table 22: Comparison of velopharyngeal and acoustic measurements.

Vowel *i*

	Mean(%)	Std Dev (σ)	Std Err	Samples
Nasal:Oral ratio	31.3	19.3	3.1	40
Closure	32.5	26.8	4.2	40

Nasal:Oral ratio/Velopharyngeal closure. Students paired t-test.

----------Paired Differences----------

Mean	Std Dev	Std Err	95% CI	t value	$t_{40,0.1}$
-1.2	33.3	5.3	-11.8→9.0	-.0.22	1.30

Vowel *a*

	Mean(%)	Std Dev (σ)	Std Err	Samples
Nasal:Oral ratio	35.7	17.7	2.9	40
Closure	31.4	24.8	3.8	40

Nasal:Oral ratio/Velopharyngeal closure. Students paired t-test.

----------Paired Differences----------

Mean	Std Dev	Std Err	95% CI	t value	$t_{40,0.1}$
4.3	32.6	5.1	-7.3→13.6	0.62	1.30

The results in Table 22 show that for both vowels, the mean of the paired differences are small, -1.2 for *i* and 3.2 for *a*. The respective |t| values for each vowel are 0.22 and 0.62 which are less than the $t_{40,0.025}$ value of 1.68 . The result is significant at the 5% level. Therefore the null hypothesis is accepted, that is *the results from the two methods are comparable.*

It is important to note that, examination of the acoustic and closure measurements reveal several pairs that do not closely correspond. Similarly, from anecdotal information relating to individual patients there are clear instances in the study when perceived hypernasality has not corresponded to impaired velar function in terms of closure. These observations are further confirmed by the high standard deviations of the mean difference shown in Table 22. This tends to the conclusion that the results of the comparison may be statistically rather than practically significant in terms of the methods being interchangeable as a clinical measurement. The results do however show that there is a strong relationship between the two methods and that they are complimentary rather than equivalent.

Chapter 7

Conclusions and further work

The overall conclusion following the design, development and clinical implementation of the Nasal Resonometer and the videofluoroscopic measurement system has been very positive. The measurement techniques are now routinely used in conjuction with complimentary clinical assessments of velopharyngeal competence.

7.1 Nasal Resonometer

The Nasal Resonometer has been in clinical use for over three years and has been found to be a useful additional measurement tool for speech assessment. The original request was for an instrument designed to aid in the clinical assessment of speech in cleft palate children. In conjunction with nasendoscopy, lateral videofluoroscopy, computer aided analysis of x-ray images, speech assessment and clinical examination, the instrument's results are routinely reported to the patient's referring clinician. The application of the instrument has broadened to encompass non-cleft conditions such as palato-pharyngeal disproportion, dysarthria and velopharyngeal incompetence.

The application of the Nasal Resonometer to the orthodontic study in Section 4.2.1 highlights the instrument's usefulness in easily providing comparative data, between two separate anatomical conditions in the same patient, due to the presence of a prosthetic device. It was of particular interest to the orthodontist to discover that the improvement in speech quality due to the presence of the prosthesis was not necessarily due to the reduction in the nasal:oral resonant balance. In addition, the

perception of hypernasality by the speech therapist was also re-examined in the light of the Resonometer results.

The instrument can also be utilized in the comparison of the efficacy of different surgical techniques in achieving a reduction in nasal:oral ratio. The study described in Section 4.2.2 is an example of such a comparison and, although the numbers of patients at the time of writing are to small to allow definitive conclusions, the measurements have enabled a number of tentative inferences to be made. For example, the lack of evidence of any systematic reduction in nasal:oral ratio during nasalised phonations in the post-operative pharygoplasty group is contrary to the notion that this surgical technique carries significant risk of inducing hypo-nasality. Further measurements are being accumulated from patients within these surgical categories.

The original design criterion of the Nasal Resonometer was to enable clinicians to undertake pre and post-operative assessments of hyper and hypo-nasal speech. The specific patient studies in Sections 4.2.2 and 6.1 demonstrate the effectiveness of the instrument in making comparative measurements of this nature for individual cases. Further accumulation of pre and post-operative comparative data from individual patients is continuing and with sufficient numbers more general conclusions relating to the efficacy of surgical techniques may be drawn.

A specific study of a group of patients suffering various degrees of deafness is planned for the instrument. This subject group present an interesting opportunity to study the effect of the lack of acoustic feedback during speech generation. The hypothesis that

the speech quality of the deaf is reduced, due to the consistent presence of hyponasality, can be carefully examined with this technique.

In a technical sense the ongoing work planned for the instrument amounts to the transfer of the whole system into an IBM PC. The sound separation, dynamic filtering, and frequency tracking will still be handled by external analogue devices. However the presentation of results and comparison with normative or preoperative data will take advantage of the PC's graphics, speed and memory capabilities. There remains the possibility of modifying the sound separation devices to encompass anemometric transducers, thus enabling the measurement of nasal:oral sound and airflow balance simultaneously.

7.2 Velopharyngeal measurements.

The velopharyngeal measurement system has been in clinical use for three years and has made a useful contribution to the assessment of cleft palate repair. In conjunction with other measurement techniques used during routine cleft clinics, the results from velopharyngeal measurements are routinely reported to referring clinicians. The measurement technique has found application in patients with non-cleft conditions such as dysarthria, palato-pharyngeal disproportion and velopharyngeal incompetence.

The original design criterion of the measurement system was to enable speech therapists and plastic surgeons to assess closure of the velopharyngeal port pre and post-operatively. The single study shown in Section 6.1.3 of a patient undergoing palate re-repair demonstrates the clarity of the comparison of pre and post-operative

closure and time of closure. Additional normative data is at present being added to that shown and this will enable a more confident conclusion to be drawn on the post-operative rate of closure that the velum achieves. This parameter is of particular importance following the repositioning of the levator muscles that perform the lifting and acceleration of the soft palate mass.

The application of the technique shown in Section 6.2 in comparing the pre and post-operative results from a particular surgical procedure has enabled a useful new comparison to be made. The results from the study were objectively measured in a randomized procedure that has enabled a confident assessment of the effect of surgery on the closure of the velopharyngeal port. The measurement technique itself has been carefully analyzed in Section 5.3.2 which has resulted in a clear understanding of the measurement uncertainty.

The measurement system has enabled the procedures described by the international standardization of measurement of velopharyngeal closure to be retrospectively applied to archive material. In this manner further studies of surgical techniques are planned for the future. Of particular interest is the comparison of pre and post - operative data measurements of velopharyngeal port as a result of the Furlow surgical technique. This surgical procedure is radically different from palate re-repair but has the same aim in increasing the extensibility of the soft palate. A comparison of closure results from the two techniques will also be studied.

Additional measurement facilities are being added to the measurement system. The assessment of extensibility of the soft palate in terms of the increase in length when extended per unit length when relaxed is of particular interest to the plastic surgeon. The need for the assessment of this parameter arises from the concern that repositioning of muscle groups may lead to scarring of hitherto elastic tissues and a consequent reduction in the elasticity of the soft palate. The timing of movement of the soft palate with respect to the onset of sound at the glottis is of fundamental importance to the change of acoustic impedance of the vocal tract during phonations. In order to study the positioning of the palate with respect to the onset of individual vowel sounds the temporal resolution of the system will have to be improved by at least an order of magnitude. A proposed extension to the existing system is the addition of a very high frame rate camera to the imaging chain which it is hoped will decrease the measurement uncertainty due to image blurring. This addition will also be a prerequisite of a velar movement with respect to acoustic onset measurement.

References

1. Moll, K.L ., A cinefluorograhic study of velopharyngeal function in normals during various activities. *Cleft Palate J.* ,2 112-122, 1965

2. Bloomer, H., Observations on palatopharyngeal movements in speech and deglutination. *J Speech Hear Dis.* 18, 230-246, 1953

3. Shprintzen R., A Three Dimensional Cinefluoroscopic Analysis of Velopharyngeal Closure during Speech and Nonspeech Activities in Normals. *Cleft Palate J,* 11, 412, 1947.

4. Podvinec, s,. The Physiology and Pathology of the Soft Palate. *J. Laryngol.* 66, 452-461, 1952.

5. Fant G., Acoustic Theory of Speech Production. Mouton and Co,. 1960

6. House A.S, Stevens K.N., Analog Studies of the Nasalisation of Vowels. *J. Speech Hearing Dis.,* 21, 218-232, 1956

7. Horii, Y. An Accelerometric Approach to Nasality Measurement: A Preliminary Report. *Cleft Palate Journal,* 17, 254-261, 1980.

8. Warren, D. Nasal Emission of Air and Velopharyngeal Function. *Cleft Palate Journal* 4, 148-156, 1967.

9. Warren, D. et al. Nasal Pathway Resistance in Normal and Cleft Lip and Palate Patients. *Cleft Palate Journal,* 6, 134-140, 1969.

10. Lubker, J., et al. Nasal Air Flow Characteristics during Speech in Prosthetically Managed Cleft Palate Speakers. *Journal of Speech and Hearing Research.* 13, 326-338, 1970.

11. Dickson, S. et al. Aerodynamic Studies of Cleft Palate Speech. *Journal of Speech and Hearing Disorders.* 43, 160-167, 1978.

12. Kelleher, R. et al. Nasal and Oral Airflow in Normal and Cleft Palate Speech. *Cleft Palate Bulletin.* 10, 66, 1960.

13. Quigley, L. et al. Velocity and volume Measurements in Nasal and Oral Airflow ...Warm-wire Flowmeter... *Journal of Dental Research.* 42, 42, 1520-1527, 1963.

14 Quigley, L. et al. Measuring Palatopharyngeal Competence with the Nasal Anemometer. *Cleft Palate Journal.* 1, 304-314, 1964.

15 Warren, D. Velopharyngeal Orifice Size and Upper Pharyngeal Pressure-Flow Patterns in Cleft Palate Speech. A Preliminary Study. *Plastic and Reconstructive Surgery.* 33/34, 82-84/15-26, 1964

16 Warren D. et al. A Pressure Flow Technique for Measuring Velopharyngeal Orifice Area... *Cleft Palate Journal.* 1, 52-71, 1964

17 Hixon T. A New Technique for Measuring Velopharyngeal Orifice Area.. *Journal of Speech and Hearing Research.* 19, 601-607, 1976.

18 Emanuel, F. Some Characteristics of Oral and Nasal Air Flow during Plosive Consonant Production. *Cleft Palate Journal.* 7, 249-260, 1970

19 Counihan, D.T. Oral and Nasal Sound Pressure Measures. In Bzoch, K.R(Ed). *Communication Disorders Related to Cleft Lip and Palate.* Little, Brown, 186-193, 1972.

20 Zemlin, W.R. and Fant, G. The Effect of a Velopharyngeal Shunt upon Vocal Tract Damping Times: An Analog Study. *Speech Transmission Laboratory Quarterly Progress and Status Report.*4, 6-10, 1972

21 Plattner, J. Weinberg, B. and Horii, Y. Performance of Normal Speakers on an Index of Velopharyngeal Function. *Cleft Palate Journal,* 17, 205-215, 1980.

22 Hattori, S. Yamamoto, K. Fujimura, O. Nasalisation of Vowels in Relation to Nasals. *Journal of the Acoustical Society of America.* 30 267-274, 1958.

23 Bloomer, H. Peterson, G. A Spectrgraphic Study of Hypernasality. *Cleft Palate Bulletin.* 5, 5-6, 1955

24 Dickson, D. A Acoustic Study of Nasality. *Journal of Speech and Hearing Research.* 5, 103-111, 1962.

25 Stevens, K. Nickerson, R. Boothroyd, A. Rollins, A. Assessment of Nasalisation in the Speech of Deaf Children. *Journal of Speech and Hearing Research.* 19, 393-416, 1976.

26 Dunn, H. The Calculation of Vowel Resonances and an Electrical Vocal Tract. *J Acous Soc Amer.* 22, 740-753, 1950.

27 Hultzen L. Apparatus for Demonstrating Nasality. *Journal of Speech Disorders.* 7, 5-6, 1942.

28 House, A. Stevens, K. Analog Studies of Nasalisation of Vowels. *J.Speech Hearing Dis.*21, 218-232, 1956.

29 Curtis, J. The Acoustics of Nasalised Speech. *Cleft Palate Journal.* 7, 380-396, 1970.

30 Watterson, T. Emanuel, F. Effects of Oral Nasal Coupling on Whispered Vowel Spectra. *Cleft Palate Journal.* 18, 24-38, 1981.

31 Bernthal, J. Beukelman, D. The Effect of Changes in Velopharyngeal Orifice Area on Vowel Intensity. *Cleft Palate Journal.* 14, 63-77, 1977.

32 Hanson, M. A Study of Velopharyngeal Competence in Children with Repaired Cleft Palates. *Cleft Palate Journal.* 1, 217-231, 1964.

33 Fujimura, O. Spectra of Nasalised Vowels. *Quarterly Progress Report of the Research Laboratory of Electronics (MIT).*15, 214-218, 1960.

34 Hirano, M. Takeuchi, Y. Hiroto, I. Intranasal Sound Pressure During Speech Sounds. *Folia Phoniattrica.* 18, 369-381, 1966.

35 Shelton, R. Knox, A. Arndt, W. Elbert, M. The Relationship Between Nasality Scores and Oral and Nasal Sound Pressure Level. *Journal of Speech and Hearing Research.* 40, 232-244, 1975.

36 Fletcher, S. Theory and Instrumentation for Quantitative Measurement of Nasality. *Cleft Palate Journal.* 7, 601-609, 1970.

37 Horii, Y. An Accelerometric Approach to Nasality Measurement: A Preliminary Report. *Cleft Palate Journal,* 17, 254-261, 1980.

38 Horii, Y. An Accelerometric Measure as a Physical Correlate of Perceived Hypernasality in Speech. *Journal of Speech and Hearing Research.* 26, 476-480, 1983.

39 Redenbaugh, M. Reich, A. Correspondence Between an Accelerometric Nasal/Voice Amplitude Ratio and Listeners' Direct Magnitude

Estimation of Hypernasality. *Journal of Speech and Research.* 28, 273-281, 1985.

40 Pigott, R. Bensen, J. White, F. Nasendoscopy in the Diagnosis of Velopharyngeal Incompetence. *Plastic and Reconstructive Surgery,* 43, 141-147, 1969.

41 Skolnick, M. Cohn, E. Videofluoroscopic Studies of Speech in Patients with Cleft Palate. Springer-Verlag. 1989.

42 Taub, S. The Taub Oral Panendoscope: A New Technique. *Cleft Palate Journal.* 3, 328-346, 1966a

43 Peterson, G., Barney H., Control Methods used in a Study of Vowels. *J Acoust Soc Am.* 24, 175, 1952.

44 Willis, C., Stutz, M., The Clinical Use of the Taub Oral Panendoscope in the Observation of Velopharyngeal Function. *Journal of Speech and Hearing Disorders.* 37, 495-502, 1972.

45 Henningsson, G., Isberg, A., Comparison between Multiview Videofluoroscopy and Nasendoscopy of Velopharyngeal Movements. *Cleft Palate Journal.* 28, 417-418, 1991

46 Moll, K., Daniloff, R. Investigation of the Timing of Velar Movements during Speech. *J Acoust Soc Am.* 50, 678-684, 1971.

47 Kuehn, D. A Cineradiographic Investigation of Velar Movement Variables in Two Normals. *Cleft Palate Journal.* 13, 88-103, 1976

48 Birch, M. Sommerlad, B. Image Analysis of Lateral Velopharyngeal Closure in Cleft Palate and Normals. *Brit J Plast Surg.*47, 400-405,1994

49 Coffey, J., Hamilton, D., Fitzsimons, M., Freyne, P. Image Processing of Patients with Velopharyngeal Insufficiency and Hypernasal Speech. *Clinical Radiology.* 48, 260-263, 1993.

50 Cowen, A., Hartley, P., Workman, A. The Computer Enhancement of Digital Grey-Scale Fluorography Images. *The British Journal of Radiology.* 61, 492-500, 1987.

51 Isberg, A., Per Julin, D., Kraepelien, T., Henrikson, C. Absorbed Dose and Energy Imparted from Radiographic Examination of Velopharyngeal Function During Speech. *Cleft Palate Journal.* 26, 105-109, 1989.

52 Golding-Kushner K. *et al.* Standardization for the Reporting of Nasophayrngoscopy and Multiview Videofluoroscopy: A Report from and International Working Group. *Cleft Palate Journal.* 27, 337-348, 1990.

53 Stevens KN, House AS. An Acoustical Theory of Vowel Production and some of it's Implications. *J Speech Hear Res.* 4, 303-320, 1961.

54 Dunn H., Methods of Measuring Vowel Formant Bandwidths. *J Acoust Soc Am.* 33, 1737, 1961.

55 Birch MJ. Initial clinical study of nasal resonance in phonation and a draft instrument specification. Internal report Dept of Medical Physics, The Royal London Hospital. No: 2705, Class No 12.5. June 1990.

56 Birch MJ. Instrument to assess hearing aid performance. Internal report Dept of Medical Physics, The Royal London Hospital. No: 2267, Class 7.2. March 1985.

57. Skolnick M.,Ellen R. Videofluoroscopic studies of speech in patients with cleft palate. Springer-Verlag. New York Inc. 1989.

58. Lubker JF. An electromyographic-cinefluorographic investigation of velar function during normal speech production. Cleft Palate J. 5:1-18 1968

59. Moll. KL, Shriner TA. Preliminary investigation of a new concept in velar activity during speech. Cleft Palate J. 4:58-69. 1967

60. Kuehn DP. A cineradiographic investigation of velar movement in two normals. Cleft Palate J. 13:88-103. 1976.

61. Cowen AR, Haywood JM, Clarke OF, Rouse S. Digital grey-scale fluorography: A new approach to digital radiographic imaging. British Journal of Radiology, 57, 533-538, 1984

62. Skolnick ML. The use and limitations of the barium phyaryngogram in the detection of velopharyngeal insufficiency. Radiology 135:301 1980.

63. Bhatt A. Measurement error in a videofluoroscopic study of cleft palate repair. BSc Project. University of London. The London Hospital Medical College. Sept 1993.

64. Birch MJ, Humphries C, Stock C. Nasal Resonometer: An instrument for the assessment and treatment of hypernasality. J. Biomed Eng, 13,429-432, 1991.

65. Sommerlad B, Henley M, Birch M, Harland K, Boorman J and Moiemen N. Cleft palate re-repair - A clinical and radiographic study of 33 consecutive cases. Brit J Plast Surg. 47, 406-410, 1994.

66. Gardner F. Phaselock techniques. J. Wiley & Sons. 1979. ISBN 0-471-04294-3.

67. Tausworthe R. Design of lock detectors. Jet Propulsion Laboratory. Pasadena, JPL SPS. 37-43, Vol III, 71-75, 1967.

68. Sommerlad B, Birch M, Moimen N, Henley M. Velar velocity, extensibility and lift in the normal and the cleft. Presentation to the European Association of Plastic Surgeons. 5th Annual Meeting. May 1994.

69. IEEE Standards Board. Specification for a standard 8 bit backplane interface. Draft 3.2. IEEE, New York, NY10017. USA. Jan, 1986.

70. Horowitz P, Hill W. The Art of Electronics. 2nd Edition. Cambridge University Press. 1989. ISBN 0-521-37095-7.

71. Sommerlad BC, Rowland N, Harland K. Lateral videofluoroscopy: a modification to aid in velopharyngeal assessmentr and measurement. Cleft Palate craniofac J 1994; 31: 134-5.

72. Mirlohi HR, Kelly SW, Manley CG. New technique for assessment of velopharyngeal function. *Med Biol Eng Comput.*32, 562-566, 1994.

73. Parker AJ, Maw AR. An objective method of assessing nasality.A possible aid in the selection of patients for adenoidectomy. *Clin Otolaryngol.*14, 161-166, 1989.

74. Dalston RM. Using simultaneous photodetection and nasometry to monitor velopharyngeal behaviour during speech. *Journal of Speech and Hearing Research.*32, 195-202, 1989.

75 Cowen AR, Haywood JM, Workman A, Coleman NJ, McArdle S, Clarke OF. Leeds DSF Test Objects. Protocol and Instruction Manual. The Radiological Imaging Group. University of Leeds. March 1987.

76 Saurashima M, Ushijima T. Use of the fiberscope in in speech resonance. Annual Bulletin. Research Inst. Logopaedics and Phiniatrics. Univ Tokyo. 5, 25-34, 1971.

77 Maisomy SB. Developments in rigid endoscopy. Revue Stomatologie. 39, 733-754, 1937.

Appendix 1: Phonetic Information.

Vowel Symbol	Vowel Sound
a	As in c*a*r
i	As in f*ee*t
u	As in f*oo*d
ae	As in h*a*t
>	As in m*o*re

Speech sample, extended non-nasalised passage.
Look at this book with us. It is a story about a zoo. That is where bears go. Today it is very cold out of doors, but we see a cloud overhead that's a pretty white, fluffy shape. We hear that straw covers the floor of cages to keep the chill away.

Non-nasalised words
Feet, book, peat, hat, talk, cat, food, car.

Nasalised words
More, man, mean, nook, morn.

Non-nasalised sentences	**Denoted in the text**
What's the day today.	Day
The colourful jigsaw puzzle.	Jigsaw
But a book ought to be bought.	Book
The ship sails to the shore.	Ship
Pat the puppy.	Pat

Nasalised sentences.	
Bang the nail in with a hammer.	Bang
Many men make much noise.	Many
Marmalade in the morning.	Marmalade

Appendix 2: Equipment Specification

Spectral Dynamics SD345 Spectrascope III

Frequency range:	1 Hz to 100kHz	Dynamic range:	65dB
Weighting :	Acoustic A and C	Linearity:	0.05%
Frequency resolution	5Hz at 2kHz	Input Impedance	100KΩ

Sennheiser MKE2 Microphone

Frequency range:	40Hz to 20kHz	Pressure transducer mode	
Sensitivity:	5.1 mV/Pa +/- 2.5dB	Input Impedance:	130Ω
Signal/Noise	> 56dB	Minimum load :	300Ω

Bruel and Kjaer Sound Level Meter Type 2230

Frequency range:	40Hz to 20kHz	Dynamic range:	70dB(A)
Weighting :	Acoustic A, C, linear	Resolution:	0.1dB

KEF C series loudspeaker Type 101

Frequency range:	60Hz to 20kHz	Dynamic range:	100dB
Distortion:	< 1%, 2nd Harmonic		
Directional:	2dB, +/-5°vertical, +/- 20° horizontal		

Toshiba stereo cassette deck Type D10

Frequency range:	35Hz to 18kHz	Dynamic range:	100dB
Signal/noise:	>62dB	Distortion:	0.05%
Line input:	> 50kΩ		

PanasonicVCR

Horizontal resolution	300 lines	Video in level:	$1.0V_{p-p}$, 75Ω
Vertical resolution	625 lines	Field rate:	50 fields/sec

Appendix 3: Partial Software Listing of Data Acquisition code.

Module : Opsyscode(part only).

```
;opsyscode contains various z80 code subroutines
;they are called from c routines with parameters as shown
;    1:AUDIO(&on/off,&level,&o/n)
;    2:KEYFETCH()
;    3:THRESHOLD(&level)
;    4:DATACQ(hor_fsd)
;    5:FETCHPIX(data_curs)
;    6:PRINT_OP(dot)
;OR THEY ARE HARDWARE TEST ROUTINES AS SHOWN
;    1:AUDTEST-O/P DATAWORDS TO THE AUDIO BOARD
;    2:KEYFETCH-CHECKS FOR ANY KEY AND DEBOUNCES.RETURNS KEY ;
       1-16 IN ACC
;    3:KEYTEST-O/P'S KEYLINES,CHECKS FOR VALID RETURN,ID'S KEY
;    4:HAR_TEST-o/p,s datawords to the harmonic select port
;    5:AD_ACQ-o/p's channel and awaits interrupt from EOC then continues
;    6:CALLDAT-calls C_INTERRUPT()




PLL         EQU     0A0H        ;harmonic address
FIRST       EQU     3           ;first harmonic
SECOND      EQU     2           ;second
THIRD       EQU     1           ;third
FOURTH      EQU     0           ;fourth
CTC0        EQU     8
CTC1        EQU     9
CTC2        EQU     0AH
CTC3        EQU     0BH
ORAL        EQU     090H        ;tracking band pass filtered
NASAL       EQU     091H        ;tracking band pass filtered
LOCK_QUAL   EQU     092H        ;PLL lock quality
ORAL_LP     EQU     093H        ;low pass filtered


            PUBLIC THRESHOLD
            CSEG
THRESHOLD:  EI
            LD      BC,ORAL_LP      ;check low pass oral signal
            CALL    DATA2           ;fetch mike1 in af'
            EX      AF,AF'
            SUB     08H
```

```
                JR          C,LESSTHAN
                LD          (ORAL_FLAG),A     ;oral level detected
                RET                           ;exceeds threshold, acc is set
LESSTHAN:       XOR         A                 ;not threshold, acc is reset
                LD          (ORAL_FLAG),A
                RET                           ;C checks for NZ acc

DATA2:          LD          A,11000111B       ;set ctc3 to int on eoc
                OUT         (CTC3),A
                LD          A,01
                OUT         (CTC3),A
                XOR         A
                OUT         (C),A             ;BC holds A/D address
                HALT                          ;await eoc
                RET


ZEROES          DCB         6,0
        PUBLIC DATACQ
        CSEG
DATACQ:         LD          (HOR_FSD),HL      ;c calls with hor_fsd in HL
                XOR         A
                LD          BC,5
                LD          HL,ZEROES
                LD          DE,LSB_NASAL
                LDIR                          ;zeroes nasal, oral, xslot
                NOP
ACQLOOP:        LD          A,08BH            ;xslot > 139?
                LD          HL,XSLOT
                XOR         (HL)
                JR          Z,EXIT
                CALL        KEYFETCH          ;check for key
                XOR         0
                            JR          NZ,EXIT
                CALL        THRESHOLD         ;set's oral flag once per meas'
                                              ;cycle
                CALL        SET_SCN_INT       ;set's and enables screen int
                            LD    D,0         ;D is loop lock counter
                            JP    ACQLOOP1
EXIT:       DI
                RET

ACQLOOP1: LD                BC,PLL
                LD          A,FIRST
                OUT         (C),A             ;set filter to fundamental
                CALL        CHECK_SCN_INT     ;request for scn service?
                JR          NZ,C_INT          ;z flag set for scn int
                CALL        LOCK_QUALY        ;check for phase lock
```

```
                LD      (LAST_LOCK),A   ;> 100 Hz
                SUB     2FH             ;data in last lock
                JR      C,ACQLOOP1      ;no lock, try again
                LD      A,(LAST_LOCK)
                SUB     0C4H            ;< 600 Hz
                JR      NC,ACQLOOP1     ;no lock, try again
                LD      BC,LOCK_QUAL    ;lock in limits
                LD      A,10100111B
                OUT     (CTC3),A
                LD      A,20H           ;4.6mS for df/dt
                OUT     (CTC3),A
                HALT                    ;awaiting int
                CALL     LOCK_QUALY
                LD      L,A             ;temp store in L
                LD      A,(LAST_LOCK)   ;last lock in acc
                SUB     L               ;find diff between
                                        ;successive
                JR      NC,POS          ;readings, adjust for -ve
                CPL
POS:            SUB     04H             ;compare against max
                                        ;allowable diff
                JR      C,INC_COUNT     ;if < inc lock counter,if>
                LD      D,0             ;then zero lock counter
                LD      A,L             ;and
                LD      (LAST_LOCK),A   ;update last lock
                JP      ACQLOOP1

INC_COUNT:      LD      A,L
                LD      (LAST_LOCK),A   ;update last lock
                INC     D
                LD      A,03H           ;3 tests
                CP      D
                JR      Z,GET_DATA      ;in lock limits so get data
                JP      ACQLOOP1        ;else loop again
                LD      D,0             ;reset lock counter
GET_DATA:       LD      BC,PLL          ;locked, fetch harmonic data
                LD      A,FIRST         ;set  1st harmonic
                OUT     (C),A
                LD      E,0FFH          ;16mS settling
                CALL    HARMONIC_DELAY  ;settling delay
                LD      A,FIRST         ;read 1st harmonic data
                LD      E,1             ;no settling
                CALL    HARMONIC_DELAY  ;after delay
                LD      A,SECOND        ;read 2nd harmonic
                LD      E,0FFH          ;16mS settling
                CALL    HARMONIC_DELAY  ;after delay
                LD      A,SECOND        ;read 3rd harmonic data
                LD      E,1             ;16mS settling
```

```
                CALL    HARMONIC_DELAY  ;after delay
                CALL    CHECK_SCN_INT   ;returns set z flag for scn int
                JR      Z,GET_DATA      ;no-loop back for more data
C_INT:          CALL    C_INTERRUPT     ;yes-service the screen
                LD      BC,4
                LD      HL,ZEROES
                LD      DE,LSB_NASAL
                LDIR                    ;zeroes 16 bit accs
                XOR     A
                LD      (ORAL_FLAG),A   ;reset oral detect flag
                JP      ACQLOOP

CHECK_SCN_INT:  CALL    THRESHOLD       ;check for oral signal and set flag
                LD      HL,SCNFLAG      ;request for scn service?
                XOR     A
                CP      (HL)            ;set zero flag for service
                RET

        PUBLIC SET_SCN_INT
        CSEG
SET_SCN_INT:    EI
                XOR     A
                LD      (SCNFLAG),A     ;reset scn flag pending int
                LD      A,11010101B     ;counter, rising edge
                OUT     (CTC2),A
                LD      A,(HOR_FSD)     ;load current x-axis fsd
                OUT     (CTC2),A
                LD      A,00100111B     ;timer for screen int's
                OUT     (CTC1),A
                LD      A,113           ;7.25mS multiple
                OUT     (CTC1),A        ;zc1 triggers ctc2
                RET

        PUBLIC HARMONIC_DELAY
        CSEG
HARMONIC_DELAY: LD      BC,PLL          ;select harmonic(passed in A)
                OUT     (C),A
                LD      BC,ORAL         ;dummy read during int routine
                LD      A,10100111B
                OUT     (CTC3),A
                LD      A,E             ;harmonic delay  in E
                OUT     (CTC3),A
                HALT                    ;await int
                CALL    DATA1           ;get data
                RET


                                        ;9 readings/harmonic
                                        ;4 harmonics/channel/cycle
```

```
        PUBLIC DATA1                        ;7 cycles max = 252 readings max
        CSEG
DATA1:  LD      HL,READINGS
        LD      (HL),9                      ;take 9 readings/harmonic
DATA3:  LD      A,10100111B
        OUT     (CTC3),A
        LD      A,10H
        OUT     (CTC3),A
        HALT                                ;1mS per reading
        LD      A,11000111B                 ;set ctc3 to int on eoc
        OUT     (CTC3),A
        LD      A,01
        OUT     (CTC3),A
        LD      BC,ORAL
        XOR     A
        OUT     (C),A                       ;A/D oral channel
        HALT                                ;await eoc_int(ctc3_reset)
        LD      HL,(LSB_ORAL)
        CALL    SUM                         ;16 bit add result in hl
        LD      (LSB_ORAL),HL
        LD      A,11000111B                 ;set ctc3 to int on eoc
        OUT     (CTC3),A
        LD      A,01
        OUT     (CTC3),A
        LD      BC,NASAL
        XOR     A
        OUT     (C),A                       ;A/D nasal channel
        HALT                                ;await eoc_int _reset)
        LD      HL,(LSB_NASAL)              ;reti here with nasal data in A
        CALL    SUM                         ;add it to current nasal total
        LD      (LSB_NASAL),HL
        LD      HL,READINGS
        DEC     (HL)
        JR      NZ,DATA3
        RET


SUM:    EX      AF,AF'                      ;A' is data from oral/nasal
        LD      E,A                         ;adds A to HL, no carry
        LD      D,0
        ADD     HL,DE
        RET

        PUBLIC LOCK_QUALY
        CSEG
LOCK_QUALY:
        LD      BC,LOCK_QUAL                ;fetch lock quality and
        CALL    DATA2                       ;ret it in acc and L
        EX      AF',AF
```

```
                RET

        PUBLIC HAR_TEST
        CSEG

HAR_TEST:       LD      BC,PLL          ;sends bytes to pll card
                LD      A,0FEH
HAR:            OUT     (C),A
                RLCA
                JP      HAR

XSLOT           EQU      0C004H         ;x axis counter
LSB_NASAL       EQU     0C000H          ;16 bit nasal data
MSB_NASAL       EQU     0C001H
LSB_ORAL        EQU     0C002H          ;16 bit oral data
MSB_ORAL        EQU     0C003H
HOR_FSD         EQU     0C005H          ;x axis fsd
READINGS        EQU     0C006H          ;readings/cycle
SCNFLAG         EQU     0C007H          ;screen update required
FAULTS          EQU     0C008H          ;fault type passed to main-.c
ORAL_FLAG       EQU     0C009H          ;oral level detected
LAST_LOCK EQU           0C00AH          ;last phase lock value

        PUBLIC AD_ACQ_T
        CSEG

AD_ACQ_T:       LD      BC,ORAL
                IN      A,(C)           ;reset A/D
                LD      BC,CTC0
                LD      A,0E0H
                OUT     (C),A           ;test vector is 3fex
                LD      BC,CTC3
                LD      A,11000111B     ;counter mode
                OUT     (C),A
                LD      A,01H           ;int on first edge
                OUT     (C),A
                LD      A,11000001B     ;ready for int
                OUT     (C),A           ;
                EI
AD_ACQ1_T:      LD      BC,ORAL         ;mike1
                AND     0
                OUT     (C),A           ;creates a falling edge
                OR      0FFH            ;loop here awaiting int
NEXT2:          DEC     A
                JR      NZ,NEXT2        ;
                JP      AD_ACQ1_T       ;reti here
```

```
;interrupts are arranged as 8 vectors placed at 3fe0 - 3fef
;these jump to routines located at 3fa0 - 3fdf, 8 bytes per routine
;these routines call the interrupt routines then EI and RETI

        PUBLIC VECTABLE_T   ;8 vectors 3FE0 - 3FEF
        ASEG
        ORG   03FE0H                    ;test interrupt addresses
VECTABLE_T:     DEFW   03FA0H                   ;dummy vector
                DEFW   03FA8H                   ; "
                DEFW   03FB0H                   ; "
                DEFW   03FB8H           ;test routine AD_ACQ of
                                        ;CTC3

        PUBLIC VECTABLE                 ;prog  vec's start at 3FE8
VECTABLE:       DEFW   03FC0H           ;CTC0 routine at 3FC0 (ctc0 reset)
                DEFW   03FC8H           ;CTC1 routine at 3FC8 (fault)
                DEFW   03FD0H           ;CTC2 routine at 3FD0 (scn_int)
                DEFW   03FD8H           ;CTC3 routine at 3FD8 (ctc3 reset)

        PUBLIC INTROUTINES
        ASEG


        ORG 03FC0H
INTROUTINES:    CALL        CTC0_RESET
                EI
                RETI

        ORG 03FC8H
        HALT

        ORG 03FD0H                      ;CTC2 screen interrupt routine
                CALL        SCN_INT
                EI
                RETI

        ORG 03FD8H                      ;CTC3 disabled
                CALL        CTC3_RESET
                EI
                RETI

        ORG 03FB8H                      ;CTC3 test routine dat_acq
                CALL        DAT_ACQ_T_INT
                EI
                RETI

        PUBLIC SCN_INT
```

```
        EXTRN  C_INTERRUPT
        CSEG
SCN_INT:        PUSH    AF
                PUSH    BC
                PUSH    DE
                PUSH    HL
                LD      A,00100011B
                OUT     (CTC1),A        ;reset screen int timer
                LD      HL,XSLOT
                INC     (HL)            ;increment x_axis position
                LD      A,1
                LD      (SCNFLAG),A     ;update scn at end of data loop
                POP     HL
                POP     DE
                POP     BC
                POP     AF
                RET

        PUBLIC CTC3_RESET
        CSEG
CTC3_RESET:     PUSH    AF
                PUSH    BC
                PUSH    DE
                PUSH    HL
                LD      A,01000011B
                OUT     (CTC3),A        ;resets ctc3
                IN      A,(C)           ;enters with BC pointing at
                EX      AF,AF'
                POP     HL              ;oral or nasal, leaves with
                POP     DE              ;data in A' and a/d reset
                POP     BC
                POP     AF
                RET

        PUBLIC CTC0_RESET
        CSEG
CTC0_RESET:     PUSH    AF
                PUSH    BC
                PUSH    DE
                PUSH    HL
                LD      A,00100011B     ;reset tc0
                OUT     (CTC0),A
                POP             HL
                POP     DE
                POP     BC
                POP     AF
                RET
```

```
        PUBLIC DAT_ACQ_T_INT
        CSEG
DAT_ACQ_T_INT: DI
               LD          BC,ORAL
               IN          A,(C)        ;get the data and reset the hardware
               RET
```

Module : C_Interrupt(From FNC2 module)

```
/*Function 2 is the function called from Main when funcflag=2,*/
/*it cls,o/p's the background axis and text  then loops on */
/*the keyboard awaiting a threshold on Mike 1 indicating data acq*/
/*or a help request key, in which case  the helpscreen is shown*/
/*or an arrow key to change the cursor position or x axis scale*/
/*or a print screen request*/
/*when a threshold is detected control is passed to DATACQ in OPSYSCODE*/
/*where 138 samples of 4 harmonics in nasal and oral channels are taken*/
/*each processed by C_INTERRUPT in this module*/
/*data is only passed when the system is phase locked  o a nasal tone*/
/*a test average is displayed and passed to FNC3, a success time is passed*/
/*to FNC4*/

FNC2()
{
   DRAW_SCREEN2();
   OP_OLD_DATA();
   KEYLOOP2();                          /*returns only fungflag*/
   return;                              /*return to LOOP in MAIN*/
}

KEYLOOP2()
{
   for (;;){
      short int i,tn;
         blink = 0x20;
       if (THRESHOLD()){                /*check mike1 for start*/
         average = 0;                   /*reset last test average*/
         success = 0;                   /*reset last success score*/
         xdata = 0;                     /*reset res data counter*/
         tn = 0;                        /*inc test number in TEST_AVERAGE*/
         DATACQ(hor_fsd);               /*DATACQ completes all screen2 functions*/
         TEST_AVERAGE(average,tn);      /*writes test average to scns 2 + 3*/
         TEST_SUCCESS();                /*writes test success to scn 4*/
         SCATTER();                     /*writes scatter to scn2*/
         TIME_RESON();                  /*writes % time resonant to scn2*/
         HORIAXIS();                    /*rewrite x axis pips*/
```

```
  DELAY();
  DELAY();                    /*delay for short test key i/p*/
  DELAY();
  if(test_number > 23){       /*scn3/4 full so display scn3*/
   fncflag = 3;
   return;
   }
  RESET_LOOP();               /*await reset key,reset screen and*/
                              /*rearm THRESHOLD*/
  }

i = KEYFETCH();
if(i == 0)
  continue;                   /* no key so loop*/


else if(i == 9){              /*reset key so redraw screen*/
  DRAW_SCREEN2();
  DELAY();
  }

else if(i == 10){
  HELP();                     /*help page key = 0*/
  DELAY();
  return;                     /*redraw screen via MAIN*/
  }

else if(i == 8 || i== 5){
  MOVCURS2(i);                /*vertical arrow key so change cursor*/
  DELAY();
  }

else if(i == 6 || i == 7){
  X_AXIS(i);                  /*horizontal arrow key so adjust */
  DELAY();                    /*  x  axis scale */
  }

else if(i == 11)
  PRINT_SCREEN2();            /*op this screen to printer*/

else if(i <= 4 && i >= 1) {
  fncflag = i;                /*function key so set flag*/
  DELAY();                    /* and return via KEYLOOP2*/
  return;                     /*to MAIN LOOP*/
  }

else continue;
}
```

```
}

C_INTERRUPT()                                   /*called from screen update*/
{                                               /*int req in DATACQ*/
nasal = 0;
oral =0;
      G_PUTCUR(curlo = 0x95 + XSLOT/2,curhi = 6,car = (blink ^= 0x0a));
/*o/p to screen, moving blinker on x axis*/
      nasal = ((nasal | MSB_NASAL) << 8) | LSB_NASAL;
      oral =  ((oral | MSB_ORAL) << 8) | LSB_ORAL;
     if(oral == 0 && ORAL_FLAG == 0){           /*no phase lock/no oral */
         ydata_hist[XSLOT] = 0;
         return;
         }
      else if(oral == 0 && ORAL_FLAG > 0){      /*no phase lock/oral detected*/
         ydata_hist[XSLOT] = 0;
         xdata += 1;                            /*so inc data counter*/
         return;
         }
      xdata += 1;                               /*count data points*/
      yslot = (nasal * 60)/(oral + nasal) ;     /*0-60 y-axis slots*/
      ydata_hist[XSLOT] = yslot;                /*keep record of ydata*/
      average += yslot;                         /*sum of data*/
      OP_SCN_DATA();
}

OP_SCN_DATA()
{
int *pyaddr = yaddr;                            /*point to yaxis start*/
      data_curs = *(pyaddr + yslot/3) ;
   if(data_curs > start_curs)
      success += 1;
/*success counts time slots below cursor*/
      data_curs += XSLOT/2;
/*data_curs made from 1st addr of 1-20 lines + x axis car pos*/
      data_car = 8 >> (XSLOT % 2) * 3;          /*start at pixcell 4/1?*/
      data_car <<= yslot % 3;                   /*shift 0,1,2 places?*/
/*data_car made from 1 of 6 cars,ie 3 rows 2 columns pixcell*/
      data_car |= FETCHPIX(data_curs);
/*data_curs or with current screen pixcell*/
      G_PUTCUR(curlo = data_curs & 0xff,curhi = data_curs >> 8,car =
data_car | 0x40);
}
```